STUDIES OF STRUCTURE-FUNCTION RELATIONSHIP OF ALPHA-MANNOSIDASE FROM *ASPERGILLUS FISCHERI* NCIM 508

Thesis submitted to University Of Pune

For the degree of

DOCTOR OF PHILOSOPHY

IN

CHEMISTRY (BIOCHEMISTRY)

By

SHASHIDHARA, K. S.

Under the guidance of

DR. SUSHAMA M. GAIKWAD

&

DR. M. I. KHAN

DIVISION OF BIOCHEMICAL SCIENCES
NATIONAL CHEMICAL LABORATORY
PUNE -411 008 (INDIA)

JULY 2009

Dedicated to

My Parents and Grandmother

CONTENTS

Acknowledgements

I take this opportunity to gratefully acknowledge my research mentor Dr. Sushama M. Gaikwad for her invaluable guidance, unending support and keen interest during the course of this investigation. She has given me the freedom to think and work; and I shall cherish my learning experience under her. Although this eulogy is insufficient, I preserve on everlasting gratitude for her.

I am grateful to Dr. M. I. Khan, my research co-guide, for his valuable suggestions, help in learning many techniques and devoting his valuable time in putting my work in the form of thesis into perfect shape.

I would also like to extend my sincere thanks to: Dr. B. M. Khan, Plant Tissue Culture, NCL, for providing lab facility for molecular biology work, Dr. (Mrs.) Vyjayanthi A. Kumar, Organic Chemistry Division, NCL, for permission to use CD facility, Dr. Mahesh Kulkarni, Centre for Material Characterization, NCL, for help in MALDI-ToF facility.

I am also grateful Dr. C. G. Suresh, Dr. Absar Ahmed, Dr. S. S. Deshmukh and Dr. Mala Rao for their valuable suggestions during the course of investigation.

I express my deep feelings and love for my friends and my lab mates Feroz, Anil, Atul, Siddharth, Nagaraj, Sajid, JP, Late. Rohtas, Sreekanth, Ansari, Avinash, Madhurima, Asad, Shabab, Shadab, Ashutosh, Santosh (bond), Vaibhav and Ravi for their help, cooperation and maintaining pleasant and healthy atmosphere throughout my doctorate course and Prasanna, Sateesh, Sumanth, Manjegowda, Suresh poojari, Kiran Toti, Govindraju and Sharat for their good company in the hostel stay and for countless things they have done for me and for always being there with me whenever I needed them.

I would like to express my deep felt gratitude to my friends Sameer, Noor, Rishi, Somesh, Santhosh, Abhishek, Abhilash, Ambrish, Anish, Yadav, Ashish, Bhuban,

Bhushan, Chetan, Fazal, Pushkar, Kishore, Manish, Nishant (Rambo), Nitin, Nookaraju, Pandey, pankaj, Pawan, Poorva, Urvashi, Rhodu, Santosh, Sarvesh, Prabhas, Prabhakar, yashwant, Gnanaprakash, Vishnu, Roopesh, Suresh, Sridevi, Ashwini, Harry, Suhas, Sumita, Ruby, Trupti, Pallavi, Sushim, Raakesh for help, support and charming company.

I also would like to thank scientists, staff of Biochemical Sciences Division, NCL, helping me directly or indirectly during course of my stay in the division.

I find no words for my parents, grandmother, my brother and sister who have been constant inspiration for me and this work would not have been possible without their constant support and sacrifices.

Finally, I thank Heads, Division of Biochemical Sciences and the Director of National Chemical Laboratory and for permitting me to submit this work in the form of the thesis and Council of Scientific and Industrial Research, India, for financial assistance.

Shashidhara

CERTIFICATE

Certified that the work incorporated in the thesis entitled **"Studies of structure-function relationship of alpha-mannosidase from *Aspergillus fischeri* NCIM 508"** submitted by Mr. Shashidhara, K. S. was carried out under my supervision. Such materials has been obtained from other sources has been duly acknowledged in the thesis.

Dr. Sushama M. Gaikwad
Research Guide

Dr. M. I. Khan
Research Co-guide

DECLARATION OF THE CANDIDATE

I declare that the thesis entitled **"Studies of structure-function relationship of alpha-mannosidase from *Aspergillus fischeri* NCIM 508"** submitted by me for the degree of Doctor of Philosophy is the record of work carried out by me during the period from **3rd August, 2004 to 12th July, 2009** under the guidance of **Dr. Sushama M. Gaikwad** and has not formed the basis for the award of any degree, diploma, associateship, fellowship, titles in this or any other University or other institute of Higher learning. I further declare that the material obtained from other sources has been duly acknowledged in the thesis.

Signature of the Candidate

Date . . . . . **Shashidhara, K. S.**

LIST OF ABBREVIATIONS USED

ANS	1-anilino-8-naphthalenesulfonate
Arg	arginine
Asn	asparagine
Asp	aspartic acid
Bn	benzyl
CD	circular dichroism
Da	dalton
DEAE	di ethyl amino ethyl
DEPC	diethylpyrocarbonate
DMJ	1-deoxymannonojirimycin
DMSO	dimethylsulfoxide
DNA, cDNA	deoxyribonucleic acid, complementary DNA
DNJ	deoxynojirimycin
DTNB	2, 2'-dithiobisnitrobenzoic acid
EDAC	1-Ethyl-3-(3-dimethylaminopropyl) carbodiimiide
ER	endoplasmic reticulum
ERMI	endoplasmic reticulum α-mannosidase I
Gal	galactose
GdnHCl	guanidium hydrochloride
Glc	glucose
GlcI	α-glucosidase I
GlcII	α-glucosidase II
GlcNAc	*N*-acethylglucosamine
GlcNAcTI	*N*-acetylglucosamine transferase I
GlcNAcTV	*N*-acetylglucosamine transferase V
GMI	golgi α-mannosidase I
GMII	golgi α-mannosidase II
GMIII	golgi α-mannosidase III
GMX	golgi α-mannosidase IIx
HEPES	4-(2-hydroxyethyl)-1-piperazineethanesulfonic acid
hGMII	human golgi α-mannosidase II
His	histidine
HIV	human immunodeficiency virus
HPLC	high pressure liquid chromatography
IC_{50}	concentration of an inhibitor required for 50% inhibition of the enzyme
IUPAC	international union of pure and applied chemistry
Ka	association constant
k_{cat}	catalytic Efficiency
K_i	inhibition constant
K_M	Michaelis-Menten constant
K_{sv}	Stern-Volmer quenching constant
LB	Luria Bertani Broth
MALDI	matrix assisted laser desorption ionization

Man	mannose
MeUmbαMan	4-methyl umbelliferyl α-D-mannopyranoside
MRE	mean residue ellipticity
mRNA	messenger ribonucleic acid
$NaBH_4$	sodium borohydride
NAI	N-acetyl imidazole
NBS	N-bromo succinimide
NEM	N-ethylmaleimide
NJ	nojirimycin
NTEE	nitro tyrosine ethyl ester
PAGE	polyacrylamide gel electrophoresis
PCR	polymerase chain reaction
PDB	protein data bank
Ph	phenyl
pHMB	p-hydroxymercurybenzoate
pKa	acid dissociation constant
PMSF	phenylmethylsulfonyl fluoride
PNPαMan	para nitro phenyl α-D-mannopyranoside
PNPG	p-nitrylphenylglyoxal
rpm	revolutions per minute
RMSD,	SD root mean square deviation, standard deviation
S	substrate
SDS	sodium dodecyl sulphate
Ser	serine
Swa	swainsonine
Thr	threonine
Tlc	thin layer chromatography
TNBS	trinitrobenzenesulphonic acid
TOF	time of flight mass spectrometry
Trp	triptophan
Tyr	tyrosine
UV	ultra violet
V, Vmax	rate of an enzyme-catalyzed reaction, maximum reaction rate

ABSTRACT

Glycosidases have proved to be useful tools for probing structural features of cell surface glycoconjugates. α-Mannosidase (α-D-mannoside mannohydrolase, EC 3.2.1.24) plays a very important role in the mannose-trimming reaction during the biosynthesis of glycoproteins of higher eukaryotes, and a deficiency of this enzyme leads to mannosidosis, a lethal disease in human and cattle. α-mannosidase is also intimately involved in the quality control, a process that facilitates proper folding of newly formed polypeptide chains leading to retention and/or degradation of malfolded proteins in the Endoplasmic Reticulum (ER). There has been widespread interest in α-mannosidase in recent years, in particular, mammalian Golgi mannosidase-II involved in glycoprotein biosynthesis and is currently an important therapeutic target for the development of anticancer agents.

Aspergillus species are used in the fermentation industry. *Aspergilli* are the major producers of the α-mannosidases. Investigation was carried out to purify and characterize α-mannosidase from *Aspergillus fischeri* (*Neosartorya fischeri*), to study substrate and inhibition kinetics and to determine its structure-function relationship. The thesis is divided into six chapters.

Chapter 1: Introduction

This part comprises biological role of sugars and a literature survey of α-mannosidase with reference to the classification, isolation, purification, properties and applications.

Chapter 2: Biochemical characterization of α-mannosidase

Production of α-mannosidase enzyme from the fungus *Aspergillus fischeri* was carried out in shake flasks by growing the organism in a yeast extract containing medium for seven days. The enzyme was purified to homogeneity using following steps. (i) Ammonium sulfate precipitation (90%) (ii) Ion exchange chromatography on DEAE-Sepharose (iii) Preparative Gel Electrophoresis (5%) with final recovery of 4.5%. The pH activity profile of the enzyme revealed the participation of two ionizable groups with a

pKa of pH5.75 and 7.84 indicating involvement of carboxylic group and Histidine/Cysteine at active site, respectively.

The activity staining of the enzyme in the gel after PAGE was standardized. The enzyme showed fluorescent bands at different stages of purification in activity staining of non-denaturing gel with fluorescent substrate 4-methylumbelliferil α-D-Mannopyranoside. Amino acid analysis of the protein revealed 18.43% hydrophobic amino acids, 16.00% (AsX + GlX) amino acids, 17.5% basic amino acids and 20.59% Glycine composition in α-mannosidase. Among the metal ions checked, Cu^{++} (K_i = 21nM) and Se^{++} ions (K_i =32 μM) showed noncompetitive and Co^{++} (K_i = 1.195 mM) showed competitive inhibition of the enzyme activity with insignificant change in the secondary structure of the protein. These studies exhibit the potential of the enzyme in studying the effect of anticancer drugs. Treatment of the enzyme with group specific reagents showed the presence of carboxylate, Arg and Cys at the active site. Substrate protection studies and kinetics of the modified enzyme confirmed the above results. Trp and His at the active site were observed to be in proximity.

Chapter 3: Energetics of catalysis and inhibition of α-mannosidase

The enzyme used in the present work is a Class II α-mannosidase from *A. fischeri* as revealed by the substrate specificity and independency on the metal ion/s for activity (18). TLC plates shows the rate of hydrolysis of the three mannose disaccharides as Man (α1-3) Man>Man (α1-2) Man>Man (α1-6) Man by the enzyme.

Energetics of the catalysis of Class II α-mannosidase (E.C.3.2.1.24) from *Aspergillus fischeri* was studied. The enzyme hydrolyzed mannose disaccharides in the order of Manα(1-3)> Manα(1-2)> Manα(1-6). The enzyme showed K_{cat}/K_m for Man (α1-3) Man, Man (α1-2) Man and Man (α1-6) Man as 7488, 5376 and 3690M^{-1} min^{-1}, respectively. The activation energy, E_a was 15.14, 47.43 and 71.21 kJ/mol for α1-3, α1-2 and α1-6 linked mannobioses, respectively, reflecting the energy barrier in the hydrolysis of latter two substrates. The enzyme showed K_{cat}/K_m as 3.56×105 and 4.61×105M^{-1} min^{-1} and E_a as 38.7 and 8.92 kJ/mol, towards pNPαMan and 4-MeUmbαMan, respectively. Binding of Swainsonine (Ki=101μM) to the enzyme is stronger than that of 1-

deoxymannojirimycin (Ki=286 μM). Among the polyhydroxy substituted derivatives, compounds **20**, **32** and **39** showed significant level of inhibition towards the enzyme.

Chapter 4: Folding - unfolding studies

The conformational transitions of an oligomeric and high molecular weight class II α-mannosidase from *Aspergillus fischeri* were examined using fluorescence and CD spectroscopy under various denaturing conditions. The enzyme activity was labile i) above 55 ^{0}C ii) in presence of 1.0 M GdnHCl iii) below pH 5.0 or above pH 8.0. The enzyme lost the biological activity first and then the overall folded conformation and secondary structure. The midpoint values of GdnHCl mediated changes measured by inactivation, fluorescence and negative ellipticity were 0.48 M, 1.5 M and 1.9 M, respectively. The protein almost completely unfolded in 4.0 M GdnHCl but not at 90 ^{0}C. The inactivation and unfolding were irreversible. The protein exhibited molten-globule like intermediate with rearranged secondary and tertiary structures and exposed hydrophobic amino acids on the surface. This species showed not only increased accessibility of Trp to the neutral and anionic quenchers but also got denatured with GdnHCl in a different manner than that of the native enzyme. The insoluble aggregates of a thermally denatured protein could be detected only in the presence of 0.25 – 0.75 M GdnHCl.

Chapter 5: Steady state and Time Resolved Fluorescence study

Apart from the vital role in glycoprotein biosynthesis and degradation, α-mannosidase is currently an important therapeutic target for the development of anticancer agents. Fluorescence quenching and time-resolved fluorescence of α-mannosidase, a multitryptophan protein from Aspergillus fischeri were carried out to investigate the tryptophan environment. The tryptophans were found to be differentially exposed to the solvent and were not fully accessible to the neutral quencher indicating heterogeneity in the environment. Quenching of the fluorescence by acrylamide was collisional. Surface tryptophans were found to have predominantly positively charged amino acids around them and differentially accessible to the ionic quenchers.

Denaturation led to more exposure of tryptophans to the solvent and consequently in the significant increase in quenching with all the quenchers. The native enzyme showed two different lifetimes, τ_1 (1.51 ns) and τ_2 (5.99 ns). The average lifetime of the native protein (τ) (3.187 ns) was not affected much after denaturation (τ) (3.219 ns), while average lifetime of the quenched protein samples was drastically reduced (1.995 ns for acrylamide and 1.537 ns for iodide). This is an attempt towards the conformational studies of α-mannosidase.

Chapter 5: General discussion and conclusion

In this chapter the properties of α-mannosidase from *Aspergillus fischeri* are compared with other mannosidases with respect to substrate specificity, inhibition constants, active site characterization, tryptophan environment and other biophysical properties.

Appendix

This chapter records the gene isolation, cloning and characterization of α-mannosidase from *Aspergillus fischeri*.

LIST OF PUBLICATIONS:

- **K. S. Shashidhara**, Sushama M. Gaikwad. (2009) Class II α-Mannosidase from Aspergillus fischeri: Energetics of Catalysis and Inhibition. *Intl. J. Biol. Macromol.,* 44, 112-115.
- **K.S. Shashidhara** and Sushama M. Gaikwad. (2007) Fluorescence quenching and Time Resolved Fluorescence studies of α-Mannosidase from *Aspergillus fischeri* (NCIM 508). *J. of Fluorescence* 17(6): 599-605.
- **K.S. Shashidhara**, Sushama M. Gaikwad, M Islam Khan, Kishor C. Bharadwaj, Ganesh Pandey. (2009) Interaction of α-mannosidase from *Aspergillus fischeri* with glycosidase inhibitors, metal ions and group specific reagents. (Communicated).
- **K.S. Shashidhara,** Sushama M. Gaikwad. (2009) Conformational and functional transitions of Class II alpha-mannosidase from *Aspergillus fischeri*. (Communicated).
- Ganesh Pandey, Debasish Grahacharya, **K. S. Shashidhara,** M. Islam Khan and Vedavati G. Puranik. (2009) Synthesis of polyfunctional quinolizidine alkaloids: development towards selective glycosidase inhibitors. *Org. Biomol. Chem.*, DOI: 10.1039/b907007a.
- Ganesh Pandey, Kishor Chandra Bharadwaj, M. Islam Khan, **K. S. Shashidhara** and Vedavati G. Puranik. (2008) Synthesis of Polyhydroxylated Piperidines and their Analogues: A novel approach for selective inhibitors of alpha- glucosidase. *Org. Biomol. Chem.,* 6, 2587–2595.
- Debendra K. Mohapatra, Debabrata Bhattasali, Mukund K. Gurjar, M. Islam Khan, and **K. S. Shashidhara.** (2008) First Asymmetric Total Synthesis of Penarolide Sulfate A1. *Eur. J. Org. Chem.* 6213–6224.

CHAPTER: 1

INTRODUCTION

Glycosylation is one of the most widespread, and yet poorly understood modifications of proteins. Every cell in nature is coated with a dense layer of carbohydrates at its surface. Decorating intra- and extracellular proteins with large carbohydrate chains is a costly endeavour for a cell to undertake, yet it is seen in ubiquity, indicating that it has great importance. Carbohydrates comprise significant amount of the mass in biological systems, yet were long considered to be useful in little more than energy storage. The landmark discovery that the molecular determinant of blood type was a carbohydrate began the notion that sugars played a functional role in biological systems [1]. Research in recent decades has highlighted many detailed and important functions of these molecules.

Biological role of sugars

Carbohydrates or saccharides (Greek *sakcharon*: "sugar") are simple molecules present in all living species and display numerous properties such as the storage and transport of energy or act as structural components (cellulose in plants or chitin in insects). Additionally, carbohydrates and their derivatives play major roles in the activity of the immune system, fertilization, cell growth, pathogenesis, blood clotting, inflammation and interactions and adhesions [2,3].

Carbohydrates differ from proteins and nucleic acids in two important characteristics. They can be highly branched molecules and their monomeric units may be connected to one another by many different linkage types whereas proteins and nucleic acids are almost exclusively linear and they only display a single type of linkage. This complexity allows carbohydrates to provide almost unlimited variations in their structures. Although carbohydrates can be present without being attached to other molecules, the majority of them are attached to proteins, lipids or nucleosides. The terminology glycoproteins and glycolipids are used to reflect this conjugation. Lectins are carbohydrate-binding proteins able to recognize glycoproteins and/or glycolipids and can consequently mediate many specific biological functions such as immune defense (mannose binding protein) and cell-cell adhesion (selectins) [4-6].

Biosynthesis of glycoproteins

Most of the soluble and membrane-bound proteins synthesized in the ER are glycosylated.

Structure and diversity of N-linked and O-linked glycans

The majority of cell surface and secreted proteins are glycosylated with carbohydrates covalently attached through either a nitrogen atom (*via* the amino group of an asparagine residue) or an oxygen atom (*via* the hydroxyl group of serine or threonine). Glycoproteins are thus classified as *N*-linked or *O*-linked depending on the nature of the glycosidic bond between the protein and the polysaccharide. With a molecular weight up to 3 kDa, the oligosaccharide groups in mammalian glycoproteins cover a large fraction of its surface and form flexible and hydrated branches that can extend 3 nm or further into the extracellular medium. This carbohydrate moiety may thus participate directly in recognition events but it may also modify the conformation [7] and the stability [8] of the protein.

N-linked glycoproteins are widespread due to the importance of their role in biological functions. The advances in techniques for oligosaccharide structural analysis have made it possible to deduce the complete structure of hundreds of asparagine-linked oligosaccharides from a variety of plant and animal sources. When these structures are examined, they fall into three main categories [9] termed high mannose, hybrid and complex (Fig. 1.1). They share the common structure: Manα1,3(Manα1,6) Manβ1,4 GlcNAcβ1,4 GlcNAc-Asn (boxed area in Fig. 1.1, Man (mannose), GlcNAc (*N*-acetylglucosamine), Asn (asparagine)). The high mannose-type oligosaccharide has typically two to six additional mannose residues linked to the pentasaccharide core. The complex-type glycans contain no other mannose residues except those of the core but are often multibranched with GlcNac, galactose (Gal) and sialic acid residues (SA). The hybrid-type molecules display features of both high-mannose and complex-type oligosaccharides: one or two mannose residues are linked to the Manα1,6 arm of the core

(as in high mannose-type glycans) and usually one or two branches (as found in complex-type glycans) are linked to Manα1,3 of the core.

Biosynthesis of N-linked oligosaccharides

Protein N-glycosylation occurs primarily in the endoplasmic reticulum (ER) and Golgi apparatus, and involves a series of discrete catalytic steps. A diverse series of enzymes have evolved to carry out the complex steps of this pathway.

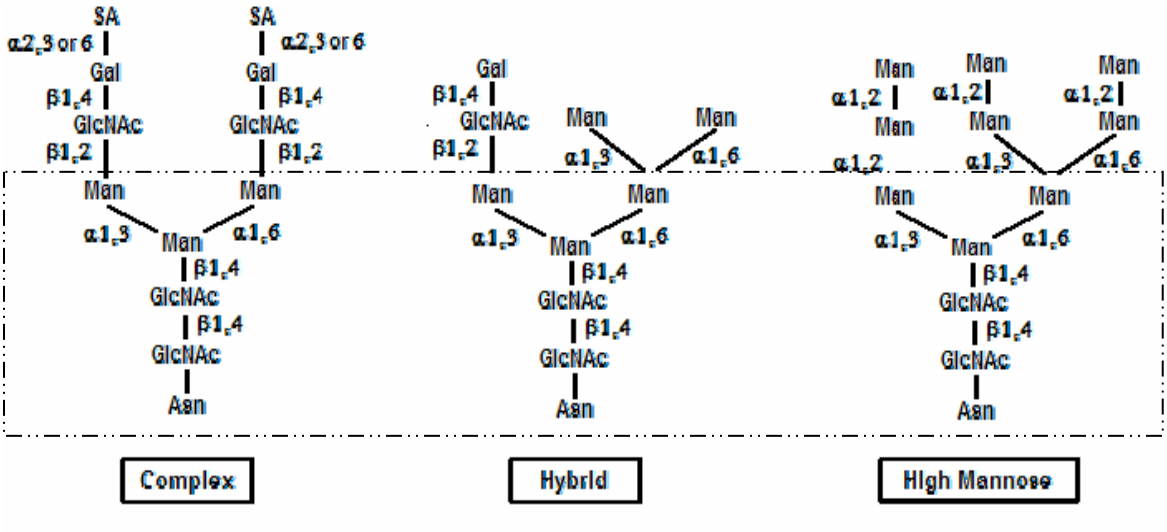

Figure 1.1: Structures of the major types of asparagine-linked oligosaccharides. The boxed area encloses the pentasaccharide core common to all *N*-linked structures.

It is becoming clear that for many of these catalytic steps, gene families have evolved to generate a number of similar genes to perform a diversity of specialized yet related functions [10].

The N-glycosylation synthesis pathways have been fairly well characterized in mammalian systems [9] and yeast expression systems [11,12], but are not as well characterized in filamentous fungi.

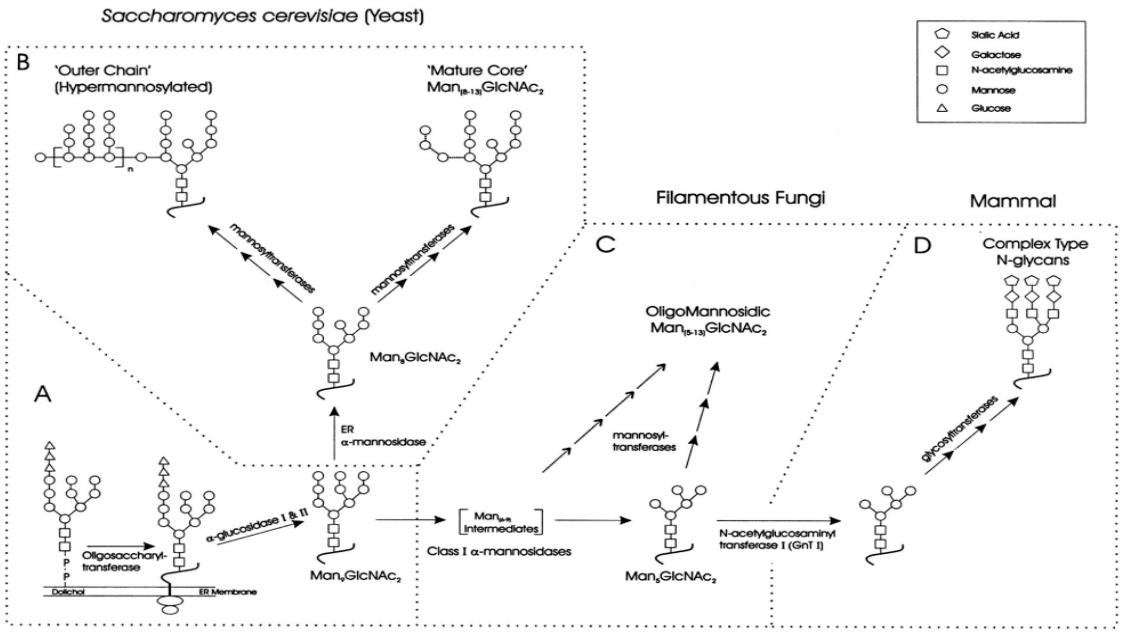

Figure 1.2: N-glycosylation synthesis pathway. The initial stages of the pathway are common to all systems [A]. Modification of $Man_9GlcNAc_2$ produces different final N-glycan structures in yeast [B], filamentous fungi [C], and mammalian systems [D]. The final structures shown represent the most common structures found in these species. Variations on these structures are found in some species[10].

In the biosynthesis of glycoproteins the sugars are added to the nascent protein, synthesized in the ER, as a core oligosaccharide unit, which is then extensively modified by removal and addition of sugar residues in the ER and the Golgi complex. The core oligosaccharides have a clearly defined structure composed of a branched unit made of three glucoses, nine mannoses and two *N*-acetyl-glucosamines ($Glc_3Man_9GlcNAc_2$) (Figure 1.3) [13,14]**.** This "14-saccharide core" unit is assembled as a membrane-bound dolicholpyrophosphate precursor by enzymes located on both sides of the ER membrane [15].

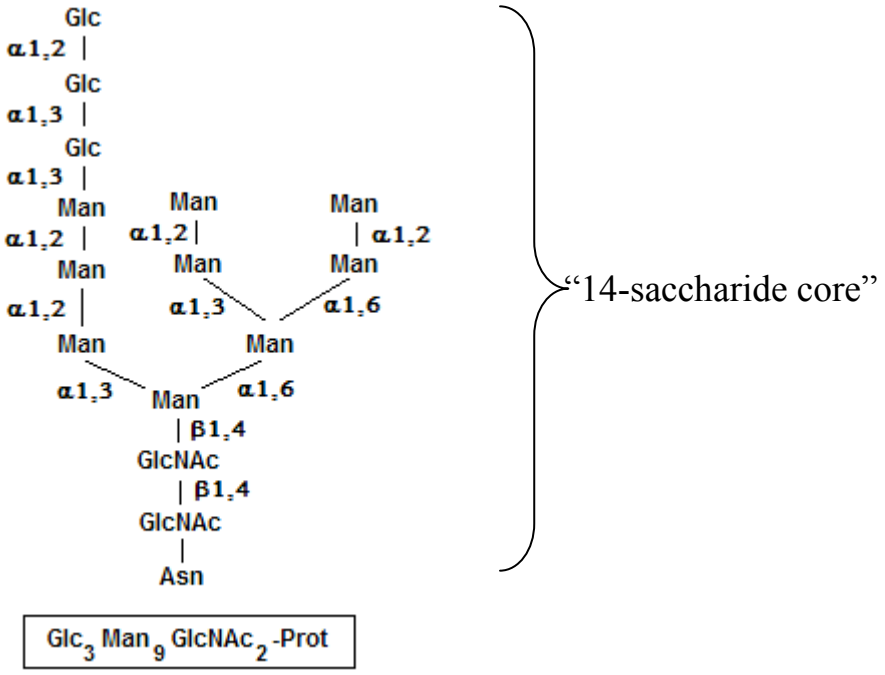

Figure 1.3: Structure of the untrimmed "14-saccharide core" *N*-glycosidic oligosaccharide $Glc_3Man_9GlcNAc_2$- protein.

The completed core oligosaccharide is transferred by a flipping mechanism from the dolichylpyrophosphate carrier to a growing nascent polypeptide chain, and is coupled through a *N*-glycosidic bond to the side chain of an asparagine residue. The oligosaccharyltransferase recognizes a specific conformation of the glycosylation sequence (Asn-X-Ser/Thr) formed when the polypeptide chain emerges, where X can be any amino acid except proline [16]. At this stage all glycoproteins bear the same carbohydrate structure in the ER.

Then a second phase of ordered trimming of selected monosaccharides by glycosidases and addition of others by glycosyltransferases begins in the ER and continues in the Golgi apparatus. This enzymatic pathway and the cellular location of the various reactions in that sequence are depicted in Figure 1.4 and Figure 1.5.

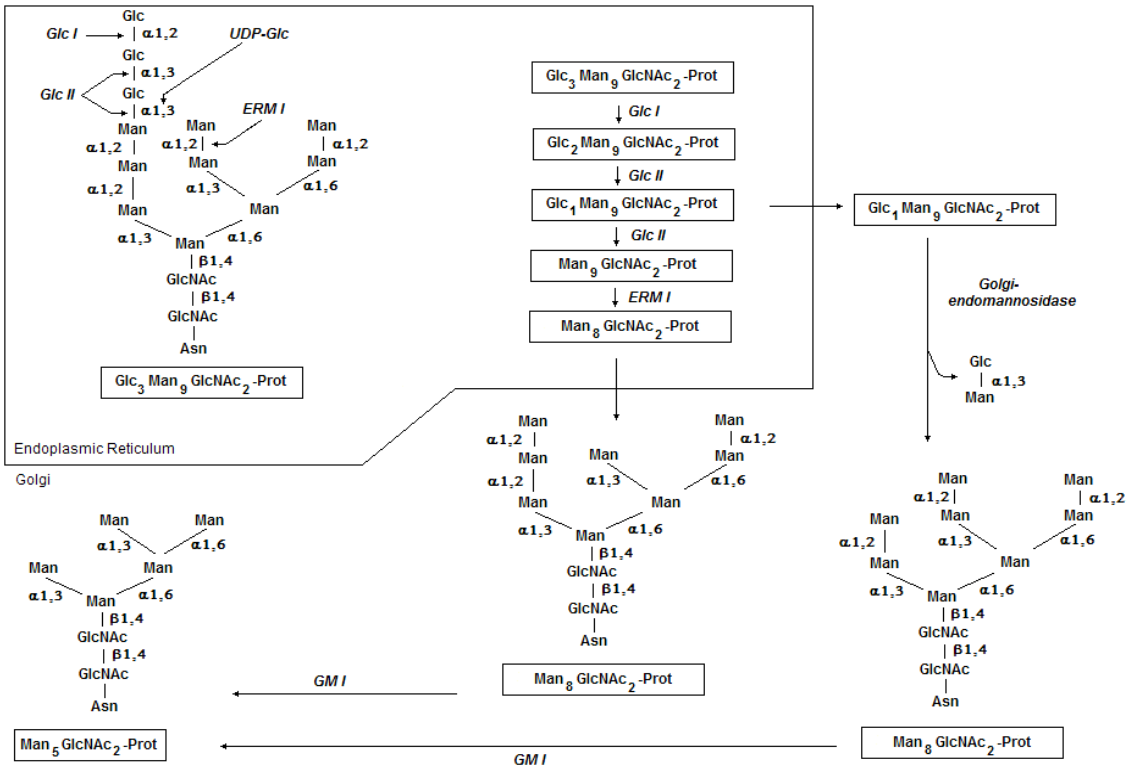

Figure 1.4: Detailed glycoprotein processing pathway (first part).

This oligosaccharide processing is predetermined, protein selective and cell-specific, but does not request a template as is necessary for the synthesis of DNA, RNA or proteins.

The newly synthesized glycoproteins are next transported to the *cis* Golgi cisternae by vesicles which are believed to bud from the ER and then fuse with the Golgi membrane [17]. This high mannose oligosaccharide can be further trimmed by Class I Golgi α1,2-mannosidase (GMI) to yield a $Man_5GlcNAc_2$-protein.

The hydrolytic steps in the maturation of *N*-glycans had originally been proposed to occur exclusively by the stepwise removal of single sugar residues (called in this introduction "traditional pathway"). But an alternative pathway has been identified due to the discovery of a processing endomannosidase which is able to cleave of an oligosaccharide (Glc3-1Man) from the $Glc_{3\text{-}1}Man_{9\text{-}4}GlcNAc_2$-protein to yield $Man_{8\text{-}}$

$_3$GlcNAc$_2$-protein [18]. The Man$_8$GlcNAc$_2$-protein chain formed by the action of this Golgi endomannosidase on Glc1Man$_9$GlcNAc$_2$-protein is distinct from the one detected *in vivo* following digestion of Man$_9$GlcNAc$_2$-protein by the ERMI (Fig. 1.4) [19]. *In vitro*, the Golgi endomannosidase has been shown to prefer the monoglucosylated oligosaccharides with the release of a α1,3-Glcα1,3-Man disaccharide [20], but has the capacity to process di- and tri-glucosylated species with the excision of Glc$_2$Man and Glc$_3$Man, respectively [21]. Afterwards, the Man$_8$GlcNAc$_2$-protein chain can further be trimmed by the GMI to yield the conventional Man$_5$GlcNAc$_2$-protein.

A second alternative route to the traditional pathway was discovered in GMII-*null* mice that developed a dyserythropoietic anemia. Cells from GMII-*null* mice, that lack the GMII activity, were found to accumulate hybrid and complex-type oligosaccharides. This finding indicates that complex oligosaccharides can be synthesized by a GMII-independent pathway, leading to the proposal of an alternative pathway and the prediction of a new α-mannosidase, designated α-mannosidase III (GMIII, Fig. 1.5). GMIII hydrolyzes two α-mannosyl residues in Man$_5$GlcNAc$_2$-protein and produces Man$_3$GlcNAc$_2$-protein which is further converted to the conventional GlcNAcMan$_3$GlcNAc$_2$-protein by GlcNAcTI [22]. This new mannosidase might be identical to the mannosidase discovered by Bonay and Hughes in rat liver [23].

A third alternative route to the traditional pathway was discovered when Fukuda *et al*., screened human-genomic and cDNA libraries by cross-hybridization with human GMII cDNA. They identified an α-mannosidase IIx that they called GMX [24]. This new enzyme composed of 1139 amino-acid residues presents 66% identity with the peptide sequence of GMII [25]. In the presence of GMX, Man$_6$GlcNAc$_2$-protein was converted to the corresponding Man$_4$GlcNAc$_2$-protein after removal of α1,6-Man and α1,3-Man residues (Fig 1.5) [26]. The proposed specificity of GMX is analogous to the action of GMII, which removes α1,6-Man and α1,3-Man residues from GlcNAcMan$_5$GlcNAc$_2$-protein. After removal of the two mannosyl residues by GMX, the substrate Man$_4$GlcNAc$_2$-protein was further converted to Man$_3$GlcNAc$_2$-protein by GMI, which is known to be a substrate for GlcNAcTI [27].

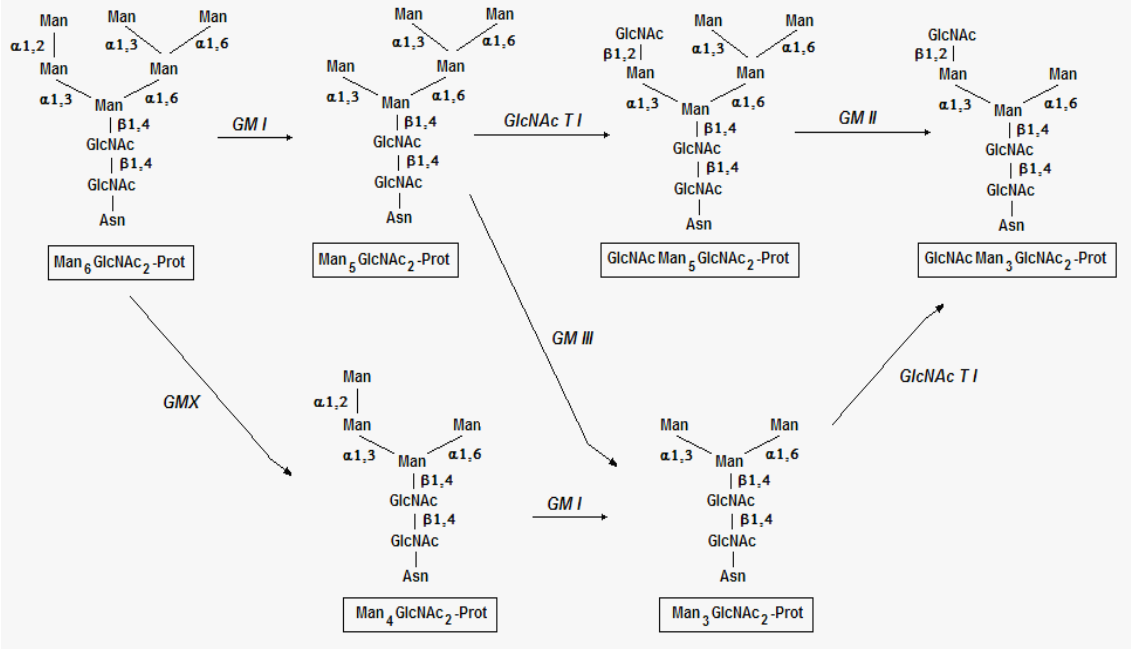

Figure 1.5: Detailed glycoprotein processing pathway (second part).

Glycosidases

Glycosidases play important roles in biological systems ranging from the degradation of polysaccharides to the manipulation of the structures of glycoconjugates at the surface of proteins. They are involved in biological processes such as the digestion, the biosynthesis of glycoproteins and the catabolism of glycoconjugates [28]. The glycosidic bond, between two glucosyl residues in cellulose or starch is one of the most stable linkage with a half-life for spontaneous hydrolysis being in the range of 5 million years. But hydrolysis carried out by enzyme is accomplished with rate constants up to $1000s^{-1}$, which make these enzymes some of the most efficient catalysts [29].

Classification of glycoside hydrolases, or glycosidases, based on amino acid sequences was first performed in the early 1990's [30]. It was determined that the 301 known glycoside hydrolases sequences could be grouped into 35 families. The substrate specificities and reaction mechanisms of the classified enzymes corresponded to their family placement. Currently, the carbohydrate-active enzyme database (CAZy;

www.cazy.org) has classified thousands of glycoside hydrolases into more than one hundred families [31]. The member enzymes of a given family come from a wide variety of organisms, but retain similarity in the types of reactions catalyzed, and the mechanism employed. This indicates that, despite the increase in sequence data, the classification scheme remains robust, as it has been validated by biochemical means.

Mechanism for enzymatic hydrolysis of glycosides

Basic mechanisms of the hydrolysis of interglycosidic bonds were proposed in 1953 by Kohsland [32]. Indeed, hydrolysis of the glycosidic bond can occur with one of two possible stereochemical outcomes: inversion or retention of anomeric configuration [33-35]. Both mechanisms involve oxocarbenium-ion like transition states and a pair of carboxylic acids in the active site of the enzyme.

With inverting β-glycosidases, as described by Kohsland, hydrolysis proceeds via a singlestep mechanism in which the sugar anomeric centre is attacked by a water molecule that acts as a nucleophile (Fig. 1.6). This reaction is catalysed by two carboxylic acid moieties both present in the active site. Deprotonation of the water molecule by the carboxylate enhances its nucleophilicity and allow it to attack the anomeric position. The glycosidic bond is cleaved and releases the alcohol which results in the inversion of the anomeric centre of the cleaved sugar.

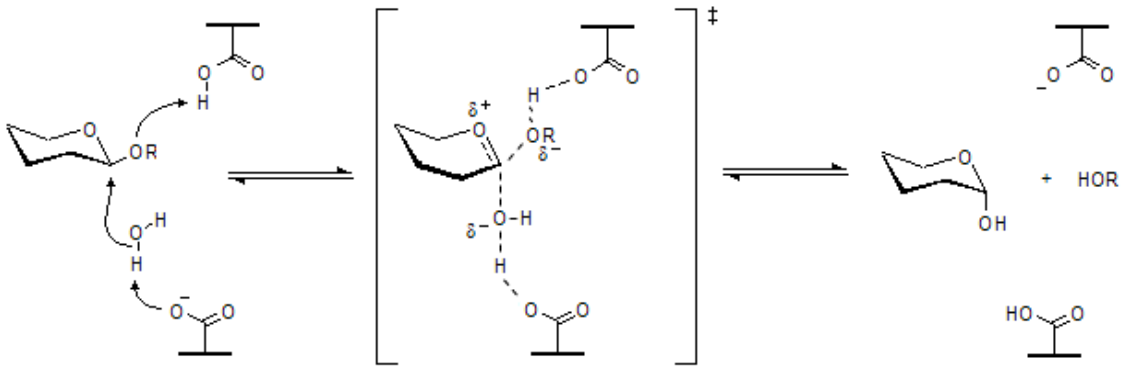

Figure 1.6: General mechanism of inverting β-glycosidases.

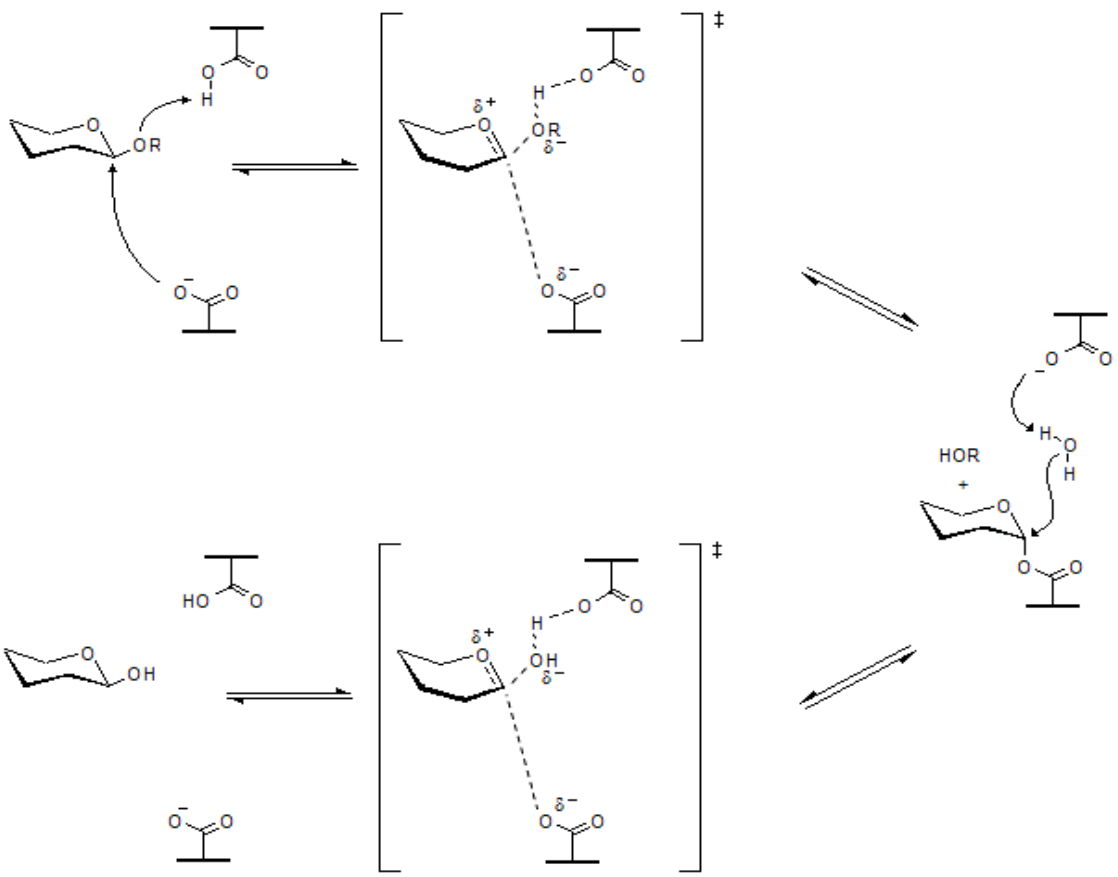

Figure 1.7: General mechanism of retaining β-glycosidases.

In contrast, retaining β-glycosidases proceed via a double-step mechanism (Fig. 1.7). The first carboxylate attacks the anomeric position and cleaves the glycosidic bond with release of an alcohol. A water molecule then attacks the remaining sugar which is bound to the first carboxylic acid. This step is catalysed by the second carboxylic acid which deprotonates the water molecule so enhancing its nucleophilicity. The reaction affords the cleaved sugar without inversion of the anomeric center [36].

Retaining and inverting β-glycosidases differ mainly by the distance separating the two carboxylic groups of the active site. This distance is around 5 Å in retaining enzymes and around 10 Å in inverting enzymes. The greater span found in inverters is necessary to accommodate the nucleophilic water molecule. The hydrolysis processes have been more

thoroughly studied for β-glycosidases. Nevertheless, it has been reported that α-glycosidases act through a similar pathway to β-glycosidases [37]. The mechanisms have been evidenced by the isolation of α-linked intermediates [38].

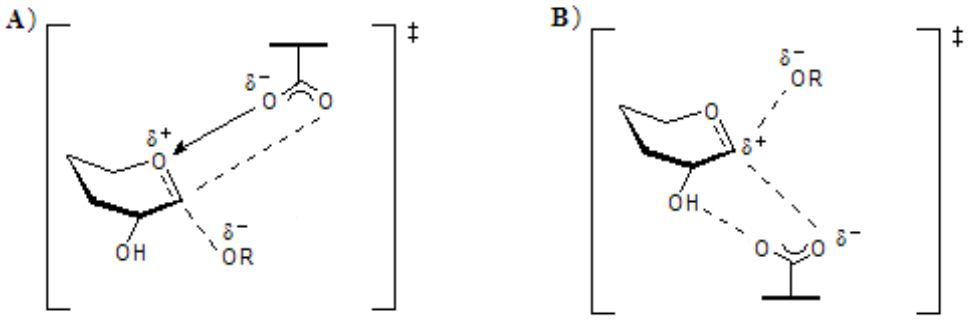

Figure 1.8: Comparison of the transition states for **A**) α- and **B**) β- retaining glycosidases.

However, subtle differences, between α- and β-glycosidases seem to exist in the oxocarbenium ion character of the transition state [33]. For β-glycosidases, the interactions involving the nucleophilic carboxyl oxygens, the anomeric center and the alcohol at C(2) position support delocalization of the positive charge on the anomeric carbon (Fig. 1.8B). On the other hand, for α-glycosidases, these interactions occur between the carboxyl oxygen, the endocyclic oxygen and the anomeric center resulting in the delocalization of the positive charge on the anomeric oxygen (Fig. 1.8A) [39].

Glycosidases as therapeutic targets

The post-translational glycosylation patterns of proteins in various cellular compartments determines not only the function, structure, physical and biochemical properties, but also the fate of a protein, such as retention in a determined cell compartment, secretion, degradation, insertion in the cell membranes or interactions with other molecules and binding to membrane receptor. Therefore, inhibition of the activity of selected enzymes involved in protein glycosylation, in particular in the latter phases of the biosynthesis, may alter the function of the target protein and its role in important biological processes. Glycosylation pathways as drug targets have remained relatively little studied until very

recently. Nevertheless, the specific inhibition of α-glucosidases and α-mannosidases involved in the trimming of glycoproteins represent promising therapeutic options.

In addition to natural inhibitors, the disclosure of the function of the active site of glycosidases involved in the biosynthesis of glycoproteins has led to the development of synthetic inhibitors.

Therapeutic applications of glycosidase inhibitors

Because enzyme-catalyzed carbohydrate hydrolysis is a biologically widespread process, glycosidase inhibitors have many potential applications as agrochemicals and as therapeutic agents. Inhibition of glycosidases in living material can have profound effects on the quality control, maturation, transport, and secretion of glycoproteins, and can alter cell-cell or cell- pathogens recognition processes suggesting potential use of glycosidase inhibitors against viral and bacterial infections and cancer [40].

Mannosidase

Mannosidases are Glycohydrolases involved in the processing of mannose containing glycans in vivo. They are involved in the maturation and degradation of glycoprotein-linked oligosaccharides. Use of natural substrates for specificity determination, antibodies from subcellular localization, specific enzymic inhibitors and mutant cell lines, has revealed the presence of different α-mannosidase isoenzymes. This suggests that α-mannosidases have multiple functions in glycoprotein metabolism [41].

Types

1. Alpha-Mannosidase [α-D-mannoside mannohydrolase]: are involved in hydrolysis of terminal α-D-mannose residues in α-D-mannosides.
   EC 3.2.1.24

2. Beta-Mannosidase [mannanase, mannase, β-mannoside mannohydrolase]: are involved in the hydrolysis of terminal non-reducing β-D-mannose residues in β-D-mannosides.
   EC 3.2.1.25

Classification of α-Mannosidase

There are two classes of processing α-mannosidase based on their distinctive substrate specificity, responses to inhibitors, cation requirements, protein molecular weights, subcellular localization, enzyme mechanisms and characteristic regions of conserved amino acid sequences [41-43]. There is significant correlation of biochemical and physiological roles of the various member genes for each of these two classes.

Table 1.1: Classification of α-mannosidases.

SL. No.	**Properties**	**Class I α-Mannosidase**	**Class II α-Mannosidase**
1	Substrate Specificity	α-1,2 mannoside linkages	α-1,2 α-1,3 and α-1,6 mannoside linkages
2	Artificial substrates (aryl mannosides)	Inactive	Active
3	Ca^{2+}	Required for activity	Not required for activity
4	Inhibition	1-deoxymannojirimycin (dMNJ) and Kifunensine (KF)	Swainsonine and 1,4-dideoxy-1,4-imino-D-mannitol (DIM)
5	Cleavage of glycosidic linkage	By Inversion of configuration of the released mannose [44,45]	By Retention of configuration of released mannose [46]
6	Glycohydrolase Family	47	38

Processing mannosidases are located in both the ER and Golgi of mammalian cells. The differential activity of Class II α-mannosidase towards artificial substrates has important practical ramifications. Because Class II enzymes are readily assayed with aryl mannosides, they are almost always employed for the initial screening of new potential inhibitors. Class I enzymes are not as easily assayed, so good inhibitors of these may be missed or incompletely characterized [41].

Class I α-mannosidases

Trimming of α1,2-linked mannose residues to form $Man_5GlcNAc_2$ in mammalian cells was originally attributed to a Golgi enzyme called α-mannosidase I [9]. It is now clear that, in addition to the ER enzymes, there are at least two Golgi α1,2-mannosidases in mammalian cells which are called Class IA and IB. Partial amino acid sequence information derived from purified enzymes was used for TR-PCR to isolate human [47], murine [48], and porcine [49] cDNAs encoding enzymes designated as α-mannosidase IA. Regions of conserved sequence were used to isolate murine and human Golgi α-mannosidase IB cDNAs by RT-PCR [50].

Mammalian α-mannosidase IA and IB are type II Ca^{2+}-dependent transmembrane enzymes. Their N-terminal transmembrane domain is flanked by a variable cytoplasmic domain of about 10-35 amino acids and a `stem region' that is not required for enzyme activity and is followed by a large C-terminal catalytic domain. These class-I α-mannosidases are inhibited by 1-deoxymannojirimycin and related compounds, but not by swainsonine. Although their N-terminal regions may differ, their catalytic domains have been conserved through eukaryotic evolution. Within the same species the catalytic domains of α-mannosidases IA and IB are about 65% identical in amino acid sequence while they are around 90% identical between mammalian species for each α-mannosidase IA and IB. The mammalian α-mannosidases exhibit about 35% amino acid identity with non-mammalian α1,2-mannosidases, including the yeast ER processing α-mannosidase.

Mammalian α-mannosidases IA and IB are derived from distinct genes. The murine and human α1,2-mannosidase IB genes span 60-80 kb of the genome, and consist of 13 exons with identical intron-exon structures [51,52].

The multiple Class I α-mannosidases found in *A. nidulans* [53] and *O. novo-ulmi* (Accession#: AF12945) also appear to have arisen from recent duplication events, in that these proteins are more similar to each other than to either of the mammalian Class I α-mannosidases. This is significant, because it suggests that the Class I α-mannosidase gene families in both lineages have independently undergone expansion and evolution through gene duplication and divergence.

Class II α-mannosidases

The second family of mannosidases, the Class II α-mannosidases are more diverse in their biochemical properties and physiological functions [41]. The majority of class II α-mannosidase enzymes that have been characterized, catalyze the degradation of Asn-linked oligosaccharides. This group of enzymes consists of three subfamilies of genes (Classes IIA, IIB and IIC) with distinct cellular functions. Enzymes of this class also have a wider range of cellular compartmentalization and can be localized to the cytosol and lysosomes in addition to the Golgi complex [54]. The Class IIA subfamily is involved in N-glycan synthesis in the Golgi, while the Class IIB and Class IIC are involved in N-glycan breakdown, removal and recycling in the cytoplasm, lysosome and vacuole. The first subfamily of Class II genes (Class IIA) are responsible for removal of α-1,3- and α-1,6-linked mannose residues from N-glycans during their synthesis (Fig. 1.9), a process which occurs in the higher eukaryotes, but does not occur in lower eukaryotes, such as fungi.

The second subfamily (Class IIB) is found in higher eukaryotes. These enzymes are involved in N-glycan degradation in the lysosome. The third subfamily (Class IIC) contains a more heterogeneous set of enzymes, with a diversity of functions and cellular localizations. Members of this family are found in higher and lower eukaryotes and are

likely involved in many aspects of N-glycan degradation and recycling. Sequence analysis clearly resolves the various inter-relationships of these proteins [55].

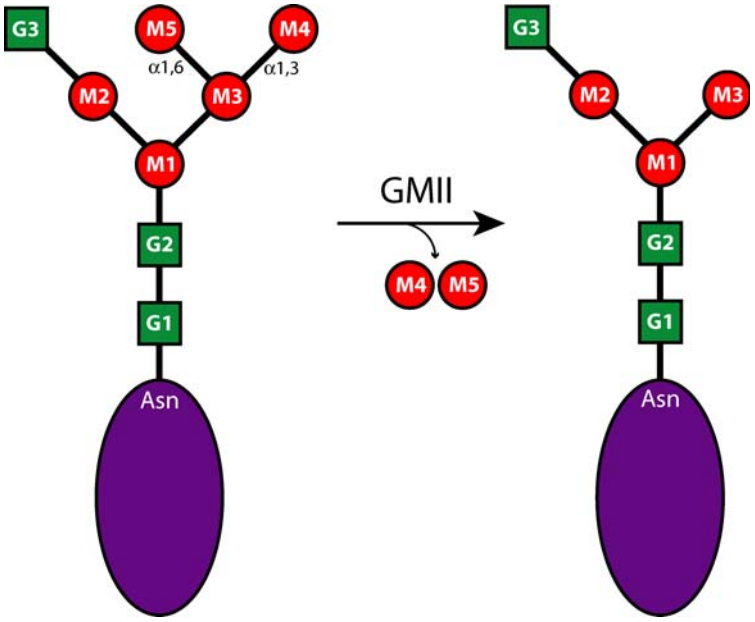

Figure 1.9: Golgi α-mannosidase II catalyzes the cleavage of two mannosyl linkages, an α1,3-linkage between M3 and M4 and an α1,6-linkage between M3 and M5, converting $GnMan_5Gn_2$to $GnMan_3Gn_2$. The reaction proceeds via a retaining mechanism and a glycosyl-enzyme intermediate.

The Class IIC subfamily has very low sequence similarity to the other two subfamilies. Phylogenetic analysis of the sequences shows that the Class IIA and Class IIB subfamilies have diverged more recently than the Class IIC subfamily. A likely scenario is that a single common ancestor was duplicated after the divergence of lower eukaryotes, such as fungi, from the higher eukaryotes. The lower eukaryotes thus only contain the orthologue of the common ancestor. Subsequent duplication in the higher eukaryotes led to the formation of the three subfamilies of Class II genes found in higher eukaryotes. These gene sequences diverged and evolved more specialized functions, such as the more

complex N-glycan pathways (Class IIA), and more efficient degradation pathways (Class IIB).

It is intriguing that the two classes of α-mannosidases have such similar and overlapping functions. The Class I genes and the Class IIA genes have complementary functions in the N-glycans synthesis pathway of higher eukaryotes. The other Class II genes have broad substrate specificities and are able to cleave α-1,2 (as well as α-1,3, and α-1,6) mannose linkages, a property it shares with the Class I genes. The Class I and Class II genes show no sequence similarity and appear to have originated independently and represent a classic case of convergent evolution [10].

Class III α-mannosidases

α-Mannosidases that can provide an alternative route independent of α-mannosidase II for the synthesis of complex N-glycans have been described in mammals like rat brain that lacks α-mannosidase II activity [56], in rat liver [23,57,58] and in several tissues of the α-mannosidase II knockout mice [22]. These enzymes can produce Man_3-$GlcNAc_2$ without the prior action of GlcNAc transferase I. The rat brain α-mannosidase cleaves $Man_{4-9}GlcNAc$ to $Man_3GlcNAc$ and is resistant to swainsonine and 1-deoxymannojirimycin. Unlike α-mannosidase II, it does not utilize p-nitrophenyl α-mannopyranoside. A Co^{2+}-dependent α-mannosidase that can trim $Man_{4-9}GlcNAc$ to $Man_3GlcNAc$ has been purified from rat liver [23,57,58]. It is relatively resistant to swainsonine and 1-deoxymannojirimycin. This enzyme was immunolocalized to the ER, Golgi and endosomes of rat liver. A Co^{2+}-dependent enzyme activity that trims $Man_5GlcNAc_2$ to $Man_3GlcNAc_2$ was found in tissues of the α-mannosidase II knock-out mice and called α-mannosidase III [22]. The α-mannosidase from lepidopteran insect cell line, Sf9 [59] is an integral membrane glycoprotein with type II topology. It can hydrolyze p-nitrophenyl α-D-mannopyranoside, ant it is inhibited by swainsonine. This enzyme is actually different form Golgi II α-mannosidase as its activity is stimulated by cobalt and it can hydrolyze various substrates containing terminal mannose residues but not $GlcNAcMan_5GlcNAc_2$. So this enzyme also has been designated as Sf9 α-mannosidase III (Sf9ManIII) and its functions in an alternate N-glycan processing

pathway in Sf9 cells [60]. The relationship between these various enzymes that can form $Man_3GlcNAc_2$ is not known, but they may be related to each other since they are all stabilized by Co^{2+}, as are the cytosolic enzymes. Additional work is required to establish the role of these enzymes in the processing pathway and their relationship to each other and to the product of the α-mannosidase IIx gene [61].

Endo α-mannosidase

There is an alternative pathway for trimming glucose residues from the oligosaccharide precursor (Fig. 1.4). A specific endo α-mannosidase purified from Golgi membrane fractions was discovered in Spiro's laboratory [43,62]. This enzyme is the only processing glycosidase that cleaves an internal glycosidic linkage, producing $Man_8GlcNAc_2$ isomer A from $Glc_{1-3}Man_9GlcNAc_2$. The endo α-mannosidase prefers monoglucosylated oligosaccharides as substrates, but it can cleave $Glc_{1-3}Man_{4-9}GlcNAc$ to yield $Man_{3-8}GlcNAc$ and $Glc_{1-3}Man$ in vitro. In contrast to α-glucosidases I and II, its activity is enhanced with glucosylated oligosaccharide substrates lacking mannose residues on adjacent branches of the oligosaccharide. Some evidence demonstrating endo α-mannosidase activity in vivo in the absence of an α-glucosidase blockade has been obtained [63], but the importance of the endo-mannosidase in glycoprotein maturation is cell-specific [64].

The enzyme has no divalent ion requirement, has a neutral pH optimum and is specifically inhibited by the disaccharides Glcα1,3-(1-deoxy)mannojirimycin and Glcα1,3-(1,2-dideoxy)mannose [65]. It has been purified by ligand affinity chromatography from rat liver Golgi membranes along with calreticulin [66]. A rat liver endo α-mannosidase cDNA has been isolated [67]. It encodes a 52 kDa protein with distinct levels of tissue-specific expression. There is no related protein found in the data base, consistent with the observation that its appearance is a relatively late event during eukaryotic evolution [68].

Inhibitors of α-mannosidases and their biological activities

Several alkaloids isolated from plants and microorganisms display inhibitory ability against α-mannosidases. For instance, 1-deoxymannonojirimycin (DMJ) was first isolated from the seeds of the legume *Lonchocarpus sericeus*, a native plant of the West Indies and tropical America [69] and was later isolated from the tropical *Omphalea diandra* and *Angylocalyx pynaertii*, [70] an edible vegetable growing in tropical African forest. In 1979, the discovery of DMJ revealed the second example after Nojirimyciin (NJ) of a sugar analogue, containing a nitrogen atom instead of an oxygen atom in the sugar ring. DMJ has been found to be a selective inhibitor of rat liver Golgi α-mannosidase I but did not affect ER α-mannosidase or Golgi α-mannosidase II. Nevertheless high concentrations of this compound are necessary for inhibition [71-73].

Mannostatins

Mannostatin A and B were discovered by Aoyagi and collaborators in 1989 and so named because of their highly potent inhibition of α- and β-mannosidase activities. They were isolated from the soil microorganism *Streptoverticillum verticillus* during screening of culture broths for mannosidase inhibitors [74]. Inhibition by mannostatin A and B of α-mannosidases prepared from epididymes of adult rats has been shown to be competitive. When tested on various glycosidases, Mannostatin A was inactive toward β-glucosidase, α- and β-galactosidase, β-mannosidase but was a potent inhibitor of jack bean α-mannosidase. Mannostatin A also proved to be an effective competitive inhibitor of the glycoprotein-processing enzyme α-mannosidase II but was inactive toward α-mannosidase I [75,76].

Kifunensine

Kifunensine, initially isolated from the culture broth of the actinomycete *Kitasatosporia kifunensine* 9482 [77], was reported to be a weak inhibitor of jack bean α-mannosidase but was a very potent and selective inhibitor of α-mannosidase I from mung bean seedlings. Studies with rat liver microsomes indicated that kifunensine selectively

inhibited Golgi α-mannosidase I but did not inhibit the ER mannosidase. Moreover, introduction of kifunensine in cells culture medium at 1 µg/ml or higher concentration resulted in the production of $Man_9GlcNAc_2$ chains rather than complex structures [78].

Swainsonine

Swainsonine, a polyhydroxylated indolizidine alkaloid, discovered in 1978 by Dorling *et al.*, [79] displayed reversible inhibition of class II α-mannosidases (lysosomal and Golgi α-mannosidases). Swainsonine was first isolated in Australia from the plant *Swainsona canescens* [80], which was toxic to livestock. Swainsonine has then been identified as the toxic principle of locoism, a syndrome developed by animals ingesting the locoweed infested species *Astragalus* and *Oxytropis* species [81], and more recently in the poisonous plant *Ipomea carnea* [82], and the fungus *Rhizoctonia leguminocola* [83].

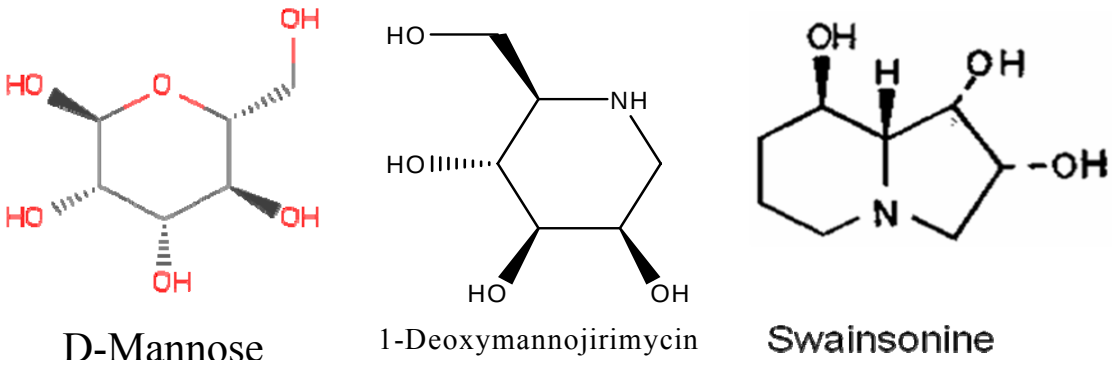

Figure 1.10: Structures of Mannose, 1-Deoxymannonojirimycin and Swainsonine.

The clinical signs of locoism include nervousness, aggression, hyperactivity, increasing misco-ordination, head tremors, loss of weight, reproductive alterations, weakness and death. These symptoms are attributed to lysosomal storage disease which is characterized by cytoplasmic vacuolation of cells of the central nervous system. However, purified Swainsonine alone is now known not to be neurotoxic, but loco syndrome may be caused

by ingestion of a combination of alkaloids found in *Swainsona canescens* or *Astragalus* [84].

Dorling *et al.*, recognized that the lysosomal storage disorder induced in animals grazing *Swainsona* species was biochemically and morphologically similar to the rare genetic mannosidosis that occurs in humans. This affection is characterized by accumulation in cells and excretion in urine of mannose-rich oligosaccharides, resulting from a deficiency of lysosomal α-mannosidase [85]. It has been found that Swainsonine concentrates and accumulates in lysosomes of normal human fibroblasts and human lymphoblasts in culture, since it is almost fully ionized within the acidic environment of this organelle [86,87].

Table 1.2: Swainsonine inhibition. IC_{50} toward various α-mannosidase enzymes.

IC_{50}	**Enzyme**
0.4-0.1 μM	α-mannosidase (jack bean)
70 nM	α-mannosidase (human liver lysosomal)
20 nM	α-mannosidase (rat lysosomal)
40 nM	α-mannosidase (human lysosomal)
n.i.	Golgi mannosidase I (rat liver)
200 nM	Golgi mannosidase II (rat liver)
160 nM	α-mannosidase (rat liver lysosomal)

n.i. = no inhibition

Such accumulation produces the inhibition of the intracellular lysosomal α-mannosidase which induces incomplete catabolism of the carbohydrate moiety of glycoproteins and storage of the remaining proteins which finally leads to disease as a consequence. It is assumed that this mode of action also occurs *in vivo*. Actually, Swainsonine provides a valuable tool for the study of human mannosidosis despite the fact it also inhibits Golgi α-mannosidase II [88,89].

Swainsonine was the first compound able to alter glycoprotein processing. It displayed inhibitory ability toward jack bean α-mannosidase, rat liver Golgi α-mannosidase II but was without effect on Golgi α-mannosidase I [90-92]. In addition, Swainsonine did not inhibit ER α-mannosidase or the soluble α-mannosidases of rat liver [93]. The selectivity of Swainsonine toward α-mannosidases was established against other glycosidases such as α-glucosidase, β-galactosidase and β-glucoronidase and lysosomal β-mannosidases [86]. The pKa of Swainsonine was determined to be 7.4 which mean that Swainsonine would be fully ionized at pH 4.0 [94]. Molecular modelling has shown that the relative positions of the cationic ammonium center and the three hydroxyl groups mimic an intermediate cationic structure of the hydrolysis mediated by α-mannosidases II and thus accounts for the apparent specificity of Swainsonine for α-mannosidases II [87].

The use of glycosidase inhibitors has recently appeared as a promising approach to treat cancers [95]. Transferases, α-glucosidases and α-mannosidases are the most relevant targets in the field of cancer for the development of cellular glycosidase inhibitors. Using Swainsonine, Humphries *et. al.*, tested the hypothesis that specific glycans structures are required for pulmonary colonization by tumor cells [96]. Furthermore, the addition of Swainsonine (2.5 μg/ml) to the drinking water of the mice further reduced the incidence of lung colonization by B16-F10 melanoma cells [97]. Since all cellular glycoproteins which normally express complex-type oligosaccharides are affected by Swainsonine treatment, investigations were carried out to determine whether the effects of Swainsonine on cellular proliferation could be widespread amongst non-transformed tissues in the body. These studies showed that the effects of this compound would appear to be cell specific, since it does not equally affect the processing of all glycoproteins [98]. Moreover, the systemic administration of high doses of Swainsonine to sheep induces mannosidosis [99,100]. However, no evidence of an over toxic reaction was observed when Swainsonine was administrated orally to rodents [101]. So it was considered that the mannosidosis induced by Swainsonine could be species- or tissue specific phenomena [102].

Synthetic Inhibitors

Several research groups have developed synthetic pathways to more complex sugar mimetics [103] hoping to achieve more potent inhibition against selected glycosidases. Some disaccharide mimics connecting 4-amino-4-deoxyerythrohtranose at C(1) to position C(3) of galactose through a CH(OH) link have been prepared as racemates and tested toward 25 commercially available glycohydrolases. One of them (**2**) is a moderate but specific (43% of inhibition at lmM) inhibitor of jack bean α-mannosidase [104]. Functionalized Pyrrolidines were shown to be inhibiting α-mannosidase activity and growth of Human Glioblastoma and Melanoma cells [105]. Mannostatin A analogue with a methoxyl instead of the methylthio, exhibited about 2-fold enhancement of the activity, indicating an importance for the methyl group rather than the sulfur atom [106]. A series of structurally related novel 7-membered iminocyclitols were synthesised and found to be inhibitors of α-mannosidase using in vitro assays. Few novel mannosidase inhibitors were used to probe the glycoprotein degradation pathway in cells [107].

Applications of α-mannosidase

Study of the biological function of glycoprotein glycans is rapidly emerging as a field of cell biology. α-Mannosidase (α-D-mannoside mannohydrolase, E.C. 3.2.1.24) is known to play an important role in the processing of mannose containing glycans *in vivo,* because a deficiency of the enzyme results in the lethal disease of mannosidosis, a hereditary disease reported in humans[108] and cattle [109].

- α-Mannosidases have been employed in the analysis of mannose containing glycans (e.g. high mannose-type sugar chains of glycoproteins) and glycolipids containing α linked mannoside residues [110].

- To elucidate the biological role and structures of the carbohydrate moieties of the mannoproteins, a highly specific α-mannosidase active on the polymannose component is required. Almond α-mannosidase as well as jack bean α-mannosidase have been used for analysis of sugar chain structures[111].

- Recombinant *Penicillium citrinum* α-1,2-mannosidase, expressed in *Aspergillus oryzae*, was employed to carry out regioselective synthesis of α-D-mannopyranosyl-(1→2)-d-mannose [112].

- Mannobioses and mannotrioses were synthesized by reverse hydrolysis using α-mannosidase from *Aspergillus niger* [113]. The synthesized oligosaccharides can potentially inhibit the adhesion of pathogens by acting as "decoys" of receptors of type-1 fimbriae carried by enterobacteria [112].

- The new invention provides means and strategies for treating the lysosomal storage disorder α-mannosidosis by enzyme replacement therapy. In particular, the reduction of stored neutral mannose-rich oligosaccharides takes place in cells within the central nervous system. Accordingly, the lysosomal α-mannosidase are used for the preparation of a medicament for reducing the intracellular levels of neutral mannose-rich oligosaccharides in cells within one or more regions of the central nervous system [114].

- Golgi α-mannosidase II is a target for inhibition of growth and metastasis of cancer cells. Golgi α-mannosidase inhibitor Swainsonine acts as anti-cancer agent [115].

- And also, α-mannosidase inhibitors and their analogs were utilized to design potential anti-HIV agents [116].

- It is essential for total hydrolysis of plant polysaccharides and may have application in pulp and paper industry in order to enhance the traditional chemical delignification [117].

- In plants, increased levels of mannosidase has been reported during the seed germination and fruit ripening [118]. Jagadeesh *et al.*, reported the increase in the activity of α-mannosidase in tomato during fruit ripening observed in the study is significant in the context of involvement of this enzyme in deglycosylation of glycoproteins resulting in release of free *N*-glycans. Free *N*-glycans (and hence *N*-glycoproteins) have a role in fruit ripening in tomato, where tunicamycin application to mature green fruit prevented both ripening and softening of the fruit [119].

Microbial α-Mannosidases

Microbial α-mannosidases are used in the analysis of glycopeptides and the developmental regulation of lysosomal enzymes.

The reports on production of α-mannosidases from bacteria include *Bacillus sp.* [120] *Acinetobacter*[121], *Arthrobacter* [122], *Flavobacterium dormitator* [123], and *Cellulomonas* [124], *Arcanobacterium haemolyticum* [125] alkaliphilic bacterium *Bacillus halodurans* [126] and *Escherichia coli* [127]. Protozoans are also known to produce α-mannosidase which is involved in the processing of high mannose oligosaccharides present in the processed proteins. Avila *et al.*, reported presence of 12 acid hydrolases including α-mannosidase from *Trypanosoma cruzi* [128] and characterization of neutral α-mannosidase from *Trypanosoma cruzi* [129] and *Trypanosoma rangeli* [130] has also been reported.

Aspergilli are the major producers, viz., *Aspergillus niger* [131,132], *Aspergillus saitoi* [133,134], *Aspergillus oryzae* [135,136], *Aspergillus* sp.,[137], *Aspergillus nidulans* [53], *Aspergillus flavus* [138] and reports concerning α-mannosidase from *Penicillium citrinum* [139], *Aspergillus fumigates* [140] and *Dictyostellium discoideum* [141] *Phellinus abietis* [142], *Trichoderma reesei* [143], *Neurospora crassa* [144] *are* also available. Among the yeasts, *Saccharomyces cerevisiae* [145] and *Candida albicans* [146] α-mannosidases are well studied.

***Aspergillus niger* α-mannosidase**

A highly purified preparation of 1,2-α-mannosidase was obtained from *Aspergillus niger* by using 2-0-α-D mannobiose as substrate. The enzyme shows a pH optimum of 4.8 and is stable in the pH range of 5.0 to 8.0. The K_m and V_{max} values for the enzyme are 2 mM and 1.3 μmoles per mg per min, respectively. The enzyme does not seem to be Zn^{++}-dependent and is inhibited only weakly by D-mannono - (l→5)-lactone. The enzyme is highly specific for 1,2-α-D-mannosidic bonds and therefore readily hydrolyzes 2-0-α-mannobiose and 2-0-α-mannotriose [131].

In another report, 100-fold purified preparation of *Aspergillus niger* α-mannosidase was obtained. The enzyme hydrolyzes specifically 1,4-α- and 1,6-α mannosidic bonds to the adjoining mannose or N-acetylglucosamine residues. Therefore, 4-O-α and 6-O-α-mannobioses and 2-acetamido-2-deoxy-4-0-α- and 6-O-α-glucoses are readily hydrolyzed. The enzyme, unlike other mannosidases, hydrolyzes p-nitrophenyl-α-D-mannopyranoside very slowly. It is inhibited strongly by D-mannono-(l→5)-lactone but does not appear to be Zn^{++}-dependent or inactivated by various chelating agents. The pH optimum for the enzyme is 4.2 [132].

***Aspergillus oryzae* α-mannosidase**

1,2-α-Mannosidase from *Aspergillus oryzae* was purified approximately 1,400-fold from an enzyme product. The α-(1→2)-linking mannose residues located at the nonreducing-ends of the substrates were selectively removed by the enzyme, whereas p-nitrophenyl α-D-mannopyranoside was completely stable to the enzyme. α-(1→2)-Linking mannose residues in intact bovine pancreatic ribonuclease B were also removed completely with the enzyme. The α-mannosidase was quite stable, and the activity was inhibited by D-mannono-gamma-lactone and by heavy metal ions, including zinc ions [135]. The enzyme purified by affinity chromatography with baker's yeast mannan gel as an adsorbent with yield of 22.9% was quite suitable for the structural analysis of glycoconjugates [147].

Table 1.2: **Properties of purified α-mannosidases from different fungal sp.**

Organism	Substrate specificity	Optimum pH	Optimum Tempt. ^{o}C	pI	Mr kDa
Aspergillus niger A	pNPM, l-4, l-6	4.8	45		
B	1-2	4.2	45		
Aspergillus saitoi II	l-3, l-6, l-2	5.0	30		
I	Yeast Mannan, 1-2	5.0	30	4.5	51
Aspergillus oryzae	1-2	4.9-5.3	37		49
A. nidulans II					118
A. fumigates IIC			37		124
Candida albicans	pNPM, 4-MUBαM	6.0	42		417
Trichoderma reesei	1-2, 1-3, 1-6, Yeast Mannan	6.5			160
Penicillium citrinum	Yeast Mannan, 1-2	5.0	50	4.6/ 4.7	53/54
Saccharomyces cerevisiae	pNPM, l-2, l-3, l-6	5.9-6.8			

***Aspergillus saitoi (Aspergillus phoenicis)* α-mannosidase**

The enzyme hydrolyzes yeast mannan partially but does not act on p-nitrophenyl α-mannopyranoside. The enzyme hydrolyzes Manα-(1→2)Man linkage but not Manα-(1→3)Man and Manα-(1→6) Man linkages at all. All Manα-(1→2) residues in intact bovine pancreatic ribonuclease B were removed completely by incubation with the α-mannosidase [148].

In another report, an α-mannosidase differing from 1,2-α-mannosidase was found in *Aspergillus saitoi*. In contrast to 1,2-α-mannosidase, the enzyme was strongly activated

by Ca^{2+} ions. p-Nitrophenyl α-mannopyranoside was not hydrolyzed by the enzyme. The enzyme cleaves the Manα-(1→3)Man linkage more than 10 times faster than the Manα-(1→6)Man and the Manα-(1→2)Man linkages [133]. 1,2α-D-Mannosidase from *Aspergillus saitoi was* inactivated by chemical modification using water-soluble carbodiimide (1-ethyl-3-(3-dimethylaminopropyl)carbodiimide) (EDC) and glycine ethyl ester (GEE). Kinetic analysis suggested one essential carboxyl group for its activity [149].

***Aspergillus nidulans* α-mannosidase**

A Class II α-mannosidase gene from the filamentous fungus *Aspergillus nidulans* was cloned and sequenced. A portion of the gene was amplified using degenerate oligonucleotide primers which were designed based on similarity between the *Saccharomyces cerevisiae* vacuolar and rat ER/cytosolic Class 2 protein sequences. The PCR amplification product was used to isolate the full length gene, and DNA sequencing revealed a 3383 bp coding region containing three introns. Although the cellular location of the *A. nidulans* mannosidase was not determined, experimental evidence suggested that it was located within a subcellular organelle. The Matchbox sequence similarity matrix indicated that the *A. nidulans* protein sequence was more highly similar to the rat ER/cytosolic and *S. cerevisiae* vacuolar α-mannosidases than the rat and yeast sequences were to each other [55].

Cloning and sequence characterization of three Class I α-1,2-mannosidase genes from the filamentous fungus *Aspergillus nidulans* was carried out. Coding regions of the genomic sequence were used to identify two additional members of the gene family by BLAST search of the *A. nidulans* EST sequencing database. Phylogenetic analysis suggests that the three *A. nidulans* Class I α-1,2-mannosidases arose from duplication events that occurred after the divergence of fungi from animals and insects [53].

***Aspergillus fumigatus* α-mannosidase**

The Afams1, a gene encoding a member of Class IIC α-mannosidases, was identified in the opportunistic pathogen *Aspergillus fumigatus*. To investigate effects of loss of function of the Af*ams1* gene in *A. fumigatus*, a null mutant was created by replacing a single copy of Af*ams1* with *pyrG*. As a result, two mutants were obtained. Deletion of the Afams1 led to a severe defect in conidial formation, especially at a higher temperature. In addition, abnormalities of polarity and septation were associated with the ΔAfams1 mutant. The results showed that the Afams1 gene, in contrast to its homolog in yeast or *A. nidulans*, was required for morphogenesis and cellular function in *A. fumigatus* [140].

***Candida albicans* α-mannosidase**

α-mannosidase from *C. albicans* has Molecular mass of 417 kDa. Optimum pH was 6.0 with 50 mM Mes-Tris when p-nitrophenyl-α-D-mannopyranoside was used as substrate. Optimum temperature was 42 ^{0}C with either 10 mM phosphate buffer (pH 6.8) or 50 mM Mes-Tris buffer (pH 6.0) and with 4-methylumbelliferyl-α-D-mannopyranoside as substrate. Apparent K_m values for p-nitrophenyl-α-D-mannopyranoside and 4-methylumbelliferyl-α-D-mannopyranoside were 3.3 mM and 0.1 mM, respectively. 1 mM 1-deoxymannojirimycin and 0.3 mM swainsonine inhibited the hydrolysis of 4-methylumbelliferyl-α-D-mannopyranoside by 67% and 83%, respectively, whereas that of p-nitrophenyl-α-D-mannopyranoside was only slightly diminished (10-15%) [150].

Other two soluble α-mannosidases, E-I and E-II, were purified from *C. albicans* yeast cells. E-I and E-II migrated as monomeric polypeptides of 54.3 and 93.3 kDa in SDS-PAGE, respectively. Hydrolysis of both substrates by either enzyme was optimum at pH 6.0 with 50 mM Mes-Tris buffer and at 42 ^{0}C. Swansonine and deoxymannojirimicin strongly inhibited the hydrolysis of 4-methylumbelliferyl-α-D-mannopyranoside by both enzymes. On the contrary, hydrolysis of p-nitrophenyl-α-D-mannopyranoside by E-I and E-II was slightly stimulated or not affected, respectively, by both inhibitors. E-I and E-II did not depend on metal ions although activity of the latter was slightly stimulated by $Mn^{2+}$and Ca^{2+}in the range of 0.5-2 mM. At the same concentrations, $Mg^{2+}$was slightly

inhibitory of both enzymes. Substrate specificity experiments revealed that both E-I and E-II preferentially cleaved alpha-1,6 and α-1,3 linkages, respectively [151].

The hydrolysis of $Man_{10}GlcNAc$ (M_{10}) by α-mannosidases from *Candida albicans* were studied. The results indicate that purified α-mannosidases participate in N-glycan processing in *C. albicans* [152].

***Trichoderma reesei* α-mannosidase**

The 160 kDa α-mannosidase (E.C. 3.2.1.24) isolated from culture filtrate of *Trichoderma reesei* showed wide aglycon specificity, cleaved the α1→2 and α1→ 3 mannosidic bonds with higher rate than α1→ 6 bond and slowly hydrolyzed yeast mannan and 1,6-α-mannan. The specific activity of the enzyme and rate constant in the reaction with p-nitrophenyl-α-D-mannopyranoside were 0.15 U/mg and 1.62 x 10^{-4} μM/min/μg, respectively, at optimal pH 6.5. In vitro, enzyme is able to cleave off 30% of total α-mannopyranosyl residues from N- and O-linked glycans of secreted glycoproteins. The activity of the α-mannosidase toward glycoproteins in vivo was studied comparing the structures of O- and N-linked glycans of glycoproteins isolated from the cultures growing with and without 1-deoxymannojirimycin, an inhibitor of α-mannosidases [153].

Structure of the *T. reesei* enzyme at 2.37 Å resolution was reported (Fig. 1.12). The enzyme folds as an $(\alpha\alpha)_7$ barrel. The substrate-binding site of the *T. reesei* mannosidase differs appreciably from the *Saccharomyces cerevisiae* enzyme. In the former, shorter loops at the surface allow substrate protein to come closer to the catalytic site. There is more internal space available, so that different oligosaccharide conformations are sterically allowed in the *T. reesei* α-1,2-mannosidase [143].

***Penicillium citrinum* α-mannosidase**

Properties of the enzyme:

Two isoforms of acidic 1,2-α-D-mannosidases were isolated from culture filtrate of *Penicillium citrinum*. The pI values of the two forms, designated 1,2-α-mannosidase Ia

and Ib, were 4.6 and 4.7 respectively. Isoenzymes Ia and Ib exhibited the same molecular mass which was determined to be 53 kDa by SDS/PAGE and 54 kDa by gel-permeation chromatography.

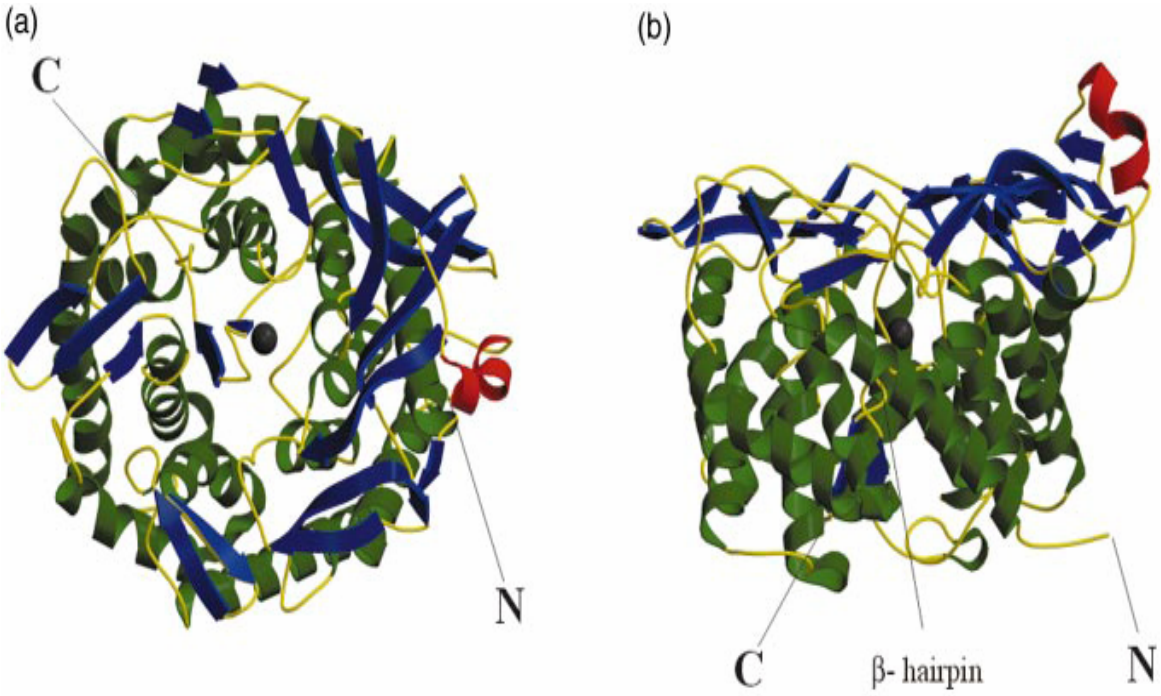

Figure 1.12: Overall structure of the *Trichoderma reesei* α-1,2-mannosidase. (a) Top view, and (b) side view of the (αα)7 barrel. β-Strands are shown in blue, and α-helices are shown in green. An extra α-helix at the substrate-binding site is represented in red.

Enzymes Ia and Ib hydrolysed yeast mannan and 1,2-α-linked mannooligosaccharides, but did not hydrolyse p-nitrophenyl α-D-mannoside. There was little difference between the enzymes with regard to their performance at acidic or alkaline pH. The N-terminal amino acid sequences of the two enzymes were identical. Analysis of C-terminal peptides, which were prepared by tryptic digestion and anhydrotrypsin-agarose chromatography, showed that Ia and Ib had the same amino acid sequences in the C-terminal region. Tryptic digestion revealed a slight difference between the isoenzymes in the pattern of cleaved peptides on SDS/PAGE [139].

Deducing the Active site residue:

1,2-α-D-Mannosidase from *Penicillium citrinum* was inactivated by chemical modification with EDC. 1-Deoxymannojirimycin (dMM), a competitive inhibitor of the enzyme, showed partial protection against the inactivation. After the modification by EDC without the presence of a nucleophile, proteolytic digests of the enzyme were analysed by reversed-phase h.p.l.c. and a unique peptide was shown to decrease when dMM was present during the modification. The peptide was absent from the digests of unmodified enzyme. The amino acid sequence of the peptide (A; Ile-Gly-Pro) was identical in part with that of the adjacent peptide (B; Ile-Gly-Pro-Asp-Ser-Trp-Gly-Trp-Asp-Pro-Lys). In the enzyme, peptide A was derived from peptide B by the modification. Consequently, Asp-4 in peptide B was assumed to be masked by dMM during the modification, and to be involved in the interaction of the enzyme with its substrate [154].

Three dimensional Structure:

The structure of the catalytic domain of the subgroup 2 (Class IB) α 1,2-mannosidase from *Penicillium citrinum* has been determined by molecular replacement at 2.2-A˚ resolution. The fungal α 1,2-mannosidase is an $(\alpha\alpha)_7$-helix barrel, very similar to the subgroup 1 yeast [155] and human [156] ER enzymes. Modeling studies of interactions between the yeast, human and fungal enzymes with different $Man_8GlcNAc_2$ isomers indicate that there is a greater degree of freedom to bind the oligosaccharide in the active site of the fungal enzyme than in the yeast and human ER α1,2-mannosidases [157].

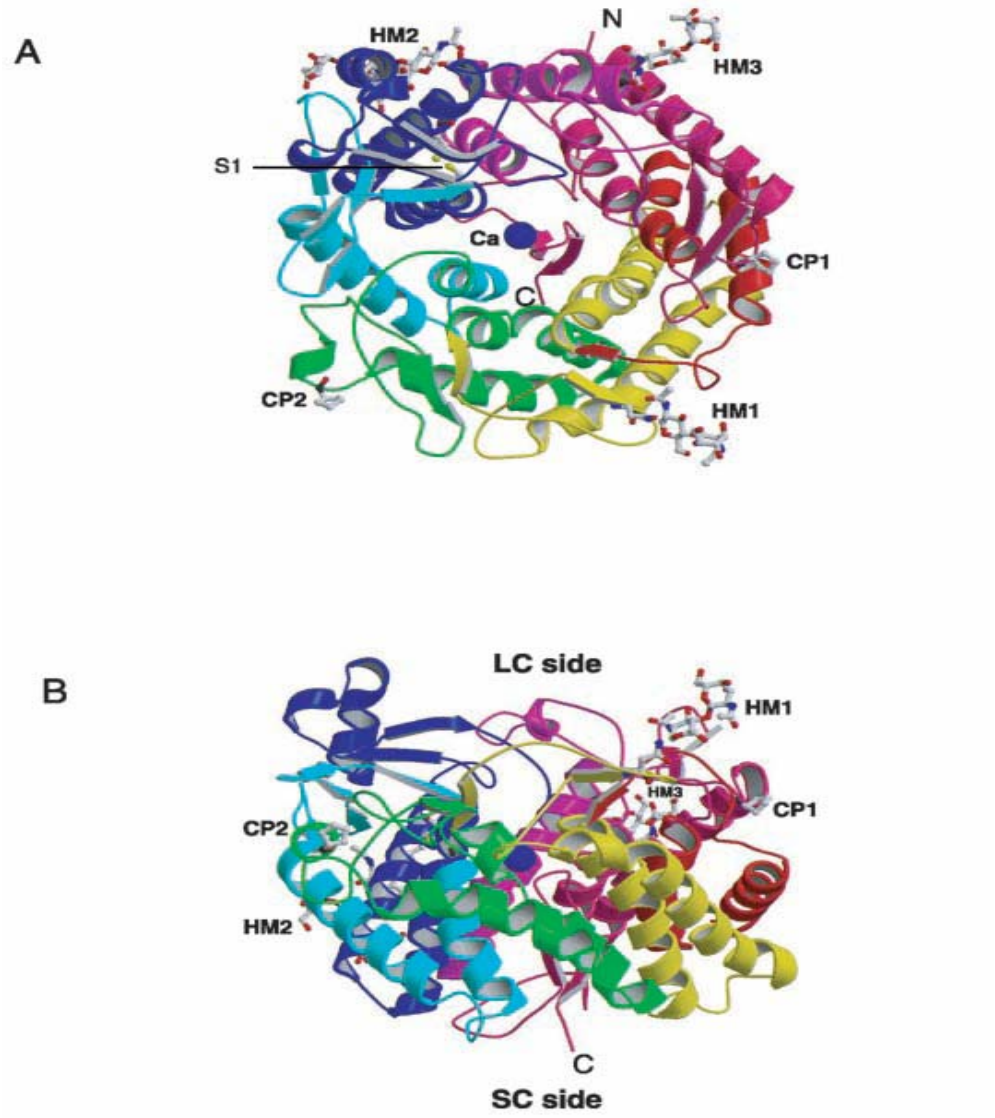

Figure 1.13: ***Penicillium citrinum* α1,2-mannosidase structure. A**, schematic ribbon representation of fungal α1,2-mannosidase viewed down the $(\alpha\alpha)_7$-barrel axis from the LC side. **B**, view at 90° orientation to **A**. In both **A** and **B**, the calcium ion is represented as a *blue sphere*, the three *N*-glycans (HM1, HM2, and HM3), the asparagine residues attached to these three *N*-glycans and one disulfide bridge (*S1*: Cys^{332}-Cys^{361}) are shown in *ball-and-stick* representation. The positions of the *cis*-prolines are indicated by the initials *CP1* and *CP2*.

***Saccharomyces cerevisiae* α-mannosidase**

There are several mannosidases reported from the yeast *Saccharomyces cerevisiae* and the enzyme from this organism is well studied in all respect including its role in N-glycosylation and structural analysis by crystallography.

The yeast α-mannosidase was purified to1160 fold. After the separation of yeast mannan during the purification procedures the enzyme became unstable but could be stored at 5 ^{0}C for three weeks with 50% loss of activity. The purified enzyme hydrolyzed both aryl and alkyl mannosides, but hydrolysis of yeast mannan proceeded slowly. The molecular weight was 450,000 Da by gel filtration [158].

Properties of the enzyme:

Two α-mannosidases from *Saccharomyces cerevisiae* were resolved and purified by X-2180 on Sepharose 6B. Fraction I which is excluded from the gel contains α-mannosidase activity toward both p-nitrophenyl-α-D-mannopyranoside and $Man_9GlcNAc$ oligosaccharide as substrates, whereas Fraction II which is included in the gel contains only oligosaccharide α-mannosidase activity. The latter enzyme is very specific and removes a single mannose residue from Man9GlcNAc, whereas the α-mannosidase activity of Fraction I removes several mannose residues from Man9GlcNAc oligosaccharide. This specific enzyme is most probably involved in processing of oligosaccharide during biosynthesis of mannoproteins. The mannose analog of 1-deoxynojirimycin (50-500 μM), dideoxy-1,5-imino-D-mannitol, inhibits the oligosaccharide α-mannosidase activities of Fractions I and II to about the same extent, but has no effect on the nonspecific α-mannosidase which acts on p-nitrophenyl-α-D-mannopyranoside [145].

Gene cloning and over expression:

The gene from *Saccharomyces cerevisiae* encoding an α-mannosidase of unique specificity has been isolated [159] which catalyzes the removal of one mannose residue from Man9GlcNAc to produce a single isomer of $Man_8GlcNAc$ [160]. Over expression

of the MNS1 gene caused an 8-10-fold increase in specific α-mannosidase activity. Disruption of the MNS1 gene resulted in undetectable specific α-mannosidase activity but no apparent effect on growth. These results demonstrate that MNS1 is the structural gene for the specific α-mannosidase and that its activity is not essential for viability [159]. The α-mannosidase encoded by MNS1 is the only enzyme responsible for mannose removal in vivo, and that this processing step is not essential for outer chain synthesis in *Saccharomyces cerevisiae* [161].

Active site and three dimensional structure:

Role of the cysteine residues in the α1,2-mannosidase involved in N-glycan biosynthesis in *Saccharomyces cerevisiae* has been revealed [162]. Kiran Dole reported the crystal structure of α1,2-mannosidase from *Saccharomyces cerevisiae* which catalyzing the conversion of $Man_9GlcNAc_2$ to $Man_8GlcNAc_2$ during the formation of N-linked oligosaccharides and is a member of the Class 1 α1,2-mannosidases conserved from yeast to mammals [163]. Vallee *et al.*, reported the crystal structure of another Class I α1,2-mannosidase that is involved in the N-glycan processing and ER quality control [155]. Ca^{2+} is shown to protect the enzyme from the thermal denaturation in *Saccharomyces cerevisiae* [164]. Active site determination of the an acidic 1,2-α-mannosidase enzyme expressed in *Saccharomyces cerevisiae* cells was performed by site-directed mutagenesis. Three glutamic acid residues, Glu-273, Glu-414, and Glu-474, are probably binding sites of the substrate [165].

Plant α-mannosidases

Several reports on α-mannosidases from plant sources are available and jack bean α-mannosidase is the most studied among for all of its characteristics.

Jack bean α-Mannosidase

An α-mannosidase which is able to hydrolyze a naturally occurring α-mannoside, yeast mannan, and several synthetic α-D-mannosides was isolated from jack bean meal. This

enzyme was used to explore the linkage of mannose in several glycoproteins. α-Mannosidase was purified approximately 500-fold from jack bean meal [166]. This enzyme was able to hydrolyze α-1,6, α-1, 2-, and α-1 ,3-linked oligomannosides. Approximately 5% of the total mannose present in the yeast mannan was set free by α-mannosidase after prolonged incubation. The fact that no sugars other than mannose were detected in the mannan digests indicates that this enzyme is not a polysaccharidase (endoenzyme) in nature. The enzyme hydrolyzes mannobiose, mannotriose, and mannotetraose derived from yeast mannan.

Metal ion requirement and inhibition:

α-Mannosidase from jack-bean meal is stabilized by Zn^{2+} addition during the purification. At pH values below neutrality, the enzyme undergoes reversible spontaneous inactivation. The enzyme is also subject to irreversible inactivation, which is prevented by the addition of albumin or by Zn^{2+}. Other cations, such as Co^{2+}, Cd^{2+} and Cu^{2+}, accelerate inactivation; an excess of Zn^{2+} again exerts a protective action, and so does EDTA in suitable concentration. It is postulated that α-mannosidase is a dissociable Zn^{2+}-protein complex in which Zn^{2+} is essential for enzyme activity [167]. The jack-bean α-mannosidase seems to exists naturally as a zinc-protein complex and may be considered as a metalloenzyme [168].

Other studies:

Jack bean α-mannosidase had a wide acceptor specificity and could transfer mannosyl residues to various acceptors such as D-fructose, L-arabinose, maltose, lactose, and sucrose [169]. The enzyme is a retaining Glycohydrolase. It was shown to be mechanistically similar to the lysosomal enzyme and would provide a useful model system in mechanistic studies and inhibitor design [170]. Two new mechanism-based inhibitors, 5-fluoro-α-D-mannosyl fluoride and 5-fluoro-β-L-gulosyl fluoride, which function by the steady state trapping of such an intermediate, were synthesized and tested. Both show high affinity and the latter has been used to label the active site nucleophile. Comparative liquid chromatographic/mass spectrometric analysis of peptic

digests of labeled and unlabeled enzyme samples confirmed the unique presence of this peptide of m/z 1180.5 in the labeled sample. They have shown presence of Aspartic acid residue at active site, contained within the peptide sequence Gly-Trp-Gln-Ile-Asp-Pro-Phe-Gly-His-Ser, which showed excellent sequence similarity with regions in mammalian lysosomal and Golgi α-mannosidase sequences, family 38 class II α-mannosidases in which the Asp in the above sequence is totally conserved [171]. Mechanism of inhibition of enzyme by swainsonine is also reported [172].

***Erythrina indica* α-mannosidase**

α-mannosidase from *Erythrina indica* seeds [173] is a Zn^{2+} dependent glycoprotein with 8.6% carbohydrate. The enzyme has energy of activation of the enzyme was found to be 23 kJ mol^{-1}. N-terminal sequence was deduced to be Asp, Thr, Gln, Glu, and Asn. Treatment of the enzyme with N-bromo succinimide (NBS) led to total loss of enzyme activity and modification of a single tryptophan residue led to inactivation. The enzyme exhibited immunological identity with α-mannosidase from *Canavalia ensiformis* but not with the same enzyme from Glycine max and *Cicer arietinum*. Incubation of *E. indica* seed lectin with α-mannosidase resulted in 35% increase in its activity. Lectin induced activation of α-mannosidase could be completely abolished in presence of lactose, a sugar specific for lectin [174].

Other sources of α-mannosidases include castor bean [175], mungbean hypocotyls [176], *Phaseolus vulgaris* [177], triticale seeds [178], *Capsicum annum* [179], papaya [180], watermelon fruit [181], pea seeds [182], Indian Lablab beans [183], soya bean [184] etc.

Animal α-mannosidases

Animal sources of α-mannosidase include humans, rat, bovine [185] and pig [186] which form very important source for the study of the enzyme widely. Apart from these, α-mannosidase has also been reported from monkey brain [187], murine [188], lepidopteran

insect [59,60], *Drosophila melanogaster* [189], Japanese Quail oviduct [190], calf liver [191], hen oviduct [192] etc.

In humans, cattle, cat and guinea pig, lack of lysosomal α-mannosidase activity causes the autosomal recessive disease called α-mannosidosis. Lysosomal α-mannosidase is a major exoglycosidase in the glycoprotein degradation pathway. Recently, great progress has been made in studying the enzyme and its deficiency. This includes cloning of the gene encoding the enzyme, characterization of mutations related to the disease, establishment of valuable animal models, and encouraging results from bone marrow transplantation experiments [193].

Human α-mannosidase

From humans, α-mannosidase (I and II) has been isolated from different parts like brain, kidney, liver, lysosomes, serum and cytosol. In a review by Daniel *et al.*, α-mannosidases were studied in detail with respect to their role in different parts of the body and classification into different groups [41]. They suggested two endoplasmic reticulum (ER) α-mannosidases, previously assigned with processing roles. They propose that the ER/cytosolic mannosidase is involved in the degradation of dolichol intermediates that are not needed for protein glycosylation, whereas the soluble form of Man_9-Mannosidase is responsible for the degradation of glycans on defective or malfolded proteins that are specifically retained and broken down in the ER.

Based on inhibitor studies with pyranose and furanose analogues, α-mannosidases may be divided into two groups. Those in Class 1 are (1—>2)-specific enzymes like Golgi mannosidase I, whereas those in Class 2, like lysosomal a-mannosidase, can hydrolyse (l→2), (l→3) and (l→6) linkages. Based on this classification of the α-mannosidases, it is possible to speculate about their probable evolution from two primordial genes. The first would have been a Class 1 ER enzyme involved in the degradation of glycans on incompletely assembled or malfolded glycoproteins. The second would have been a Class 2 lysosomal enzyme responsible for turnover. Later, other α-mannosidases, with new

processing or catabolic functions, would have developed from these, by loss or gain of critical insertion or retention sequences, to yield the full complement of a-mannosidases known today.

Human lysosomal mannosidase is a retaining glycosidase [170]. Cloning and expression of the human broad specificity lysosomal α-mannosidase has been done in *Pichia pastoris* [194]. A liver α-mannosidase has been purified and characterized [195]. The purified enzyme completely removed the α-linked non-reducing terminal mannose from a trisaccharide isolated from the urine of a patient with mannosidosis. The results validate the use of synthetic substrates for determining the mannosidosis genotype. There is also further evidence that mannosidosis is a lysosomal storage disease resulting from a deficiency of acidic α-mannosidase. Molecular cloning and expression of cDNAs encoding human α-mannosidase II has been reported [196].

Figure 1.14: Structure of Human Golgi α-Mannosidase II [197].

Studies on the biological roles of complex type N-glycans have employed a variety of strategies including the treatment of cells with glycosidase inhibitors, characterization of human patients with enzymatic defects in processing enzymes, and generation of mouse models for the enzyme deficiency by selective gene disruption approaches. Studies on Golgi mannosidase II have employed swainsonine, which causes "locoism", a phenocopy of the lysosomal storage disease. The human deficiency in Golgi mannosidase II is characterized by various abnormalities and complications. Mouse models for Golgi mannosidase II deficiency recapitulate many of the pathological features of the human disease and confirm that the unexpectedly mild effects of the enzyme deficiency result from a tissue-specific and glycoprotein substrate-specific alternate pathway for synthesis of complex N-glycans. In addition, the mutant mice develop symptoms of a systemic autoimmune disorder as a consequence of the altered glycosylation [198].

There are two liver acidic α-mannosidases (A and B) reported from humans [199]. α-mannosidase A and B are immunologically identical but they differ in their range of pI values and molecular masses. Suzuki *et al.*, reported a Class 2C1 α-mannosidase [200]. Its activity was enhanced by Co^{2+}, typical of other known cytosolic α-mannosidases so far characterized from animal cells.

Protein Folding

The process by which a linear polypeptide chain transforms into three-dimensional functional structure is known as protein folding. Defining mechanism governing folding remains a central point in biophysics and molecular biology. Each amino acid in the chain can be thought of having certain ‘gross’ chemical features. These may be hydrophobic, hydrophilic or electrically charged. These amino acids interact with each other and their surroundings in the cell to produce a well-defined, three dimensional shape of the folded protein, known as the native state. Protein can fold spontaneously into functionally active conformation under *in-vitro* condition as if folding code is encoded by primary sequence of proteins. Protein folding is a topic of fundamental interest since it

concerns the mechanisms by which linear information of genetic message is transformed into three dimensional and functional structure of proteins. Protein folding problem involves a number of related questions such as how does the given sequence find its specific native structure in a finite time among the astronomical number of possible conformations that a polypeptide could adopt? How is the folding process initiated and what is (are) the pathway (s) of folding? What is the physical basis of the stability of native conformations? Are the main rules of protein folding deduced from *in-vitro* studies valid for folding *in-vivo*? Existence of folding pathways has been suggested, on which protein molecule passes through well-defined partially structured intermediates [201-203].

Protein folding intermediates:

A number of equilibrium and kinetic studies have led to structural characterization of folding/unfolding intermediates, which is a prerequisite to solve the folding problem. Partially folded states are characterized at equilibrium under mildly denaturing conditions, such as by altering pH, addition of salts and alcohols, chemical denaturants such as urea and guanidine hydrochloride or by changing temperature and pressure. Equilibrium intermediates characterized in different proteins were found to be related to kinetic folding intermediate transiently populated in early phase of folding reaction. This partially folded state was termed 'molten globule' since it had shape with loosely collapsed hydrophobic core [204].

Molten globule is a compact intermediate with high content of native-like secondary structure but fluctuating tertiary structure [205,206]. It contains accessible hydrophobic surfaces which bind a hydrophobic dye, 1-anilinonaphthalene sulfonate (ANS). The absence of near UV circular dichroism spectrum shows that in this intermediate aromatic resides can rotate in a symmetrical environment. Sub-millisecond kinetic methods have improved resolution time of kinetic studies allowing detection of early events of folding. More recently, techniques such as hydrogen exchange NMR, solution X-ray scattering, protein engineering and site-directed mutagenesis have provided detailed picture of

molten globules of many proteins. The latest experimental techniques, which are used to characterize protein folding intermediates, have been described in Table 1.3. Also, theoretical approaches based on computer simulations to understand folding process have been developed.

The ultimate objective of such studies is to define complete energy landscape for the folding reaction and to understand in detail how this is defined by the sequence. Various studies have shown that molten globule (MG) state has heterogeneous structure in which one portion of molecule is more organized and native like while other portions being less organized [207]. How much native-like structure is present depends on protein species and solution conditions and a remarkable diversity in molten-globule structure of different proteins has been observed [208,209]. Thus, it will be useful to describe MG state and other partially folded states of different globular proteins so that we can see the features in common as well as differences among the different proteins.

Protein Folding and Biotechnology:

An intense research is focused to understand the structural basis of protein folding and stability and mechanistic role of early folding intermediates. Finding a solution to protein folding problem has many practical applications.

- ***Predicting structure of protein***

  A thorough understanding of the physical principles that govern folding of globular proteins is required for rational efforts to predict the three-dimensional structure of proteins. The methodologies used can be divided into three general categories: comparitive modeling, Fold recognition or threading and Ab-initio methods. These methods involve the development of an energy function capable of identifying the most stable conformation of a protein and a scoring function for the evaluation of protein models.

- ***Solving the protein aggregation problem***

  Protein aggregation *in vivo* is widespread phenomenon that arises from early folding intermediates through kinetic competition between proper folding and

misfolding. Wide range of human diseases results due to incorrect folding of proteins, thereby leading to deposition of aggregates or plaques. A list of some human diseases is presented in Table 1.4 that have been found to be a ramification of altered protein conformation. Possible treatment of these diseases could exploit detailed knowledge of protein folding and the prevention of abnormal folding.

Table 1.3: Experimental Techniques used to monitor protein folding.

Techniques	**Information about folding process**
Protein engineering	Role of individual amino acids in stability
Laser scattering	Radius of gyration
Gel filtration chromatography	Radius of gyration
DSC	Thermodynamics of folding process
Fluorescence spectroscopy	
a. Intrinsic	Environment and orientation of Trp
b. Polarization and anisotropy	Dynamics of fluorophore
c. FRET	Distance between two point in a protein
d. Quenching	Accessibility and environment of fluorophore
e. REES	Difference between environment fluorophore
f. Stopped flow	Time scale of fluorescence changes
g. Ligand binding	Formation of native structure at active site
Circular Dichroism (CD)	
a. Far-UV	Secondary structure
b. Near-UV	Tertiary structure
c. Stopped flow	Time for secondary and tertiary structure formation
Hydrogen exchange	
a. Native state exchange	Detection of metastable state
b. NMR	Rate of formation of backbone hydrogen bonds and protection form exchange of amino acid side chains
Real time NMR	Environment of protein side chain
Dynamic NMR	Detect equilibrium species
Laser temperature jump	Trigger folding /unfolding at nano seconds

- ***De novo designing***

  Important field of research dependent upon our understanding of protein folding is de novo protein designing for constructing completely new positions with determined function. Grado *et al*., [210] have reviewed the different methods for de novo protein design, which usually consist of choosing a function of protein followed by searching a proteins scaffold capable of supporting the reactive groups in desired geometry. It is then necessary to determine an amino acid sequence able to fold into an adequate and stable three-dimensional structure, done by either exploring genetic methods or by combinatorial and computational algorithms.

Table 1.4: Some protein misfolding diseases

Diseases	**Protein involved**	**Cause**
Crueltzfeldt-jacob	Prion protein	Toxic folding /aggregation
Alzheimer's	Beta-amyloid	Toxic folding/aggregation
Cystic fibrosis	CFTR	Misfolding
Cancer	Protein 53 (transcription factor)	Misfolding
Familial amyloid polyneuropathy	Apolipoprotein	Aggregation
Parkinson	Alpha-synuclein	Amyloid fibril formation
Huntington's	Huntington	Amyloid fibril formation
Familial visceral amyloidosis	Lysozyme	Aggregation
Cataract	Crystallins	Aggregation
Marfan syndrome	Fibrillin	Misfolding
Scurvy	Collagen	Misfolding
Osteigenesis imperfect	Type 1 procollagen	Misassembly
Amyotropic lateral sclerosis	Superoxide dismutase	Misfolding
Finish type familial amyloidosis	Gesolin	Amyloid fibril formation
Kelanddic cerebral angiopathy	Cystatin C	Amyloid fibril formation
Type II diabetes	Islet amyloid polypeptide	Amyloid fibril formation

Success in functionally-active designed polypeptide has been obtained in the field of catalysis, metal ion and heme binding, and introduction of cofactors. The successful design of a four-helix bundle protein that binds four heme groups with high affinity has been reported. It is clear that *de novo* protein design represents a growing field of research that will be useful both in testing the principles of protein folding and in offering the perspectives to design new proteins with practical applications for pharmaceuticals and diagnostics.

Present investigation

Literature survey of glycosylation and the novelty and importance of the α-mannosidases has been presented in this chapter. Our group at National Chemical Laboratory (Pune, India) is working in the area of carbohydrate-protein interactions, glycosidases and protein chemistry for last 20 years. Besides the physiological and therapeutic importance of the α-mannosidase, it also serves as an interesting model to study the conformation related function of the enzyme [137,211-213]. The present fungal culture *Aspergillus fischeri* was already screened and the enzyme was studied to some extent in our lab.

The objective of the present investigation was to isolate, purify with alternate protocol and further characterize α-mannosidase enzyme from *Aspergillus fischeri* (NCIM 508) and to study its structure-function relationship. Biochemical characterization like effect of metal ions, temperature and active site modification with specific chemical reagents was carried out. Substrate kinetic parameters were determined for both natural (mannobioses) and synthetic (aryl) substrates which provides vital information regarding subtle nature of specificity of the enzyme. The inhibition studies were carried out with swainsonine, 1-deoxymannojirimycin and synthetic substrate analogs such as polyhydroxy substituted piperidine derivatives. The tryptophan environment of the enzyme was studied in detail with steady state and time resolved fluorescence. Conformational stability and its correlation with activity were also determined for different chemical and physical chaotropes.

References:

[1] Landsteiner, K. (1931) *Science* **73**, 403-409.

[2] Alberts, B., Bray, D., Lewis, J., Raff, M., Roberts, K. and Watson, J.D. (1994) *Molecular Biology of the Cell*, 3rd edition, Garland Publishing.

[3] Rudd, P.M., Elliott, T., Cresswell, P., Wilson, I.A. and Dwek, R.A. (2001) *Carbohydrate and Glycobiology* **291**, 2370-2376.

[4] Dwek, R.A. (1996) *Chem Rev* **96**, 683-720.

[5] Drickamer, K. and Taylor, M.E. (1993) *Annu Rev Cell Biol* **9**, 237-264.

[6] Hart, G.W. (1992) *Curr Opin Cell Biol* **4**, 1017-1023.

[7] Varki, A. (1993) *Glycobiology* **3**, 97-130.

[8] Opdenakker, G., Rudd, P.M., Ponting, C.P. and Dwek, R.A. (1993) *FASEB J* **7**, 1330-1337.

[9] Kornfeld, R. and Kornfeld, S. (1985) *Annu Rev Biochem* **54**, 631-664.

[10] Eades, C.J. and Hintz, W.E. (2000) *Biotechnol Bioprocess Eng* **5**, 227-233.

[11] Herscovics, A. (1999) *Biochim Biophys Acta* **1426**, 275-285.

[12] Dean, N. (1999) *Biochem Biophys Acta* **1426**, 309-322.

[13] Gahmberg, C.G. and Tolvanen, M. (1996) *Trends Biochem Sci* **21**, 308-311.

[14] Helenius, A. and Aebi, M. (2004) *Ann Rev Biochem* **73**, 1019-1049.

[15] Burda, P. and Aebi, M. (1999) *Biochim Biophys Acta* **1426**, 239-257.

[16] Knauer, R. and Lehle, L. (1999) *Biochim Biophys Acta* **1426**, 259-273.

[17] Rothblatt, J., Novick, P. and Stevens, T. (1994) *Guidebook to the Secretory Pathway*, Oxford University Press.

[18] Lubas, W.A. and Spiro, R.G. (1988) *J Biol Chem* **263**, 3990-3998.

[19] Lubas, W.A. and Spiro, R.G. (1987) *J Biol Chem* **262**, 3775-3781.

[20] Fujimoto, K. and Kornfeld, R. (1991) *J Biol Chem* **266**, 3571-3578.

[21] Moore, S.E. and Spiro, R.G. (1990) *J Biol Chem* **265**, 13104-13112.

[22] Chui, D. et al. (1997) *Cell* **90**, 157-167.

[23] Bonay, P. and Hughes, R.C. (1991) *Eur J Biochem* **197**, 229-238.

[24] Misago, M., Liao, Y.F., Kudo, S., Eto, S., Mattei, M.G., Moremen, K.W. and Fukuda, M.N. (1995) *Proc Natl Acad Sci U S A* **92**, 11766-11770.

[25] Ogawa, R., Misago, M., Fukuda, M.N., Kudo, S., Tsukada, J., Morimoto, I. and Eto, S. (1996) *Eur J Biochem* **242**, 446-453.

[26] Oh-Eda, M., Nakagawa, H., Akama, T.O., Lowitz, K., Misago, M., Moremen, K.W. and Fukuda, M.N. (2001) *Eur J Biochem* **268**, 1280-1288.

[27] Nilsson, T. and Warren, G. (1994) *Curr Opin Cell Biol* **6**, 517-521.

[28] de Melo, E.B., da Silveira Gomes, A. and Carvalho, I. (2006) *Tetrahedron* **62**, 10277-10302.

[29] Wolfenden, R., Lu, X. and Young, G. (1998) *J Am Chem Soc* **120**, 6814-6815.

[30] Henrissat, B. (1991) *Biochem J* **280**, 309-316.

[31] Coutinho, P.M. and Henrissat, B. (1999) *in: Recent Advances in Carbohydrate Bioengineering*, The Royal Society of Chemistry, Cambridge, pp 3–12.

[32] Koshland, D.E. (1953) *Biol Rev* **28**, 416-436.

[33] Zechel, D.L. and Withers, S.G. (2000) *Acc Chem Res* **33**, 11-18.

[34] Withers, S.G. (2001) *Carb Polymers* **44**, 325-327.

[35] Sinnot, M.L. (1990) *Chem Rev* **90**, 1171-1202.

[36] Vasella, A., Davies, G.J. and Böhm, M. (2002) *Curr Opin Chem Biol* **6**, 619-629.

[37] McCarter, J.D. and Withers, S.G. (1996) *J Am Chem Soc* **118**, 241-242.

[38] Uitdehaag, J.C.M., Mosi, R., Kalk, K.H., van der Veen, B.A., Dijkhuisen, L., Withers, S.G. and Dijkstra, B.W. (1999) *Nat Struct Biol* **6**, 432-436.

[39] Heightman, T.D. and Vasella, A.T. (1999) *Angew Chem Int Ed Engl* **38**, 750-770.

[40] Asano, N. (2003) *Glycobiology* **13**, 93R-104R.

[41] Daniel, P.F., Winchester, B. and Warren, C.D. (1994) *Glycobiology* **4**, 551-556.

[42] Moremen, K.W., Trimble, R.B. and Herscovics, A. (1994) *Glycobiology* **4**, 113-125.

[43] Herscovics, A. (1999) *in: B.M. Pinto (Ed.), Comprehensive Natural Products Chemistry*, **3**, Elsevier, Amsterdam, pp.13-35.

[44] Lipari, F., Gour-Salin, B.J. and Herscovics, A. (1995) *Biochem Biophys Res Commun* **209**, 322-336.

[45] Lal, A., Pang, P., Kalelkar, S., Romero, P.A., Herscovics, A. and Moremen, K.W. (1998) *Glycobiology* **8**, 981-995.

[46] Howard, S., Braun, C., McCarter, J., Moremen, K.W., Liao, Y.F. and Withers, S.G. (1997) *Biochem Biophys Res Commun* **238**, 896-898.

[47] Bause, E., Bieberich, E., Rolfs, A., Volker, C. and Schmidt, B. (1993) *Eur J Biochem* **217**, 535-540.

[48] Lal, A., Schutzbach, J.S., Forsee, W.T., Neame, P.J. and Moremen, K.W. (1994) *J Biol Chem* **269**, 9872-9981.

[49] Bieberich, E., Treml, K., Volker, C., Rolfs, A., Kalz-Fuller, B. and Bause, E. (1997) *Eur J Biochem* **246**, 681-689.

[50] Camirand, A., Heysen, A., Grondin, B. and Herscovics, A. (1991) *J Biol Chem* **266**, 15120-15127.

[51] Tremblay, L.O., Campbell Dyke, N. and Herscovics, A. (1998) *Glycobiology* **8**, 585-595.

[52] Campbell Dyke, N., Athanassiadis, A. and Herscovics, A. (1997) *Genomics* **41**, 155-159.

[53] Eades, C.J. and Hintz, W.E. (2000) *Gene* **255**, 25-34.

[54] Gonzalez, D.S. and Jordan, I.K. (2000) *Mol Biol Evol* **17**, 292-300.

[55] Eades, C.J., Gilbert, A.M., Goodman, C.D. and Hintz, W.E. (1998) *Glycobiology* **8**, 17-33.

[56] Tulsiani, D.R. and Touster, O. (1985) *J Biol Chem* **260**, 13081-13087.

[57] Monis, E., Bonay, P. and Hughes, R.C. (1987) *Eur J Biochem* **168**, 287-294.

[58] Bonay, P., Roth, J. and Hughes, R.C. (1992) *Eur J Biochem* **205**, 399-407.

[59] Jarvis, D.L., Bohlmeyer, D.A., Liao, Y.F., Lomax, K.K., Merkle, R.K., Weinkauf, C. and Moremen, K.W. (1997) *Glycobiology* **7**, 113-127.

[60] Kawar, Z., Karaveg, K., Moremen, K.W. and Jarvis, D.L. (2001) *J Biol Chem* **276**, 16335-163340.

[61] Herscovics, A. (1999) *Biochim Biophys Acta* **1473**, 96-107.

[62] Spiro, R.G. (1994) *in: J. Rothblatt, P. Novick, T. Stevens (Eds.), Guidebook to the Secretory Pathway*, Sambrook and Tooze Publication, Oxford University Press, Oxford, pp. 188-189.

[63] Weng, S. and Spiro, R.G. (1996) *Glycobiology* **6**, 861-868.

[64] Karaivanova, V.K., Luan, P. and Spiro, R.G. (1998) *Glycobiology* **8**, 725-730.

[65] Hiraizumi, S., Spohr, U. and Spiro, R.G. (1993) *J Biol Chem* **268**, 9927-9935.

[66] Spiro, R.G., Zhu, Q., Bhoyroo, V. and Soling, H.D. (1996) *J Biol Chem* **271**, 11588-94.

[67] Spiro, M.J., Bhoyroo, V.D. and Spiro, R.G. (1997) *J Biol Chem* **272**, 29356-29363.

[68] Dairaku, K. and Spiro, R.G. (1997) *Glycobiology* **7**, 579-586.

[69] Fellows, L.E., Bell, E.A., Lynn, D.G., Pilkiewicz, F., Miura, I. and Nakanishi, K. (1979) *Chem Commun* **22**, 977-978.

[70] Molyneux, R.J., Pan, Y.T., Tropea, J.E., Elbein, A.D., Lawyer, C.H., Hughes, D.J. and Fleet, G.W. (1993) *J Nat Prod* **56**, 1356-1364.

[71] Fuhrmann, U., Bause, E., Legler, G. and Ploegh, H. (1984) *Nature* **307**, 755-758.

[72] Bischoff, J. and Kornfeld, R. (1984) *Biochem Biophys Res Commun* **125**, 324-331.

[73] Hardick, D.J., Hutchinson, D.W., Trew, S.J. and Wellington, E.M.H. (1992) *Tetrahedron* **48**, 6285-6296.

[74] Aoyagi, T., Yamamoto, T., Kojiri, K., Morishima, H., Nagai, M., Hamada, M., Takeuchi, T. and Umezawa, H. (1989) *J Antibiot (Tokyo)* **42**, 883-889.

[75] Tropea, J.E., Kaushal, G.P., Pastuszak, I., Mitchell, M., Aoyagi, T., Molyneux, R.J. and Elbein, A.D. (1990) *Biochemistry* **29**, 10062-10069.

[76] Berecibar, A., Grandjean, C. and Siriwardena, A. (1999) *Chem Rev* **99**, 799-844.

[77] Kayakiri, H., Takase, S., Shibata, T., Okamoto, M., Terano, H., Hashimoto, M., Tada, T. and Koda, S. (1989) *J Org Chem* **54**, 4015-4016.

[78] Elbein, A.D., Tropea, J.E., Mitchell, M. and Kaushal, G.P. (1990) *J Biol Chem* **265**, 15599-15605.

[79] Dorling, P.R., Huxtable, C.R. and Vogel, P. (1978) *Neuropathol Appl Neurobiol* **4**, 285-295.

[80] Colegate, S.M., Dorling, P.R. and Huxtable, C.R. (1979) *Aust J Chem* **32**, 2257-2264.

[81] Molyneux, R.J. and James, L.F. (1982) *Science* **216**, 190-1901.

[82] Haraguchi, M. et al. (2003) *J Agric Food Chem* **51**, 4995-5000.

[83] Schneider, M.J., Ungemach, F.S., Broquist, H.P. and Haris, T.M. (1983) *Tetrahedron* **39**, 29-32.

[84] Bowlin, T.L. and Sunkara, P.S. (1988) *Biochem Biophys Res Commun* **151**, 859-864.

[85] Jolly, R.D., Winchester, B.G., Gehler, J., Dorling, P.R. and Dawson, G. (1981) *J Appl Biochem* **3**, 273-291.

[86] Chotai, K., Jennings, C., Winchester, B. and Dorling, P. (1983) *J Cell Biochem* **21**, 107-117.

[87] Ikeda, K., Kato, A., Adachi, I., Haraguchi, M. and Asano, N. (2003) *J Agric Food Chem* **51**, 7642-7646.

[88] Cenci di Bello, I., Dorling, P. and Winchester, B. (1983) *Biochem J* **215**, 693-696.

[89] Watson, A.A., Fleet, G.W.J., Asano, N., Molyneux, R. and Nash, R. (2001) *J Phytochemistry* **56**, 265-295.

[90] Tulsiani, D.R., Harris, T.M. and Touster, O. (1982) *J Biol Chem* **257**, 7936-7939.

[91] Tulsiani, D.R., Broquist, H.P., James, L.F. and Touster, O. (1988) *Arch Biochem Biophys* **264**, 607-617.

[92] Cenci di Bello, I., Fleet, G., Namgoong, S.K., Tadano, K. and Winchester, B. (1989) *Biochem J* **259**, 855-861.

[93] Bischoff, J. and Kornfeld, R. (1986) *J Biol Chem* **261**, 4758-4765.

[94] Dorling, P.R., Huxtable, C.R. and Colegate, S.M. (1980) *Biochem J* **191**, 649-651.

[95] Humphries, M.J. and Olden, K. (1989) *Pharmac Ther* **44**, 85-105.

[96] Humphries, M.J., Matsumoto, K., White, S.L. and Olden, K. (1986) *Proc Natl Acad Sci U S A* **83**, 1752-1756.

[97] Dennis, J.W. (1986) *Cancer Res* **46**, 5131-5136.

[98] Spearman, M.A., Damen, J.E., Kolodka, T., Greenberg, A.H., Jamieson, J.C. and Wright, J.A. (1991) *Cancer Letters* **57**, 7-13.

[99] Huxtable, C.R. and Dorling, P.R. (1982) *Am J Pathol* **107**, 124-126.

[100] Huxtable, C.R., Dorling, P.R. and Walkley, S.U. (1982) *Acta Neuropathol* **58**, 27-33.

[101] Huxtable, C.R. and Dorling, P.R. (1985) *Acta Neuropathol* **68**, 68-73.

[102] Tulsiani, D.R. and Touster, O. (1987) *J Biol Chem* **262**, 6506-6514.

[103] Robina, I. and Vogel, P. (2005) *Synthesis* **5**, 675-702.

[104] Kraehenbuehl, K., Picasso, S. and Vogel, P. (1997) *Bio organic & Medicinal Chemistry Letters*, **7**, 893-896.

[105] Fiaux, H., Popowycz, F., Favre, S., Schutz, C., Vogel, P., Gerber-Lemaire, S. and Juillerat-Jeanneret, L. (2005) *J Med Chem* **48**, 4237-4246.

[106] Ogawa, S. and Morikawa, T. (2000) *Bioorg Med Chem Lett* **10**, 1047-1050.

[107] Butters, T.D., Alonzi, D.S., Kukushkin, N.V., Ren, Y. and Bleriot, Y. (2009) *Glycoconj J*, DOI 10.1007/s10719-009-9231-3.

[108] Ockerman, P.A. (1967) *Acta Paediatr Scand*, Suppl 177:35-6.

[109] Burditt, L.J., Phillips, N.C., Robinson, D., Winchester, B.G., Van-de-Water, N.S. and Jolly, R.D. (1978) *Biochem J* **175**, 1013-1022.

[110] Bischoff, J., Liscum, L. and Kornfeld, R. (1986) *J Biol Chem* **261**, 4766-4774.

[111] Misaki, R., Fujiyama, K., Yokoyama, H., Ido, Y., Miyauchi, K., Yoshida, T. and Seki, T. (2003) *Journal of Bioscience and Bioengineering* **96**, 187-192.

[112] Maitin, V., Athanasopoulos, V. and Rastall, R.A. (2004) *Appl Microbiol Biotechnol* **63**, 666-671.

[113] Ajisaka, K., Matsuo, I., Isomura, M., Fujimoto, H., Shirakabe, M. and Okawa, M. (1995) *Carbohydr Res* **270**, 123-130.

[114] http://www.freepatentsonline.com/WO2005094874.html.

[115] van den Elsen, J.M., Kuntz, D.A. and Rose, D.R. (2001) *EMBO J* **20**, 3008-3017.

[116] Winkler, D.A. and Holan, G. (1989) *J Med Chem* **32**, 2084-2089.

[117] Suurnakki, A., Tenkanen, M., Buchert, J., Viikari, L. (1997) Hemicellulases in the bleaching of chemical pulps. In: *Adv. Biochem. Eng./Biotechnol.* Scheper T. (Ed.) **57**, 261-287.

[118] Agrawal, K.M.L. and Bahl, O.P. (1968) *J Biol Chem* **243**, 103-111.

[119] Jagadeesh, B.H., Prabha, T.N. and Srinivasan, K. (2004) *Plant Science* **166**, 1451-1459.

[120] Nankai, H., Hashimoto, W. and Murata, K. (2002) *Appl Environ Microbiol* **68**, 2731-2736.

[121] Kathoda, S., Sawaya, Y., Asatsuma, K., Suzuki, F. and Hayashibe, M. (1977) *Agric Biol Chem* **41**, 331-337.

[122] Jones, G.H. and Ballou, C.E. (1969) *J Biol Chem* **244**, 1043-1051.

[123] Yamamoto, S. and Nagasaki, S. (1975) *Agric Biol Chem* **39**, 1981-1989.

[124] Takegawa, K., Miki, S., Jikibara, T. and Iwahara, S. (1989) *Biochim Biophys Acta* **991**, 431-437.

[125] Carlson, P. and Kontiainen, S. (1994) *J Clin Microbiol* **32**, 854-855.

[126] Takami, H. et al. (2000) *Nucleic Acids Res* **28**, 4317-4331.

[127] Sampaio, M.M., Chevance, F., Dippel, R., Eppler, T., Schlegel, A., Boos, W., Lu, Y.J. and Rock, C.O. (2004) *J Biol Chem* **279**, 5537-5548.

[128] Avila, J.L., Casanova, M.A., Avila, A. and Bretaña, A. (1979) *J Protozool* **26,** 304-311.

[129] Bonay, P. and Fresno, M. (1999) *Glycobiology* **9**, 423-433.

[130] Nok, A.J., Shuaibu, M.N., Kanbara, H. and Yanagi, T. (2000) *Parasitol Res* **86**, 923-928.

[131] Swaminathan, N., Matta, K.L., Donoso, L.A. and Bahl, O.P. (1972) *J Biol Chem* **247**, 1775-1779.

[132] Matta, K.L. and Bahl, O.P. (1972) *J Biol Chem* **247**, 1780-1787.

[133] Amano, J. and Kobata, A. (1986) *J Biochem* **99**, 1645-1654.

[134] Ichishima, E., Arai, M., Shigematsu, Y., Kumagai, H. and Sumida-Tanaka, R. (1981) *Biochim Biophys Acta* **658**, 45-53.

[135] Yamamoto, K., Hitomi, J., Kobatake, K. and Yamaguchi, H. (1982) *J Biochem* **91**, 1971-1979.

[136] Akao, T. et al. (2006) *Biosci Biotechnol Biochem* **70**, 471-479.

[137] Keskar, S.S., Gaikwad, S.M., Khire, J.M. and Khan, M.I. (1993) *Biotechnol Lett* **15**, 685-690.

[138] Augustin, J. and Sikl, D. (1978) *Folia Microbiol (Praha)* **23**, 349-350.

[139] Yoshida, T., Inoue, T. and Ichishima, E. (1993) *Biochem J* **290 (Pt 2)**, 349-354.

[140] Li, Y., Fang, W., Zhang, L., Ouyang, H., Zhou, H., Luo, Y. and Jin, C. (2009) *Glycobiology* **19**, 624-32.

[141] Schatzle, J., Bush, J. and Cardelli, J. (1992) *J Biol Chem* **267**, 4000-4007.

[142] Zouchova, Z., Kocourek, J. and Musilek, V. (1977) *Folia Microbiol (Praha)* **22**, 61-65.

[143] Petergem, V.F., Contreas, H., Contreas, R., Beeumen, V.J. (2001) *J Mol Biol* **312**, 157-165.

[144] Vaughn, L.E. and Davis, R.H. (1981) *Mol Cell Biol* **1**, 797-806.

[145] Jelinek-Kelly, S., Akiyama, T., Saunier, B., Tkacz, J.S. and Herscovics, A. (1985) *J Biol Chem* **260**, 2253-2257.

[146] Ana Bertha, V.R., Rozalia, B.O. and Arturo, F.C. (1993) *FEMS Microbial Lett* **106**, 321-325.

[147] Tanimoto, K., Nishimoto, T., Saitoh, F. and Yamaguchi, H. (1986) *J Biochem* **99**, 601-4.

[148] Yamashita, K., Ichishima, E., Arai, M. and Kobata, A. (1980) *Biochem Biophys Res Commun* **96**, 1335-42.

[149] Yoshida, T., Shimizu, S., Ichisima, E., . (1994) *Phytochemistry* **35**, 267-268.

[150] Vazquez-Reyna, A.B., Balcazar-Orozco, R. and Flores-Carreon, A. (1993) *FEMS Microbiol Lett* **106**, 321-5.

[151] Vazquez-Reyna, A.B., Ponce-Noyola, P., Calvo-Mendez, C., Lopez-Romero, E. and Flores-Carreon, A. (1999) *Glycobiology* **9**, 533-7.

[152] Vazquez-Reyna, A.B., Balcazar-Orozco, R., Calvo-Mendez, C., Lopez-Romero, E. and Flores-Carreon, A. (2000) *FEMS Microbiol Lett* **185**, 37-41.

[153] Eneyskaya, E.V., Kulminskaya, A.A., Savel'ev, A.N., Shabalin, K.A., Golubev, A.M. and Neustroev, K.N. (1998) *Biochem Biophys Res Commun* **245**, 43-49.

[154] Yoshida, T., Maeda, K., Kobayashi, M. and Ichishima, E. (1994) *Biochem J* **303 (Pt 1)**, 97-103.

[155] Vallee, F., Lipari, F., Yip, P., Sleno, B., Herscovics, A. and Howell, P.L. (2000) *EMBO J* **19**, 581-588.

[156] Vallee, F., Karaveg, K., Herscovics, A., Moremen, K.W. and Howell, P.L. (2000) *J Biol Chem* **275**, 41287-41298.

[157] Lobsanov, Y.D., Vallee, F., Imberty, A., Yoshida, T., Yip, P., Herscovics, A. and Howell, P.L. (2002) *J Biol Chem* **277**, 5620-56230.

[158] Kaya, T., Shibano, M. and Kutsumi, T. (1973) *J Biochem* **73**, 181-2.

[159] Camirand, A., Heysen, A., Grondin, B. and Herscovics, A. (1991) *J Biol Chem* **266**, 15120-15127.

[160] Jelinek-Kelly, S. and Herscovics, A. (1988) *J Biol Chem* **263**, 14757-14763.

[161] Puccia, R., Grondin, B. and Herscovics, A. (1993) *Biochem J* **290**, 21-26.

[162] Lipari, F. and Herscovics, A. (1996) *J Biol Chem* **271**, 27615-22.

[163] Dole, K., Lipari, F., Herscovics, A. and Howell, P.L. (1997) *J Struct Biol* **120**, 69-72.

[164] Lipari, F. and Herscovics, A. (1999) *Biochemistry* **38**, 1111-1118.

[165] Fujita, A., Yoshida, T. and Ichishima, E. (1997) *Biochem Biophys Res Commun* **238**, 779-83.

[166] Li, Y.T. (1967) *J Biol Chem* **242**, 5474-80.

[167] Snaith, S.M. and Levvy, G.A. (1968) *Biochem J* **110**, 663-70.

[168] Snaith, S.M. (1975) *Biochem J* **147**, 83-90.

[169] Hara, K., Fujita, K., Nakano, H., Kuwahara, N., Tanimoto, T., Hashimoto, H., Koizumi, K. and Kitahata, S. (1994) *Biosci Biotechnol Biochem* **58**, 60-3.

[170] Howard, S., Braun, C., McCarter, J., Moremen, K.W., Liao, Y.F. and Withers, S.G. (1997) *Biochem Biophys Res Commun* **238**, 896-8.

[171] Howard, S., He, S. and Withers, S.G. (1998) *J Biol Chem* **273**, 2067-72.

[172] Kang, M.S. and Elbein, A.D. (1983) *Plant Physiol* **71**, 551-554.

[173] Kestwal, R.M. and Bhide, S.V. (2005) *Indian J Biochem Biophys* **42**, 159-160.

[174] Kestwal, R.M., Konozy, E.H., Hsiao, C.D., Roque-Barreira, M.C. and Bhide, S.V. (2007) *Biochim Biophys Acta* **1770**, 24-8.

[175] Kimura, Y., Yamaguchi, O., Suehisa, H. and Takagi, S. (1991) *Biochim Biophys Acta* **1075**, 6-11.

[176] Forsee, W.T. (1985) *Arch Biochem Biophys* **242**, 48-57.

[177] Paus, E. (1976) *FEBS Lett* **72**, 39-42.

[178] Subha Mahadevi, A., Vegiraju Suryanarayana, R. and Siva Kumar, N. (2002) *J Biochem Mol Biol Biophys* **6**, 397-400.

[179] Sethu, K.M.P. and Prabha, T.N. (1997) *Phytochemistry* **44**, 383-387.

[180] Ohtana, K. and Akira, M. (1983) *Agric Biol Chem* **47**, 2441-2451.

[181] Nakagawa, H., Noriyuki, E., Makio, A. and Uda, Y. (1988) *Agric Biol Chem* **52**, 2223-2230.

[182] Krishna, T.G. and Murray, D.R. (1990) *J Plant Physiol* **135**, 618-622.

[183] Tulasi, R.B. and Nadimpalli, S.K. (1997) *Biochem Mol Biol Int* **41**, 925-31.

[184] Kimura, Y. and Kitahara, E. (2000) *Biosci Biotechnol Biochem* **64**, 1847-55.

[185] Heikinheimo, P. et al. (2003) *J Mol Biol* **327**, 631-44.

[186] Bause, E., Breuer, W., Schweden, J., Roeser, R. and Geyer, R. (1992) *Eur J Biochem* **208**, 451-7.

[187] Mathur, R., Alvares, K. and Balasubramanian, A.S. (1984) *Biochem Biophys Res Commun* **123**, 1185-93.

[188] Merkle, R.K., Zhang, Y., Ruest, P.J., Lal, A., Liao, Y.F. and Moremen, K.W. (1997) *Biochim Biophys Acta* **1336**, 132-46.

[189] Numao, S., Kuntz, D.A., Withers, S.G. and Rose, D.R. (2003) *J Biol Chem* **278**, 48074-48083.

[190] Oku, H., Hase, S. and Ikenaka, T. (1991) *J Biochem* **110**, 29-34.

[191] Schweden, J., Legler, G. and Bause, E. (1986) *Eur J Biochem* **157**, 563-570.

[192] Yamashiro, K., Itoh, H., Yamagishi, M., Natsuka, S., Mega, T. and Hase, S. (1997) *J Biochem* **122**, 1174-81.

[193] Sun, H. and Wolfe, J.H. (2001) *Exp Mol Med* **33**, 1-7.

[194] Liao, Y.F., Lal, A. and Moremen, K.W. (1996) *J Biol Chem* **271**, 28348-58.

[195] Phillips, N.C., Robinson, D. and Winchester, B.G. (1976) *Biochem J* **153**, 579-87.

[196] Misago, M., Liao, Y.F., Kudo, S., Eto, S., Mattei, M.G., Moremen, K.W. and Fukuda, M.N. (1995) *Proc Natl Acad Sci U S A* **92**, 11766-70.

[197] Fiaux, H., Kuntz, D.A., Hoffman, D., Janzer, R.C., Gerber-Lemaire, S., Rose, D.R. and Juillerat-Jeanneret, L. (2008) *Bioorg Med Chem* **16**, 7337-7346.

[198] Moremen, K.W. (2002) *Biochim Biophys Acta* **1573**, 225-35.

[199] Cheng, S.H., Malcolm, S., Pemble, S. and Winchester, B. (1986) *Biochem J* **233**, 65-72.

[200] Suzuki, T., Hara, I., Nakano, M., Shigeta, M., Nakagawa, T., Kondo, A., Funakoshi, Y. and Taniguchi, N. (2006) *Biochem J* **400**, 33-41.

[201] Oas, T.G. and Kim, P.S. (1988) *Nature* **336**, 42-48.

[202] Feng, H., Zhou, Z. and Bai, Y. (2005) *PNAS, United States of America* **102**, 5026-5031.

[203] Simmons, D.A. and Konermann, L. (2002) *Biochemistry* **41**, 1906-1914.

[204] Kuwajima, K. (1989) *Proteins: Structure, Function, and Genetics* **6**, 87-103.

[205] Dolgikh, D.A., Gilmanshin, R.I., Brazhnikov, E.V., Bychkova, V.E., Semisotnov, G.V., Venyaminov, S.Y. and Ptitsyn, O.B. (1981) *FEBS Letters* **136**, 311-315.

[206] Ptitsyn, O.B. (1987) *J Protein Chem* **6**, 277-293.

[207] Arai, M., Kuwajima, K. (2000) *Adv Protein Chem* **53**, 209-271.

[208] Haq, S.K., Rasheedi, S. and Khan, R.H. (2002) *European Journal of Biochemistry* **269**, 47-52.

[209] Privalov, P.L. (1996) *Journal of Molecular Biology* **258**, 707-725.

[210] DeGrado, W.F., Wasserman, Z.R. and Lear, J.D. (1989) *Science* **243**, 622-628.

[211] Keskar, S.S., Gaikwad, S.M., Khan, M.I. . (1996) *Enz Micro Tech* **18**, 602-604.

[212] Gaikwad, S.M., Keskar, S.S. and Khan, M.I. (1995) *Biochim Biophys Acta* **1250**, 144-8.

[213] Sushama, M.G., M. Islam, Khan and Sulbha, S. Keskar. (1997) *Biotechnology and Applied Biochemistry* **25**, 105-108.

CHAPTER: 2

BIOCHEMICAL CHARACTERIZATION OF α-MANNOSIDASE

Summary: Production of α-mannosidase enzyme from the fungus *Aspergillus fischeri* was carried out in shake flasks by growing the organism in a yeast extract containing medium for seven days. The enzyme was purified to homogeneity using following steps. (i) Ammonium sulfate precipitation (90%) (ii) Ion exchange chromatography on DEAE-Sepharose (iii) Preparative Gel Electrophoresis (5%) with final yield of 2.5 mg from 1 litter of culture broth. The activity staining of the enzyme in the gel after PAGE was standardized. The enzyme showed fluorescent bands at different stages of purification in activity staining of non-denaturing gel with fluorescent substrate 4-methylumbelliferil α-D-Mannopyranoside. Amino acid analysis of the protein revealed 18.43% hydrophobic amino acids, 16.00% (AsX + GlX) amino acids, 17.5% basic amino acids and 20.59% Glycine composition in α-mannosidase. Among the metal ions checked, Cu^{++} (K_i = 21nM) and Se^{++} ions (K_i =32 μM) showed noncompetitive and Co^{++} (K_i = 1.195 mM) showed competitive inhibition of the enzyme activity with insignificant change in the secondary structure of the protein. These studies exhibit the potential of the enzyme in studying the effect of anticancer drugs. The pH activity profile of the enzyme revealed the participation of two ionizable groups with a pKa of pH 5.75 and 7.84 indicating involvement of carboxylic group and Histidine/Cysteine at active site, respectively. Treatment of the enzyme with group specific reagents showed the presence of carboxylate, Arg and Cys at the active site. Substrate protection studies and kinetics of the modified enzyme confirmed the above results. Trp and His at the active site were observed to be in proximity.

Introduction:

There has been widespread interest in α-mannosidase in recent years, largely due to the vital role of the enzyme in number of biological systems and hence the potential as a therapeutic target. In particular, mammalian Golgi mannosidase-II is involved in glycoprotein biosynthesis and is currently an important therapeutic target for the development of anticancer agents [1]. Microbial α-mannosidases have been studied widely [2]. The enzyme is also essential for total hydrolysis of plant polysaccharides and may have application in pulp and paper industry in order to enhance the

traditional chemical delignification [3]. The use of alpha-mannosidase and related enzymes in the synthesis of oligosaccharides for medical and other purpose is also interesting [4]. During last ten years several reports on fungal α-mannosidases have been published [5-11]. The basic understanding of the active site of the enzyme and the mechanism of its inactivation are essential for studying structure-function relationship of the enzyme. X-ray crystallography gives the clear picture of spatial arrangement of essential amino acid residues. However, protein crystallography has its limitations such as difficulties in obtaining pure crystals which will diffract at higher resolution and the amount of pure protein available for the crystallization. Other than site directed mutagenesis, chemical modification is an alternative method which provides reasonably reliable information about the residues involved in the saccharide binding.

The inhibition of enzyme by metal ions is of considerable importance and has been studied extensively. Metal ions such as copper and zinc ions are physiologically important ions, and play a crucial role in many biological functions. Some Metal ions such as zinc, nickel and vanadium are reported to be helpful in the therapy of diabetes[12].

The α-mannosidase from *Aspergillus fischeri* has already been characterized partially [13,14]. The enzyme is a hexamer with molecular weight of 420 kDa for native protein and 69200 Da for each subunit. It has PI of 4.5, with optimum temperature between 50 - 55 ^{0}C and optimum pH of 6.0 to 6.5. It is a glycoprotein with 3.8% of carbohydrate content. In this chapter, we report the modified method of purification and further characterization of the α-mannosidase for its active site, amino acid analysis and effect of metal ions.

Materials and Methods:

Production of α-Mannosidase from *Aspergillus fischeri*

The seven days old fungi grown on the Potato Dextrose Agar (PDA) slants were inoculated in to medium containing $MgSO_4$ (0.1%), $(NH_4)_2SO_4$ (0.1%), KH_2PO_4 (0.2%) and Yeast Extract Powder (2%), grown for two days as starter culture. Starter

culture was inoculated in to 100 ml of medium in 500ml flasks and grown at 28 ^{0}C, at 180 rpm on shaker for seven days. The culture was harvested after seven days and filtered through muslin cloth to separate broth from mycelium.

Purification of the Enzyme

The α-Mannosidase from *Aspergillus fischeri* was purified by following procedures. The filtered culture broth was concentrated to one third of its volume by passing through 30,000da cut off Ultra Filtration membrane. The concentrated enzyme was salt precipitated using ammonium sulfate till 90% saturation by gently stirring and adding salt at 4 ^{0}C. The precipitate was collected by centrifugation at 10,000 rpm for 20 minutes and redissolved in phosphate buffer 10mM, pH 6.5 and extensively dialyzed against the same buffer.

The enzyme after the ammonium sulfate precipitation and dialysis was loaded on to the DEAE-Sepharose, an Anion Exchange matrix, which was equilibrated with 10mM phosphate buffer (PB), pH6.5 at a constant flow rate of 20ml/hr. The column was washed with the same buffer to remove unbound and excess proteins, till the O.D. at 280 drops down to 0.02. 100mM NaCl in 10mM PB, pH 6.5 was passed through the column, fractions were collected and activity was checked. 200 mM NaCl in 10 mM PB, pH 6.5 was passed through the column and fractions of 5ml were collected until O.D. at 280 nm was below 0.100. Fractions were checked for α-Mannosidase activity and those showing activity were pooled and dialyzed against 10 mM PB pH 6.5 with three to four changes.

The partially purified protein was subjected to Preparative poly acrylamide gel electrophoresis (PAGE) (5% acrylamide). The run took 22-24h. The enzyme on the gel was located by activity staining, by cutting the small vertical strips which was cut into pieces further. The pieces were crushed, suspended in buffer and substrate and incubated at 50 ^{0}C for 2 minute. The yellow color appeared within 1 minute. The portion of the gel corresponding to the piece showing α-mannosidase activity was cut finely and crushed with glass rod and 20 ml of phosphate buffer of pH 6.5 was added to the crushed gel to make it semisolid. The suspension was filtered and the filtrate was dialyzed against PB pH 6.5.

Enzyme assay

The α-Mannosidase activity was estimated by incubating suitably diluted enzyme with 500 μM para nitro phenyl-α-D-Mannopyranoside (PNPM) in 50 mM phosphate buffer, pH 6.5 in a total volume of 0.5 ml at 50 ^{0}C for 15 min. The reaction was terminated by adding 1 ml of 1M Na_2CO_3 and the p-nitrophenol released was determined from its absorbance at 405 nm. A unit of activity is defined as the amount of enzyme required to liberate 1 μmole of p-nitrophenol per min under the assay conditions. (Extinction co-efficient of para nitrophenol= 17.7 X 10^3 $M^{-1}cm^{-1}$).

Protein concentration estimation

Protein concentration was determined according to the method of Lowry [15] using bovine serum albumin as standard.

Activity staining of α-mannosidase [Zymogram]

Samples of α-mannosidase at different stages of purification; crude culture broth, ammonium sulfate precipitated and dialyzed broth, DEAE-Sepharose eluted protein and the protein eluted after Preparative PAGE were subjected to non-denaturing PAGE at pH 8.8. Once the run was over, the gel was suspended in a mixture of phosphate buffer pH 6.5 and 4-methylumbelliferyll-α-D-mannopyranoside, a fluorescent substrate, in excess, and the tray is kept in water both at 50 ^{0}C for 20 minutes. The excess substrate was washed with double distilled water and the gel was observed under UV-illuminator for fluorescent bands of active protein samples at different stages of purification.

Amino acid analysis

50 μg of purified α-mannosidase was digested with 6 N HCl at 110 ^{0}C for 24 h in vacuum-sealed tubes. The hydrolysate was then used for amino acid analysis with AccQ-Fluor kit (Waters Corporation, USA). The digested sample was lyophilized, recovered in milli Q passed water and again lyophilized to remove the acid. The digested sample was derivatized with 6-aminoquinolyl-*N*-hydroxysuccinimidyl carbamate (AQC) following manufacturer's instruction. 5 pmol of the sample was

loaded onto AccQ-tag column and eluted with acetonitrile gradient (0-60%). The eluate was monitored with a florescence detector. The amino acid peaks were compared with standard amino acids, which were derivatized and run under identical conditions. Total cysteine and tryptophan were estimated with denatured protein according to the method of Cavallini *et al.* [16] and Spande and Witkop [17], respectively.

Circular dichroism (CD) measurements

The CD spectra of the enzyme were recorded on a J-175 Spectropolarimeter with a PTC343 Peltier unit (Jasco, Tokyo, Japan) at 25 ^{0}C in a quartz cuvette. Each CD spectrum was accumulated from eight scans at 50 nm/min with a 1 nm slit width and a time constant of 1 s for a nominal resolution of 0.5 nm. Far UV CD spectra of the enzyme (2.6 μM) were collected in the range of wavelengths of 200-250 nm using a cell path length 0.1 cm for monitoring the secondary structure. All spectra were corrected for buffer contributions and observed values were converted to molar ellipticity. The tertiary structure of the enzyme (8.6 μM) was monitored with near UV CD spectra in the wavelength 250-300 nm using path length 1 cm. Results were expressed as mean residue ellipticity (MRE) in deg cm^2 dmol^{-1} defined as

$$MRE = M\ \theta_\lambda / 10\ d\ c\ r$$

Where M is the molecular weight of the protein, θ_λ is CD in millidegree, d is the path length in cm, c is the protein concentration in mg/ml and r is the average number of amino acid residues in the protein. Secondary structure elements were calculated by using CD pro software[18].

Effect of Metal Ions on α-Mannosidase

Enzyme (0.072 μM) assay was carried out in presence of metal ions such as Cu, Co, Fe, Mg, Mn, Ca, Zn, Se Cd, V, Pb, Ni and Hg at 1mM concentrations of metal ions. IC_{50}, Ki and type of inhibition was determined for promising metal ion inhibitors, by using range of concentration. K_i was determined by Dixon plot and type of inhibition was determined by LB plot. Reversibility of metal ion inhibition was checked with

various concentrations of EDTA and also by dialysing the metal ion treated enzyme. Substrate protection studies for inhibition were also carried out for most promising metal ions.

pH activity profile

V_{max} and K_m for α-mannosidase from *Aspergillus fischeri* at different pH (4.0 to 10.0) were determined under standard assay conditions. The data was fitted into non-linear regression analysis of Michaelis-Menten equation. 3-4 μg of enzyme was used for each assay.

Chemical Modification of α-Mannosidase:

Modification Carboxylate groups with 1-Ethyl-3-(3-dimethylaminopropyl) carbodiimiide (EDAC)

The enzyme solution (6μM) in 50mM MES/HEPES buffer (75:25 w/v), pH 6.0, was incubated with varying concentrations of EDAC (10-40μM) at 30 ^{0}C[19]. Aliquots were removed at suitable time intervals and the residual activity was determined under standard assay conditions. The K_m and V_{max} of partially modified and inactivated enzyme were also determined. Enzyme sample incubated in absence of EDAC served as control.

Reaction with EDAC/ Nitro tyrosine ethyl ester (NTEE):

The enzyme solution (5μM, 1ml) in 50mM MES/HEPES buffer (75:25 v/v), pH 6.0, was incubated with total of 50mM EDAC and 30mM NTEE at 30 ^{0}C for 45 min. Subsequently the reaction was arrested by the addition of 10% (w/v) TCA and the precipitated protein was collected by centrifugation, washed extensively with chilled acetone, air-dried and dissolved in 100mM sodium hydroxide. The number of nitrotyrosyl groups incorporated was determined spectrophotometrically at 430nm, using a molar absorption coefficient of 4600 $M^{-1}cm^{-1}$.

Modification of Cysteine Residues with N-ethylmaleimide (NEM)

The α-Mannosidase solution (1.65 μM) in 50 mM potassium phosphate buffer, pH6.5, was incubated with varying concentrations of NEM (3-12 mM) at 30 ^{0}C. Aliquots were removed at different time intervals and the residual activity was determined under standard assay conditions. Enzyme samples incubated without NEM served as control.

Reaction with p-hydroxymercurybenzoate (pHMB)

The enzyme solution (1.65 μM) in 50 mM potassium phosphate buffer solution, pH6.5, was incubated with varying concentrations of pHMB (10 – 40 μm) at 25 ^{0}C. Aliquots were removed at different time intervals, passed through G-25 matrix and the residual activity was determined under standard assay conditions. The K_m and V_{max} values of the partially modified enzyme were also determined.

Reaction with 2, 2'-dithiobisnitrobenzoic acid (DTNB)

The enzyme solution (1.65 μM, 1ml) in 50 mM potassium phosphate buffer, pH 7.8, was incubated with 1.0 mM of DTNB (effective concentration) at 30 ^{0}C for 45 min. The modification reaction was followed by monitoring the absorbance at 412nm and the number of sulfhydral groups modified was calculated by using a molar absorption co-efficient of 13,600 $M^{-1}cm^{-1}$.

Determination of disulfide bond with DTNB after reduction

To a test tube containing 1.44 mg of urea was added (0.1ml) 0.1M sodium EDTA, 0.5-1.0 ml of protein sample (240 μg), 1ml of 2.5% $NaBH_4$, water to 3 ml, and a drop of octyl alcohol as an antifoaming agent. The tubes were mixed at 38 ^{0}C and reduction was allowed to proceed for 30min at 38 ^{0}C, after which 0.5 ml of 1M KH_2PO_4 containing 0.2 M HCl was added and nitrogen was bubbled through for 5 min. Finally, 0.5 ml of 0.01M DTNB was added and the volume was made to 6 ml with water. Nitrogen was bubbled for 2 minutes and tube was stoppered, ensuring that the gas space was filled with nitrogen. The preparation was stabilized for 15 min, the absorbance was determined at 412 nm. Blanks containing all reactants except the protein solution were subtracted. A molar absorptivity of 12,000 $M^{-1}cm^{-1}$ was used for calculating the number of sulfhydral groups formed after reduction [20].

Modification of Arginine Residues with p-nitrylphenylglyoxal (PNPG)

The enzyme (2 μM, 1ml) in 50 mM potassium phosphate buffer, pH 7.5, was incubated with varying concentrations of pNPG (5-12.5) at 30 ^{0}C [21]. Aliquots were removed at suitable intervals and the residual activity was determined under standard assay conditions. The K_m and V_{max} values of the partially modified and inactivated enzyme were also determined.

Modification of Tryptophan Residues with N-bromosuccinimide (NBS)

The reaction was carried out by titrating 1ml of enzyme solution (10-40 μM) with freshly prepared NBS (2.5 mM) in the same buffer [17]. The NBS mediated reaction was followed by monitoring the decrease in the absorbance at 280 nm. The reagent was added in 10 installments (5 μl each) till the protein: NBS ratio reached 1:10. Similar additions were carried out in a tube containing duplicate sample and after each addition, an aliquot was removed and checked for residual activity under standard assay conditions. The K_m and V_{max} values were also determined for partially modified and inactivated enzyme. The number of Tryptophan modified was determined spectrophotometrically, by assuming a molar absorption co-efficient of 5500 $M^{-1}cm^{-1}$ for the modified Trp at 280 nm. The absorption spectral measurements were made using a Shimadzu UVB101 PC double-beam spectrophotometer.

Modification of histidine using diethylpyrocarbonate (DEPC)

Reaction mixture of 1ml contained 6 μM of α-mannosidase in 50 mM phosphate buffer, pH 6.0 and varying concentrations of DEPC (10-40 μM), freshly prepared in absolute ethanol. The ethanol concentration in the reaction mixture did not exceed 2% (v/v) and had no effect on the activity and stability of the enzyme during the incubation period. α-mannosidase samples incubated in the absence of DEPC served as control. The K_m and V_{max} values were also determined for partially inactivated enzyme.

Modification of Tyrosine Residues with N-acetyl imidazole (NAI)

This was performed as described by Riordan *et al.*, [22]. The enzyme (3.9 μM) in 50 mM phosphate buffer pH 7.5 was incubated with 1000 fold molar excess of NAI at 30 ^{0}C for 30 min followed by estimation of the residual activity after removing the excess reagent by gel filtration on Sephadex G-25 column (1x10 cm, dimension) pre-equilibrated in the same 50 mM phosphate buffer pH 7.5. The enzyme incubated in the absence of NAI served as control. The tyrosine residues modified were determined spectrophotometrically, using a molar absorption coefficient of 1160 $M^{-1}cm^{-1}$ at 278 nm.

Modification of Lysine Residues

a) Estimation of free amino groups using trinitrobenzenesulphonic acid (TNBS)

1ml of reaction mixture containing enzyme (4.7 μM) in 4% sodium carbonate buffer, pH 7.8 and 2 and 5 mM of TNBS was incubated at 30 ^{0}C temperature in dark for four hours. Aliquots were withdrawn at suitable intervals and the residual activities were determined under standard assay conditions.

b) Citraconylation

The purified α-Mannosidase (4.7 μM 1ml) in 200 mM Phosphate buffer, pH 7.85, was treated with 2 to 28 mM Citraconic anhydride at 25 ^{0}C. The amino groups of α-Mannosidase were reversibly modified by citraconic anhydride according to the Dixon and Perham [23]. Citraconic anhydride was diluted in dioxane and the concentration of the diluted reagent was estimated to be 110 mM. Purified α-Mannosidase (4.7 μM 1 ml) in 200 mM phosphate buffer, pH 7.85, was treated with a total of 2 to 28 mM Citraconic anhydride at 25 ^{0}C. After each addition, an aliquot was removed and assayed for enzyme activity and presence of free amino groups. α-mannosidase sample incubated under same conditions without citraconic anhydride served as control.

Modification of Serine Residues with phenylmethylsulfonyl fluoride (PMSF)

The reaction mixture containing enzyme (2 μM 1ml) in 50 mM phosphate buffer, pH 7.5 and 2 and 5 mM of PMSF was incubated at 30 ^{0}C for 2 hr. Aliquots were removed

at different time intervals and the residual activities were determined under standard assay conditions [24]. Enzyme sample incubated in the absence of PMSF served as control.

Substrate protection studies:

Substrate protection studies were carried out by mixing the enzyme with 0.2 – 1.25 mM pNPM before treatment with different chemical modifiers and then assaying the modified enzyme with proper controls.

Histidine – Tryptophan proximity study in α-mannosidase

To know the proximity of His and Trp at the active site of α-mannosidase, the pH dependence of fluorescence of the enzyme was studied. 1 ml of sample (1.44 μM) in 0.05 M potassium phosphate buffer, taken in cuvette and to it were added 10 μl of 300 mM HCl aliquots till the pH of sample reached 2.80 from 6.60. To ascertain change in pH, 0.05 M potassium phosphate buffer was titrated with 300 mM HCl with 10 μl aliquots and pH was noted down successively till the end. DEPC (1.4 μM) treated enzyme sample with residual activity of 58% was used to check change in fluorescence intensity due to change in pH. The fluorescence scan was taken with excitation wavelength of 295 nm and slit width of 5 mM for both excitation and emission. The fluorescence intensity at pH 6.60 was taken as 100% and successive decrease in intensity after addition of HCl aliquots was calculated appropriately. The per cent fluorescent intensity was plotted against the pH range.

Results and Discussion:

Production and Purification of α-Mannosidase from *Aspergillus fischeri*

The α-mannosidase was produced as an extracellular enzyme in a medium with yeast extract powder (2%) as carbon source as well as an inducer of α-mannosidase. The culture produced 22-25 units of enzyme from one litter of culture broth.

Table 2.1: Purification of α-mannosidase from *Aspergillus fischeri*.

Step	Fraction	Total Volume (ml)	Total Protein (mg)	Total activity (U)	Specific activity (U/mg)	Purification fold
I	Culture filtrate	1000	1750	22	0.0125	-
II	Ammonium sulfate pptn	30	220	14	0.0636	5.09
II	DEAE-Sepharose	120	42	8	0.1904	15.23
IV	Preparative PAGE (5%W/V)	5	4	1.0	0.2500	20.00

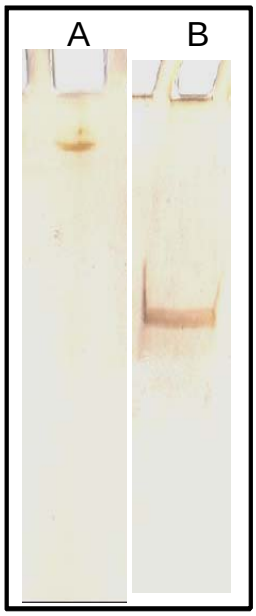

Fig. 2.1: Pure α-mannosidase (20 µg) in (A) Non-denaturing and (B) SDS PAGE 7.5 % (w/v). Protein was visualized with silver staining.

The ammonium sulfate precipitated and dialysed culture broth was subjected to DEAE-Sepharose chromatography. The enzyme got eluted in 0.2M NaCl in 10 mM Phosphate buffer. The enzyme was further concentrated after dialysis and loaded on to the preparative PAGE to get pure protein with overall 20 fold purification (Fig. 2.1).

Activity staining of α-mannosidase [Zymogram]

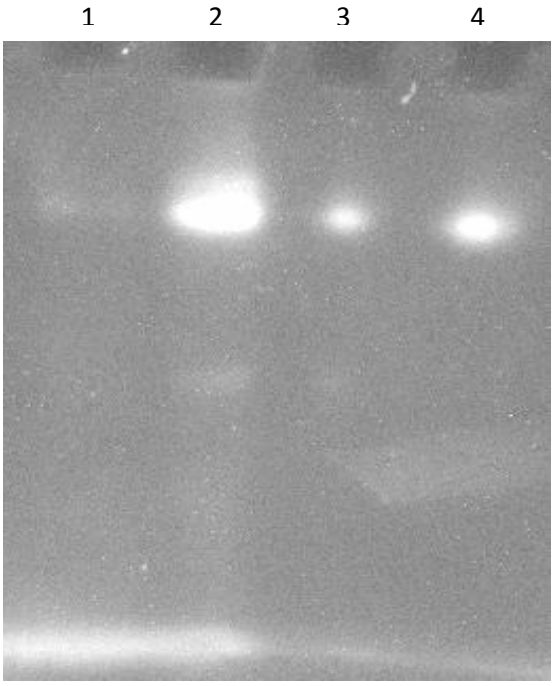

Figure 2.2: Zymogram of α-mannosidase. Non-denaturing PAGE (7.5%v/v), showing the fluorescent bands of α-mannosidase at different stages of the protein purification. Lane1- Culture Broth, Lane 2- Ammonium Sulfate Precipitated and dialyzed sample, Lane 3- Enzyme eluted from DEAE-Sepharose and Lane 4- pure protein after Preparative PAGE. Protein loaded on to the gel was around 20-40 μg.

The activity staining of the enzyme with fluorescent substrate clearly showed the presence of the active α-mannosidase at same position on gel for all the stages of purification process.

Amino acid and *N*-terminal analysis

Table 2.2: Amino acid composition of α-mannosidase from *Aspergillus fischeri*.

Amino Acid	% Amino Acid contribution	Amino Acid	% Amino Acid contribution
Aspartic acid and Aspargine	6.40	Isoleucine	2.55
Threonine	7.20	Leucine	3.07
Serine	4.80	Tyrosine	7.07
Glutamic acid and glutamate	9.40	Phenylalanine	1.97
Proline	6.20	Lysine	3.13
Glycine	20.59	Histidinine	3.19
Alanine	11.10	Arginine	11.20
Valine	2.26	Tryptophan	1.11[a]
Methionine	-	Cysteine	0.15[b]

* [a] Spade and Witkop [17], [b] Habeeb [20] determined spectroscopically.

Amino analysis revealed that α-mannosidase contains remarkably high percentage of Glycine (20.6%) , Arginine (11.2%) and Alanine (11.1%) and essential amount of hydrophobic amino acids (18.43%) and basic amino acids (17.5%) (Table 2.2). ASX and GlX were found to be 6.4% and 9.4%, respectively. The enzyme contains one cysteine residue per sub unit. There is no methionine in the protein.

Circular dichroism (CD) measurements

Far UV CD-spectrum at pH 6.5 showed a trough with minima at 210 nm and 222 nm indicating presence of both α and β structures in the enzyme (Fig. 2.3 A). The mean residue ellipticity (MRE) was calculated using the formula given in materials and methods. The secondary structure elements determined using the software CD Pro

(continell) are 24% (Helix), 23.6% (Sheet), 21.2% Turn and 31.3% unordered structure (RMSD 0.028 and NRMSD 0.012).

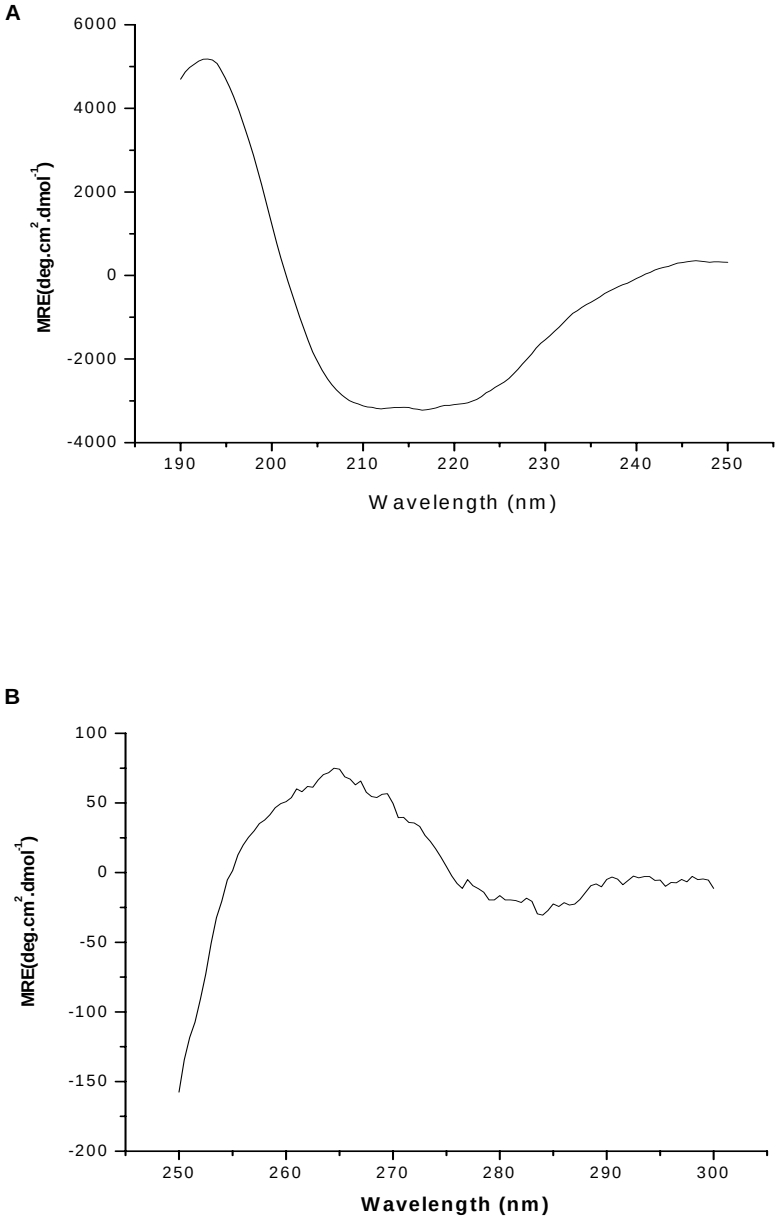

Figure 2.3: CD spectra of α-mannosidase. (A) Far UV CD spectrum (2.6 μM) and Near UV CD spectrum of α-mannosidase (8.6 μM) at pH 6.5.

Effect of metal ions on the α-mannosidase

The class II α-mannosidases are neither metal ion dependent nor they get inactivated by EDTA. The number of metal ions were checked for the effect on the enzyme. None of the metal ions showed activating effects on the enzyme. The inhibitory effect of Cu^{++}, Co^{++} and Hg^{++} has already been reported in our earlier studies. Among the other metal ions checked, Se^{++} and Pb^{++} inactivated the enzyme strongly (Table 2.3).

Table 2.3: Percent Inhibition of α-mannosidase by different metal ions at 1mM concentration.

Sr. No.	Metal Ion	% Inhibition at 1mM
1	Control	0.00
2	Cu ($CuSO_4$)	99.4
3	Co ($COCl_2$)	53.70
4	Fe (Fe_3Cl_2)	26.37
5	Mg ($Mg\ SO_4$)	23.34
6	Mn ($MnCl_2$)	6.10
7	Ca ($CaCl_2$)	1.21
8	Zn ($Zn\ SO_4$)	15.37
9	V (VCl_2)	4.50
10	Cd ($Cd\ SO_4$)	7.90
11	Se ($SeCl_4$)	96.60
12	Pb ($PbNO_3$)	80.50
13	Ni ($NiCl_2$)	37.60
14	Hg ($HgCl_2$)	89.18

Cu^{++}, Co^{++} and Se^{++} were taken up to study the mode of inhibition of the enzyme as well as their effect on the protein structure. Enzyme (0.72 μM) was incubated with

the respective concentrations of the metal ions for 10 minutes and the residual activity was determined. The α-mannosidase activity was inhibited by Cu^{++}, Se^{++} and Co^{++} ions at a very low concentration (Table 2.4) indicating that these metal ions have strong affinity for this enzyme.

Figure 2.5 shows the IC_{50} values of the above three metal ions. Copper inhibited the enzyme at nano molar level where as cobalt and selenium inhibited the enzyme at milli molar concentrations. This may be due to the binding of copper to the cysteine amino acid at or near the active site of the enzyme. Inhibition of neutral α-mannosidase from Japanese oviduct by copper has been reported [25]. Figure 2.6 shows the Lineweaver-Burk plots of the inhibited enzyme. The mode of inhibition by Cu^{++} and Se^{++} ions was noncompetitive, while that with Co^{++} ions was competitive. The K_i values determined from the Dixon plot were 22 nm, 28 μM, and 1.2 mM for Cu^{++}, Se^{++} and Co^{++} ions, respectively. The reason for Co^{++} being competitive inhibitor could be the co-ordination with carboxylate ions at the active site. Cu^{++} and Se^{++} could be interfering the catalysis since the K_m of the enzyme in presence of these metal ions remained same. But Co^{++} is known to activate the α-mannosidase from Japanese oviduct and rat liver [25,26]. Also, there was no recovery of the present enzyme activity after dialyzing out the metal ions.

Table 2.4: IC_{50}, Ki and Type of inhibition of Cu^{2+} Se^{4+} and Co^{2+} for α-mannosidase from *A. fischeri*.

Inhibitor	IC_{50} (μM)	Ki (μM)	Type of Inhibition
Cu^{2+}	0.021	0.022	Non Competitive
Se^{4+}	32.0	28.0	Non Competitive
Co^{2+}	1124	1112	Competitive

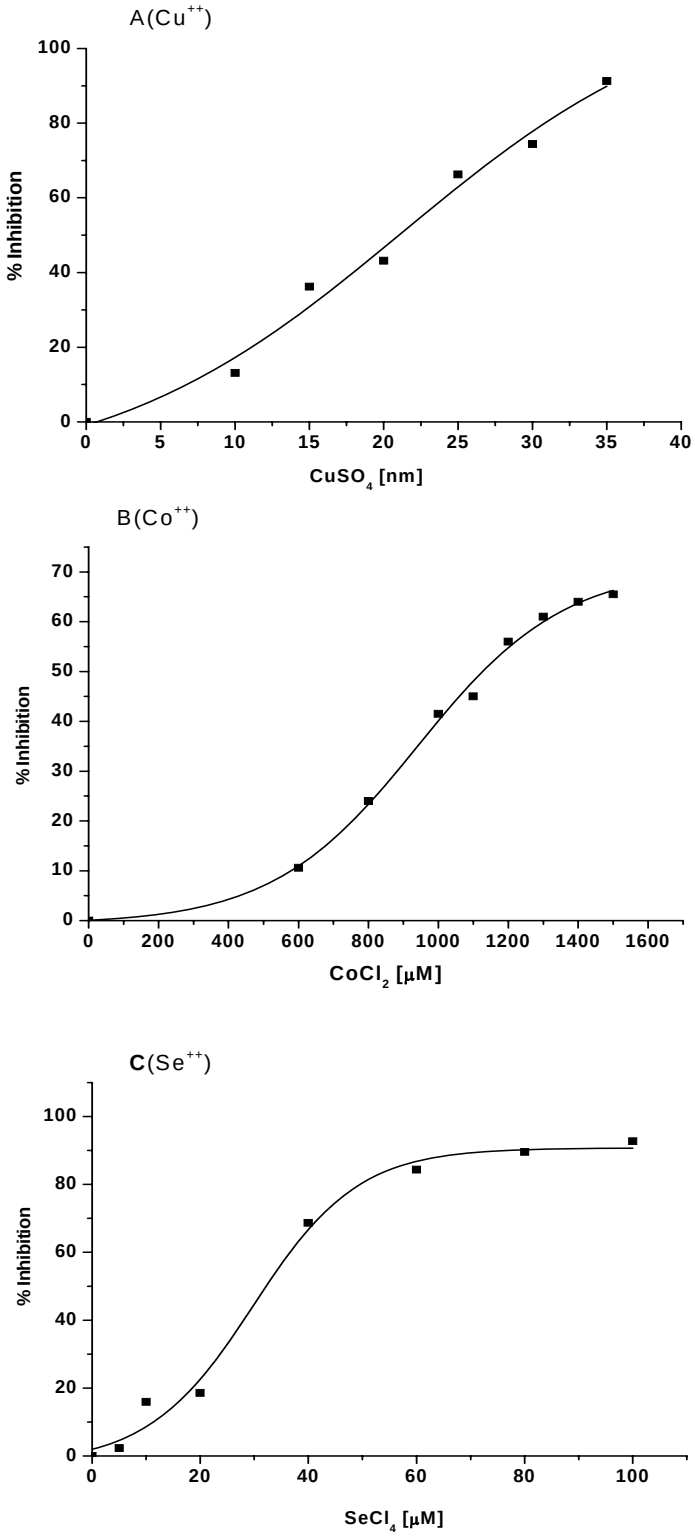

Figure 2.4: Inhibition of α-mannosidase with A) Cu^{++} B) Co^{++} and C) Se^{++}.

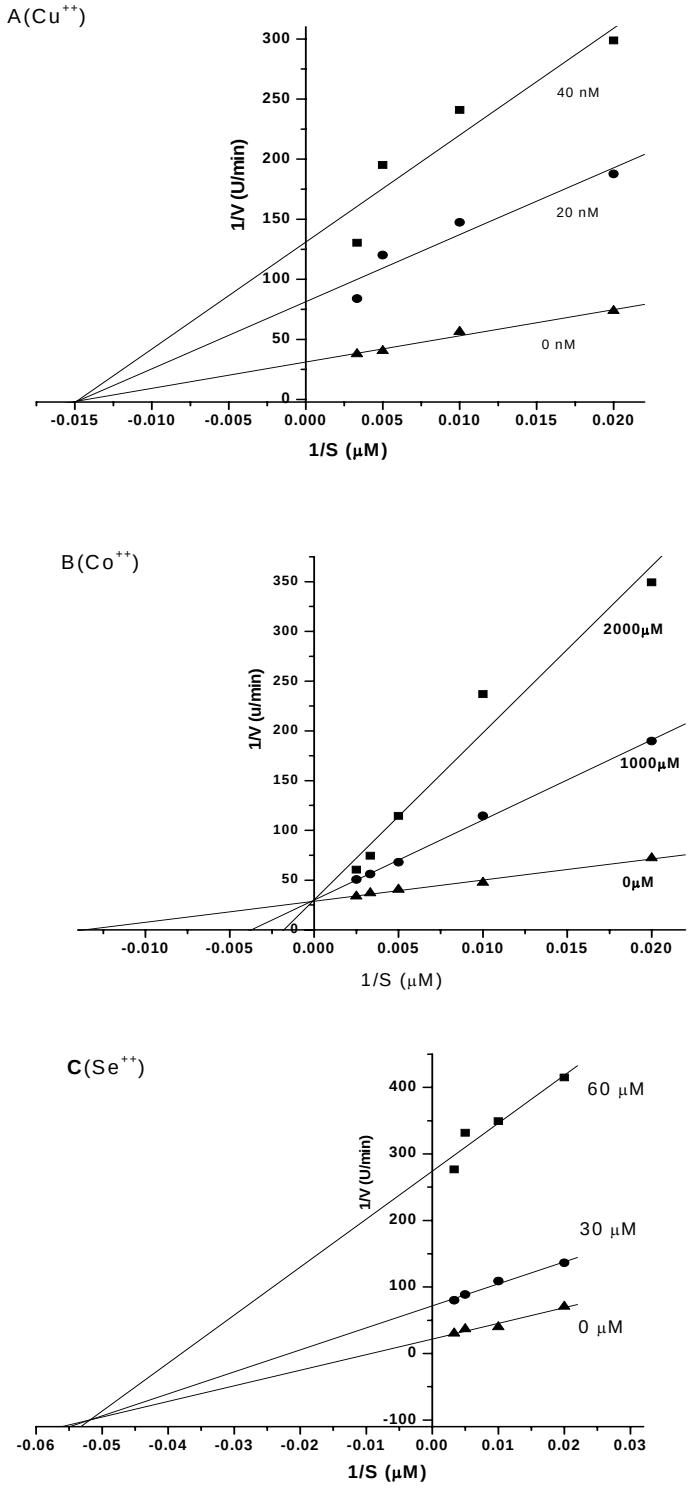

Figure 2.5: Inhibition of α-mannosidase (0.72μM) with A) Cu^{++} B) Co^{++} and C) Se^{++}. Lineweaver - Burk plot showing type of inhibition.

The conformational changes induced if any by the metal ions were studied by fluorescence and CD spectroscopy. The fluorescence titrations of the enzyme with metal ions showed 4-5 % decrease in florescence intensity indicating minor changes in the microenvironment of the tryptophan residues. Fig. 2.6 shows that Cu^{2+}, Se^{2+} and Co^{2+} ions do not induce any change in the secondary structure in spite of drastically inactivating the enzyme.

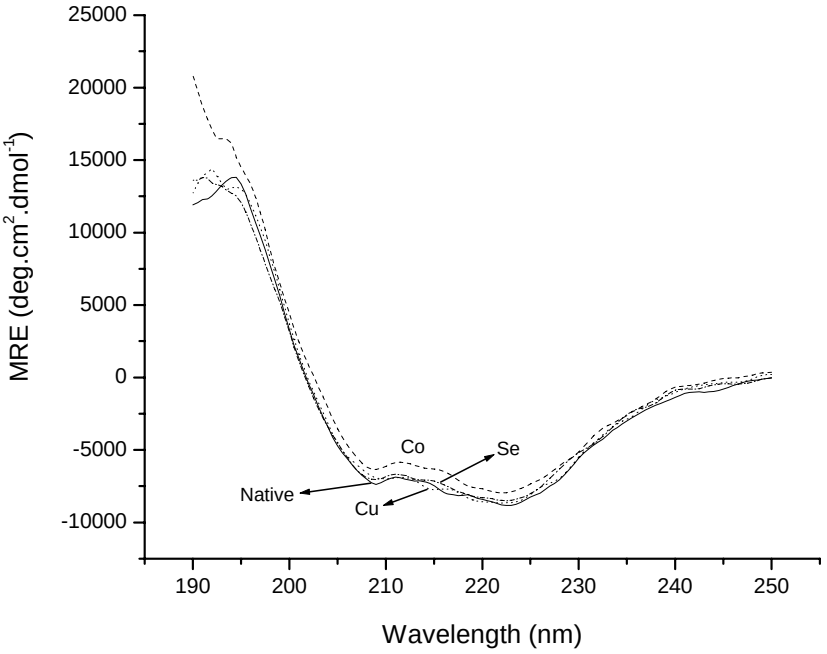

Figure 2.6: Far UV-CD spectra of the native and metal ion treated α-mannosidase. 2.3 μM protein was incubated with Cu^{++} (22 nM), Co^{++} (1112 μM) and Se^{++} (28 μM) for 20 minutes and the scans were recorded.

pH activity profile

The pH-activity profile obtained by plotting log (V_{max}/K_m) against pH of purified α-mannosidase revealed the participation of two ionizable groups with pK_a values of 5.75 and 7.84 (Fig.2.2). The pK_a of amino acid towards acidic side shows

involvement of carboxylate and the one towards basic side shows the presence of either His (pK_a values changed slightly due to change in the microenvironment) or Cys. Chemical modification of the other amino acids with the group specific reagents was taken up for detailed studies of the active site.

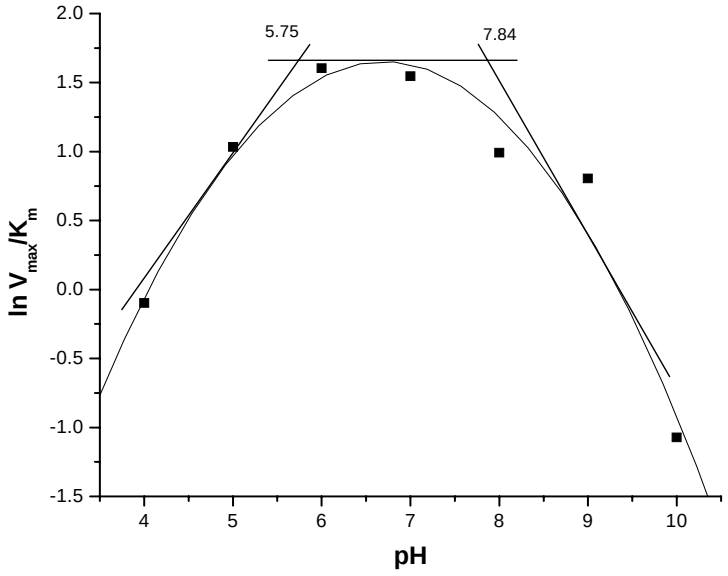

Figure 2.7: pH activity profile of α-Mannosidase: The K_m and V_{max} values of the enzyme were determined at different pH (4-10) by using the 0.2-1.5mM pNP-α-Mannopyranoside and fitting the data to linear regression using Line weaver-

Chemical Modification of α-Mannosidase:

The effect of various chemical modifiers on the activity of α-Mannosidase from *Aspergillus fischeri* is shown in the Table 2.5. Treatment of the enzyme with TNBS resulted in no loss of activity even though there is 15% loss of activity after treatment with Citraconic anhydride. Modification of enzyme with PMSF and NAI did not result in any loss of activity. The above results suggest Lysine, Serine and Tyrosine residues do not have role at the active site of the enzyme. Enzyme modification with Phenylglyoxal leads to 25% loss in the activity. The treatment with para nitrophenyl glyoxal lead to modification of one Arginine residue and resulted in 60% of activity

loss. Carboxylate, Cys, His and Trp specific reagents inactivated the enzyme indicating the possible involvement of these residues in catalytic activity.

Table 2.5: Effect of chemical modifiers on the activity of α-Mannosidase from *Aspergillus fischeri* The α-Mannosidase (6.0μM) was incubated with various reagents separately at room temperature for 5-10min and after terminating the reaction, residual activity of enzyme were measured under standard assay conditions.

Reagent	Residual activity (%)	Concentration	Buffer
None	100	-	Phosphate, 50mM, pH6.5
TNBS	100	2mM	,, 100mM, pH7.8
Citraconic anhydride	85	2mM	,, 50mM ,,
PMSF	100	5mM	,, ,, pH7.5
NAI	100	20mM	,, ,, ,,
DEP	20	40μM	,, ,, pH6.0
DTNB	30	1mM	,, ,, pH7.8
pHMB	20	40μM	,, ,, pH6.5
NEM	50	80mM	,, ,, ,,
Phenylglyoxal	75	40mM	,, ,, pH7.8
pNPG	40	10mM	,, ,, pH7.5
NBS	20	20mM	,, ,, pH6.0
HNBB	20	20mM	,, ,, ,,
EDAC	28	40mM	MES/HEPES ,, ,,

Modification and subsequent inactivation of the enzyme by EDAC (for carboxylate) or pNPG (for Arg), NEM or pHMB (for cysteine) followed pseudo-first order kinetics at any fixed concentration of the reagent. Double logarithmic plots of the rate constants versus reagent concentration deduced number of respective residues present at the active site to be one (Fig. 2.8). Kinetics of the modified enzyme was studied to know the role of respective amino acid residue at the active site. Also the modification reactions were carried out in presence of substrate to confirm the observations. The results are presented in Table 3. There was decrease in the V_{max} values of the enzyme modified with almost all the reagents. However, the K_m values of the enzyme modified with EDAC, pHMB and NBS were almost unchanged indicating that the carboxylate, cysteine and Trp residues must be involved either in the catalysis or holding the catalytic conformation. The enzyme modified with pNPG and DEPC showed increase in Km values indicating decrease in the substrate affinity, along with decrease in the V_{max}. So, Arg and His could be involved in substrate binding and holding the reactive groups in proper position. The inactivation could be prevented by the substrate to substantial extent confirming the specific modification of the amino acids at the active site.

The catalytic mechanism of α-mannosidase normally requires the presence of two carboxylate groups, one acts as a general base by removing a proton from water and the other acts as general acid by donating the proton to the leaving group [27]. The reason for getting one residue from the double reciprocal plot in the present work could be due to the fast reactive nature of one carboxylate residue. EDAC was used alone for modification which rules out the possibility of cross linking with the other amino acids. Presence of carboxylate group at the active site of α-mannosidase has been shown by chemical modification of the enzyme from *Aspergillus saitoi* [28] and *Penicillium citrinum* [29] and by radiolabelling of the enzyme from Jack bean [30]. Aspartic acid is known to be conserved in the Class II α-mannosidase active site. Thus, Asp can be assigned as one of the carboxylate amino acid present at the active site of *A. fischeri* α-mannosidase.

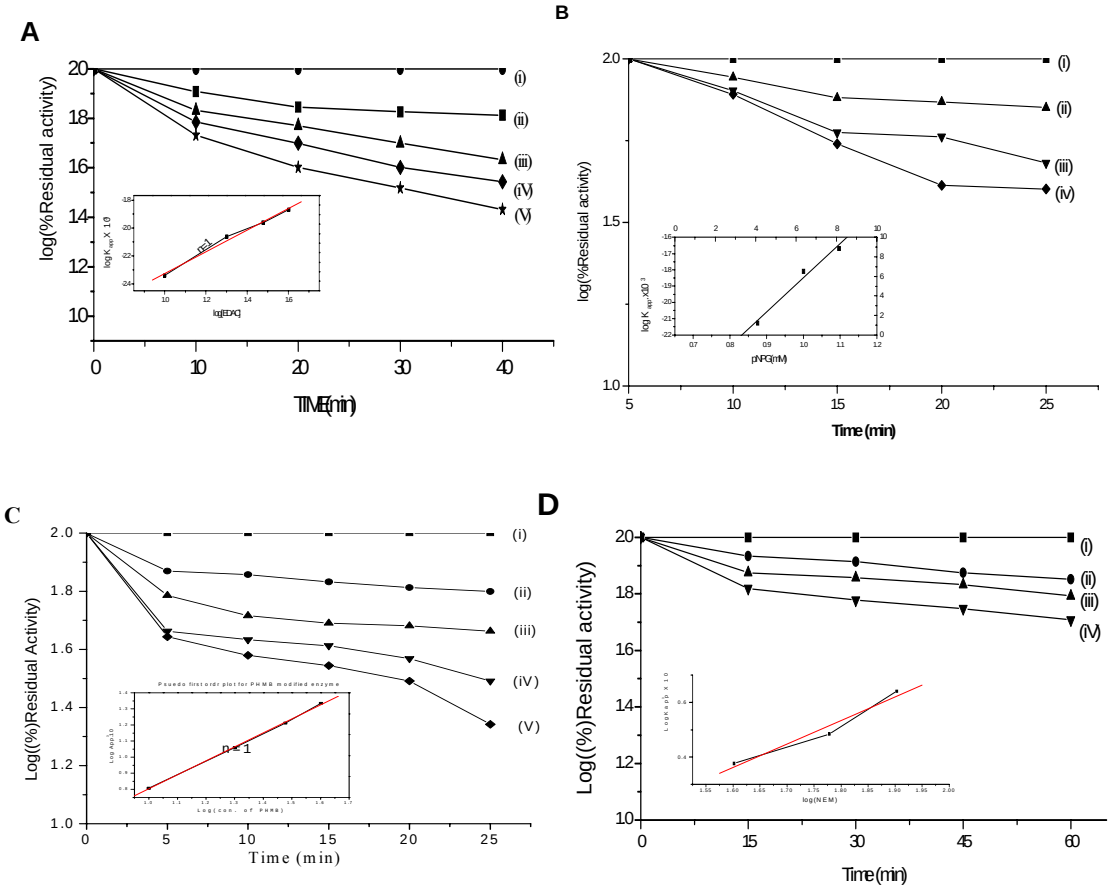

Figure 2.8: Pseudo first-order plot for inactivation of α-Mannosidase from *A. fischeri* by (A) EDAC: Concentrations of EDAC were (i) 0 mM (ii)10mM (iii) 20mM (iV) 30mM and (V) 40mM. **(B) pNPG:** Concentrations of pNPG were (i) 0 mM (ii) 7.5mM (iii) 10mM and (iv) 12.5mM. **(C) PHMB:** Concentrations of PHMB were (i) 0 mM (ii) 10mM (iii) 20mM (iv) 30mM and (v) 40mM. **(D) NEM:** Concentrations of NEM were (i) 0 mM (ii) 40mM (iii) 60mM and (iv) 80mM. Inset for all the figures from A to D are: second order plot of pseudo-first order rate constants (K_{app}) (min^{-1}) as a function of log (EDAC/pNPG/PHMB/NEM) concentration.

Effect of sulfhydryl reagents viz., DTNB, pHMB and NEM on the enzyme activity was studied. Based on the modification of the enzyme with DTNB, the number of free Cys residues per subunit was found to be one. There are no disulfide bonds in the enzyme as revealed by modification of the protein with DTNB under reducing conditions. Incubation of enzyme with β-mercaptoethanol or dithiothreotal [DTT] did

not show any effect on the activity of α-mannosidase. The Cu^{++} is known to bind cysteine residues in the protein [31]. The drastic inactivation of the present enzyme by Cu^{++} could be due to the binding of this metal ion to the cysteine near the active site.

Modification of Tryptophan and Histidine

As described in our earlier report [14], one Tryptophan and one Histidine residues are essential for the enzyme activity. Modification of Trp with NBS was accompanied by a decrease in the absorbance of modified protein at 280 nm. Based on molar absorption co-efficient of 5500 M^{-1} cm^{-1} and molecular weight of enzyme to sub unit to be 69,200 Da, the total number of Tryptophan residues in native protein was observed to be two and seven after denaturing protein, indicating two tryptophans are on the surface, while five are in the interior of the protein.

Proximity of His and Trp residues

The K_m of the α-mannosidase modified and partially inactivated by DEPC was observed to be increased and V_{max} decreased indicating the essential role of His at the active site (Table 2.6).

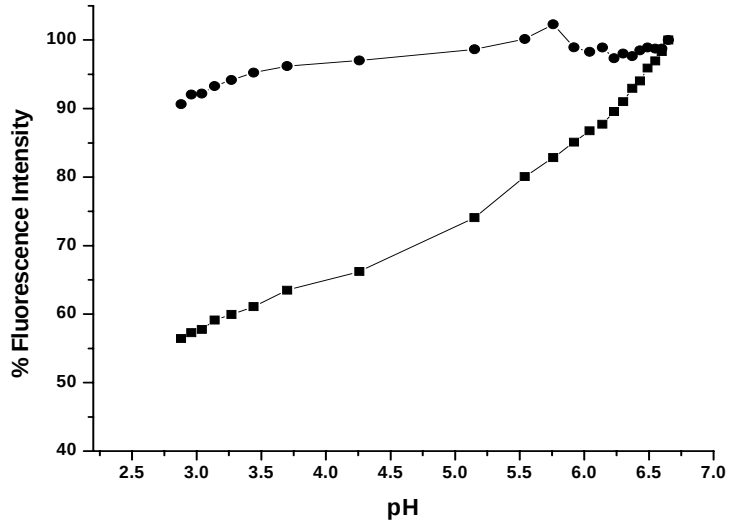

Figure 2.9: pH dependence of fluorescence intensity of α-mannosidase. Effect of gradual addition of HCl (0.3 N) into the native (●) and DEPC (80 μM) treated (■) Enzyme (1.44 μM) in 0.05 M potassium phosphate buffer, pH 7.0

Table 2.6: Kinetics and substrate protection studies of the chemically modified α-mannosidase from *Aspergillus fischeri*

Amino acid modified	Residual Activity (%)	K_m (µM)	V_{max} (µmoles/ min/mg)	Substrate protection studies	
				Conditions	Residual Activity** (%)
None	100	94	0.376	E	100
Carboxylate	60	92	0.2099	E + EDAC(30 mM)	29
				E+S(0.833 mM)+ EDAC(30mM)	69
Arginine	58	235	0.273	E+pNPG(10,12.5 mM)	74, 39
				E+S(1.88mM) + pNPG (10, 12.5mM)	100, 100
Cysteine	63	96	0.241	E+NEM(40,60,80 mM)	71,62, 51
				E+S(1.25mM)+NEM (40,60,80mM)	96, 94, 93
Tryptophan	45	98	0.122	E+NBS(20µM)	30*
				E+S(200 µM)+NBS(20 µM)	80*
Histidine	59	220	0.164	E+DEPC (60µM)	18*
				E+ S(200µM)+DEPC (60µM)	81*

* The data has been taken from Gaikwad et al (1997)[14]

** The values reported in the table vary by ±3%. E: Enzyme, S: Substrate.

Titration of the native and DEPC modified enzyme with 0.3 N HCl was carried out to check the proximity of the His with carboxylate at the active site. The fluorescence intensity of the modified enzyme was 3.5 times more than that of native enzyme (Fig.

2.9). The modified His at the active site could be masking the tryptophan due to which there is no decrease in the fluorescence intensity. This must be due to the proximity between the active site His and Trp residues can be predicted.

In conclusion, the α-mannosidase is produced on basal medium with yeast extract powder as an inducer of the enzyme and purified on DEAE-Sepharose followed by preparative PAGE. The enzyme does not require any metal ions for its activity. It is a hexameric protein with a 412 kDa mass and has pI around 4.5 [32]. The enzyme has one carboxylate, Trp, Cyst, Arg and Hist amino acids at the active site. The Hist is in proximity to the Trp at the active site.

References:

[1] Goss, P.E., Baker, M.A., Carver, J.P., Dennis, J.W. (1995) *Clinical Cancer Res.* **1**, 935-944.

[2] Keskar, S.S., Gaikwad, S.M., Khan, M.I. (1996) *Enz Micro Tech* **18**, 602-604.

[3] Suurnakki, A., Tenkanen, M., Buchert, J., Viikari, L. . (1997) *Hemicellulases in the bleaching of chemical pulps. In: Adv. Biochem. Eng./Biotechnol. Scheper T. (Ed.).* **57**, 261-287.

[4] Kobata, A. (1993) *Acc Chem Res* **26**, 319-324.

[5] Eneyskaya, E.V., Kulminskaya, A.A., Savel'ev, A.N., Shabalin, K.A., Golubev, A.M. and Neustroev, K.N. (1998) *Biochem Biophys Res Commun* **245**, 43-49.

[6] Kelly, S.J., Herscovics, A. . (1998) *J Biol Chem* **263** 14757–14763.

[7] Reyna, A.B.V., Noyola, P.P., Mendez, C.C., Romero, E.O., Carreon, A.F. . (1999) *Glycobiology* **9**, 533–537.

[8] Eades, C.J. and Hintz, W.E. (2000) *Gene* **255**, 25-34.

[9] Mares, M., Callewaert, N., Piens, K., Claeyssens, M., Martinet, W., Dewalele, S., Contreras, H., Dewerte, I., Penttila, M., Contreras, R. (2000) *J Biotechnol* **77**, 255–263.

[10] Tatara, Y., Lee, B.R., Yoshida, T., Takahashi, K. and Ichishima, E. (2003) *J Biol Chem* **278**, 25289-94.

[11] Athanasopoulos, V.I., Niranjan, K., Rastall, R.A. (2005) *Carbohydr Res* **340**, 609–617.

[12] Tsujii, E., Muroi, M., Shiragami, N. and Takatsuki, A. (1996) *Biochem Biophys Res Commun* **220**, 459–466.

[13] Gaikwad, S.M., Keskar, S.S. and Khan, M.I. (1995) *Biochim Biophys Acta* **1250**, 144-8.

[14] Sushama, M.G., M. Islam, Khan and Sulbha, S. Keskar. (1997) *Biotechnology and Applied Biochemistry* **25**, 105-108.

[15] Lowry, O.H., Rosebrough, N.J., Farr, A.L. and Randall, R.J. (1951) *J Biol Chem* **193**, 265-75.

[16] Cavallini, D., Graziani, M. T. and Dupre, S. (1966) *Nature* **212**, 294-295.

[17] Spande, T.F., and Witkop, B., . (1967) *Methods Enzymol* **11**, 498-506.

[18] Sreerama, N., Venyaminov, S. Y. and Woody, R. W. (1999) *Protein Sci* **8**, 370-380.

[19] Hoare, D.G., Koshland, D.E. (1967) *J Biol Chem* **242**, 2447-2453.

[20] Habeeb, A.F.S.A. (1872) *Methods Enzymol* **25**, 457.

[21] Takashi, K. (1968) *J Biol Chem* **243**, 6171-6179.

[22] Riordan, J.F., Wacker, W. E. C. and Valle, B. L. (1965) *Biochemistry* **4**, 1758-1764.

[23] Dixon, H.B.F.a.P., R. N. (1968) *Biochem J* **109**, 312-314.

[24] Gold, A.M., and Faheney, D. (1964) *Biochemistry* **3**, 783-791.

[25] Oku, H., Hase, S. and Ikenaka, T. (1991) *J Biochem* **110**, 29-34.

[26] Grard, T., Saint-Pol, A., Haeuw, J.F., Alonso, C., Wieruszeski, J.M., Strecker, G. and Michalski, J.C. (1994) *Eur J Biochem* **223**, 99-106.

[27] Petergem, V.F., Contreas, H., Contreas, R., Beeumen, V.J. (2001) *J Mol Biol* **312**, 157-165.

[28] Yoshida, T., Shimizu, S., Ichisima, E., . (1994) *Phytochemistry* **35**, 267-268.

[29] Yoshida, T., Maeda, K., Kobayashi, M. and Ichishima, E. (1994) *Biochem J* **303** 97-103.

[30] Howard, S., He, S. and Withers, S.G. (1998) *J Biol Chem* **273**, 2067-72.

[31] Harrison, D.C. (1927) *Biochem J* **21**, 335-346.

[32] Keskar, S.S., Gaikwad, S.M., Khire, J.M. and Khan, M.I. (1993) *Biotechnol Lett* **15**, 685-690.

CHAPTER: 3

ENERGETICS OF CATALYSIS AND INHIBITION OF α-MANNOSIDASE

Summary: Energetics of the catalysis of Class II α-mannosidase (E.C.3.2.1.24) from *Aspergillus fischeri* was studied. The enzyme hydrolyzed mannose disaccharides in the order of Manα(1-3)> Manα(1-2)> Manα(1-6). The enzyme showed K_{cat}/K_m for Man (α1-3) Man, Man (α1-2) Man and Man (α1-6) Man as 7488, 5376 and 3690M^{-1} min^{-1}, respectively. The activation energy, E_a was 15.14, 47.43 and 71.21 kJ/mol for α1-3, α1-2 and α1-6 linked mannobioses, respectively, reflecting the energy barrier in the hydrolysis of latter two substrates. The enzyme showed K_{cat}/K_m as 3.56×105 and 4.61×105M^{-1} min^{-1} and E_a as 38.7 and 8.92 kJ/mol, towards pNPαMan and 4-MeUmbαMan, respectively. Binding of Swainsonine (Ki=101μM) to the enzyme is stronger than that of 1-deoxymannojirimycin (Ki=286 μM). Among the polyhydroxy substituted derivatives, compound **20**, **32** and **39** showed significant level of inhibition for the enzyme.

Introduction:

N-linked glycosylation is a posttranslational modification found in eukaryotes [1]. In various tumor cell lines such as those from breast, colon, and skin cancer, the distribution of the cell surface N-linked sugars is altered[2]. Enzymes of this glycosylation pathway are therefore potential targets for the development of inhibitors for cancer treatments[3]. In early clinical trials, the compound Swainsonine, a well-known inhibitor for α-mannosidase was found to reduce the tumor growth and metastasis when taken orally[4].

Some detail into the catalytic mechanism of glycoside hydrolysis has been obtained from studies of various three dimensional glycosidase structures complexed with substrate analogs and also from kinetic studies of site-directed mutations of these enzymes[5,6]. The glycosidic bond is cleaved via a nucleophilic substitution at the saturated carbon of the anomeric center, resulting in either retention or inversion of the anomeric configuration. Glycosidases are thus classified as either retaining or inverting enzymes. The retaining enzymes are thought to react using a double displacement mechanism, where a nucleophile of a side chain carboxylate group attacks from the opposite side of the pyranose ring to the leaving group, producing a covalent glycosyl ester intermediate.

The transition state most likely has an oxocarbonium ion-like character which is electrostatically stabilized by an enzyme carboxylate.

It is considered that standard enthalpy is a quantitative indicator of the changes in intermolecular bond energies, such as hydrogen bonding and Van der Waals interactions, occurring during the binding. In addition, standard entropy can be considered an indicator of the rearrangements undergone by the solvent, usually water molecules, during the ligand binding [7]. The transfer of solvent molecules between the bulk of the solvent and the solvation shells of solutes is termed as 'solvent reorganization'. It is established that solvent reorganization and the *change* in solvent reorganization which may accompany reactions and spectral transitions, have thermodynamic consequences, especially in hydrogen-bonding solvents such as aqueous buffers, prevalent in biochemical reactions. As a result of which, there is enthalpy-entropy compensation to make the overall standard change in free energy (ΔG) negative and keep the reaction spontaneous. Although the change in enthalpy is measured directly by calorimetric techniques, it is frequently convenient to compare with indirect estimates using classical Vant Hoff equations [8], arising from temperature dependence of equilibrium constant as we might get during circular dichroism, fluorescence and other indirect techniques. The affinity of inhibitor is measured as the free energy difference between the free, solvated ligand and the free, solvated active site on the one hand and the complex on the other hand. The changes in affinity will reflect changes in ligand-active site interactions [9].

In the present chapter, we report the energetics of the reaction of α-mannosidase with different mannose disaccharides as well as pNPαMan and 4-methylumbelliferyl α-mannopyranoside (4- MeUmbαMan). The inhibition of the enzyme activity with potential anticancer agents Swainsonine (Class II mannosidase specific) and 1-deoxymannojirimycin (Class I mannosidase specific) and also with synthetic polyhydroxy piperidine derivatives was studied.

Materials and Methods:

Production and Purification of α-mannosidase

Production, purification and enzyme assay was carried out as described in chapter 2.

Protein concentration estimation

Protein concentration was determined according to the method of Lowry[10] using bovine serum albumin as standard.

Enzyme assay in presence of mannobioses

Assay for Manα(1-2) Man, Manα(1-3) Man or Manα(1-6) Man substrates was carried out by incubating the enzyme (1.44μM) with 100μl of 1mM mannobioses in 50mM phosphate buffer pH 6.5 in a total volume of 500μl at 50 ^{0}C for 20 min. The reaction was terminated by adding 500μl of alkaline Copper reagent solution and the mannose released was determined by the method of Somogyi[11]. One unit of enzyme activity is defined as the enzyme required for liberating 1μmol of mannose per minute under standard assay conditions.

Thin Layer Chromatography:

This technique has been used to show visually the difference in the catalytic rate of α-mannosidase enzyme for different mannobioses like Man α(1-3) man, Man α(1-2) man and Man α(1-6)[12].

A special finely grounded Silica gel-G coated on the glass plate as thin layer (0.25 cm) was used as matrix for Stationary phase. Butanol–ethanol–acetic acid–water in the ratio of 9:6:3:1 used as mobile phase for elution.

Sample preparation and loading:

The different mannobioses (0.2%) like Manα(1-3) man, Manα(1-2) man and Manα(1-6) man were incubated with 2 μM of enzyme at 50^{0}C for time intervals, 20,

40 and 60 minutes. These different mannobioses were loaded 1 cm above the base of TLC plate with glass capillary.

Developing the TLC plate:

The TLC glass chamber was saturated with the mobile phase before keeping the plate inside it. 200 ml of solvent (Butanol–ethanol–acetic acid–water 9:6:3:1) was poured 1h before keeping the TLC plate, and then the lower edge of plate was dipped in solvent. The solvent level was maintained below the spot. The solvent moves up in the matrix by capillary action and in this way it also carries along the components of the samples. The different components move with a different rate depending upon the degree of interaction with matrix and mobile phase. The polar solvent moves to top of plate. The solvent was allowed to move up in the plate until 1 cm distance was left at the top, the plate was taken out and allowed to dry completely.

TLC plates showing the hydrolytic activity of the α-D-mannosidase towards differently linked disaccharides [Manα(1-3)Man, Manα(1-2)Man and Manα(1-6)Man], monitored over 1.0 hr incubation time at 50 ^{0}C, pH 6.5, using two ascents of butanol–ethanol–acetic acid–water 9:6:3:1. The plate was removed and kept for drying. Then the plate was developed by dipping in 50 ml of 0.1M $Ce(SO_4)_2$ diluted in 100 ml of 15% v/v H_2SO_4 and the sugar spots visualized at 100 ^{0}C for 15 min.

Assay for 4-methymumbelliferyl-α-d-mannopyranoside

α-Mannosidase (0.144μM) was incubated with 10μM 4-MeUmbαMan in 50mM phosphate buffer pH 6.5 in a total reaction mixture of 500μl for15minat 50 ^{0}C. The reaction was then stopped by adding 1ml of 0.3M Na_2CO_3. The fluorescence was measured in a Perkin-Elmer Fluorescence Spectrophotometer, using excitation wavelength 360 nm and emission at 445 nm. One unit of enzyme activity is the amount of enzyme required to release 1μmol of 4-methylumbelliferon per minute under standard assay conditions.

Substrate kinetic studies

K_m and V_{max} of α-mannosidase for different substrates (mannobioses - Man (α 1-2, α 1-3 and α 1-6), PNPαMan, 4-MeUmbαMan,) were determined by Michaelis–Menten method at different temperatures ranging from30 to 50 ^{0}C by varying the substrate concentrations. The activity of the enzyme was expressed as units/µmol of enzyme/min. The K_{cat} was expressed as V_{max}/µmol of enzyme/min. The energy of activation E_a, of the enzyme with each substrate was calculated from the slope of the plot of ln V_{max} *V*s 1000/*T*, as E_a =−slope × *R* (*R*, gas constant = 8.314×10^{-3} kJ/mol).

ΔG was calculated by using the equation, $\Delta G = RT\ln K_d$ (here, the values of K_m were used for dissociation constant K_d).

Enzyme assay in presence of inhibitors

α-Mannosidase (25µl of 0.076µM) was incubated with inhibitor (Swainsonine 50–300µM or 1-deoxymannojirimycin 50–400µM) in 50mM potassium phosphate buffer of pH 6.5 and 500µM pNPαMan in total 500µl reaction volume at 50 ^{0}C for 15 min. The reaction was stopped by adding 1.0ml of 1M sodium carbonate. IC_{50} data were obtained in duplicate over a range of inhibitor concentration and then plotted as percentage inhibition versus inhibitor concentration. Determination of K_i was performed under similar conditions of IC_{50} determination, at 250 and 500µM concentrations of pNPαMan. Dixon plots [13] were used to transform the kinetic data into K_i values. The reactions were carried out at temperatures from 30 to 50 ^{0}C for 15 min. ΔH was calculated from the slope of the plot of ln K_a versus 1000/*T* (*R*=gas constant = 8.314×10^{-3} kJ/mol). $K_a=1/K_i$.

Inhibition with polyhydroxy piperidine derivatives

The inhibitors used were (3S, 4R, 5S)-1- benzyl- 3-(hydroxymethyl) piperidine-3,4,5-triol hydrochloride **(19)**, (3S, 4R, 5S)-3- (hydroxymethyl)piperidine -3,4,5-triol hydrochloride **(20)**, (3S, 5S)-1- benzyl-3,4,5-triol hydrochloride **(25)**, (3S, 5S)-piperidine -3,4,5-triol hydrochloride **(22)**, (3S, 4R, 5S)-1- benzyl- 3-((chloramino) methyl)piperidine -3,4,5-triol hydrochloride **(32)**, (3R, 4R, 5S)-3- (amino methyl)

piperidine-3,4,5-triol hydrochloride **(33)**, (3R, 4S, 5R)-1- benzyl- 3-((chloramino) methyl) piperidine-3,4,5-triol hydrochloride **(41)**, (3R, 4R, 5S)-3-((dodecyl amino) methyl)piperidine -3,4,5-triol di hydrochloride **(36)**, (3S, 4S, 5R)-5-amino piperidine-3,4,5-triol hydrochloride **(28)**, (3R, 4S, 5R)-3-(hydroxymethyl)piperidine-3,4,5-triol hydrochloride **(40)** (3R, 4S, 5R)-1-benzyl-3-(hydroxymethyl)piperidine-3,4,5-triol hydrochloride **(39)**. The synthesis of these inhibitors was described by Pandey et al[14].

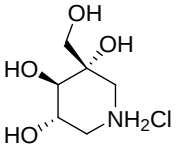

(3*S*,4*R*,5*S*)-3-(hydroxymethyl)piperidine-3,4,5-triol hydrochloride

20

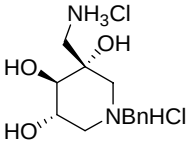

(3*S*,4*R*,5*S*)-1-benzyl-3-((chloroamino)methyl)piperidine-3,4,5-triol hydrochloride

32

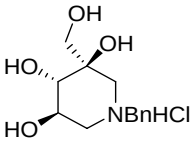

(3*R*,4*S*,5*R*)-1-benzyl-3-(hydroxymethyl)piperidine-3,4,5-triol hydrochloride

39

25 µl of α-mannosidase (0.076 µM) was incubated with the inhibitor in 50 mM potassium phosphate buffer of pH 6.5 and 500 µM pNPαMan in total reaction volume of 500 µl at 50^0 C for 15 min. The reaction was stopped by adding 1.0 ml of 1M sodium carbonate. IC_{50} data were obtained in duplicate over a range of concentration of inhibitor and then plotted as percentage inhibition versus inhibitor concentration. Determination of K_i was performed under similar conditions to IC_{50} determinations, at 250 and 500 µM pNPαMan concentrations. Dixon plots [13] were used to transform the kinetic data into

K_i values. Type of inhibition was determined from Lineweaver-Burk plot. The enzyme reaction was carried out in presence of fixed concentrations of inhibitors.

Thermodynamic parameters of Inhibition

25µl of α-mannosidase (0.09 µM) was incubated with inhibitor **20** (200-700 µM), **39** (25-200 µM) and **32** (25-250 µM) in pH 6.5, 50 mM potassium phosphate buffer and 500 µM of pNPαMan in a total volume of 500 µl at temperature range of 30-50 ^{0}C for 15 min. The reaction was stopped by addition of 1.0 ml of 1 M sodium carbonate solution. IC_{50} and K_i were determined as briefed above.

ΔG was calculated by using the equation, $\Delta G = RT\ln K_d$. (Here, the values of K_i were used for dissociation constant K_d), (R, gas constant = 8.314×10^{-3} KJ/mol). ΔH was calculated from the slope of the plot of $\ln K_a$ vs 1000/T (K_a were taken as reciprocal of the K_i values.). ΔS was calculated as per the equation $\Delta G = \Delta H - T\Delta S$.

Results and Discussion:

The enzyme used in the present work is a Class II α-mannosidase from *A. fischeri* as revealed by the substrate specificity and independency on the metal ion/s for activity (Table 3.1) [15]. Fig. 3.2 shows the TLC showing rate of hydrolysis of the three mannose disaccharides as Man (α1-3) Man>Man (α1-2) Man>Man (α1-6) Man by the enzyme.

To further investigate mechanism behind different rates of hydrolysis, the energetics of the reactions of the enzyme with mannobioses (physiological substrates), pNPαMan and 4-MeUmbαMan (synthetic substrates) was studied. The synthetic substrate used in the routine work, pNPαMan and the other fluorescencent substrate 4-MeUmbαMan were extensively used in the enzyme catalysis reactions and the results were compared. The binding parameters of the α-mannosidase specific inhibitors were also evaluated. The enzymatic reactions were carried out in the temperature range of 30–50 ^{0}C, in which the enzyme is fully stable and no inactivation or denaturation of the enzyme takes place.

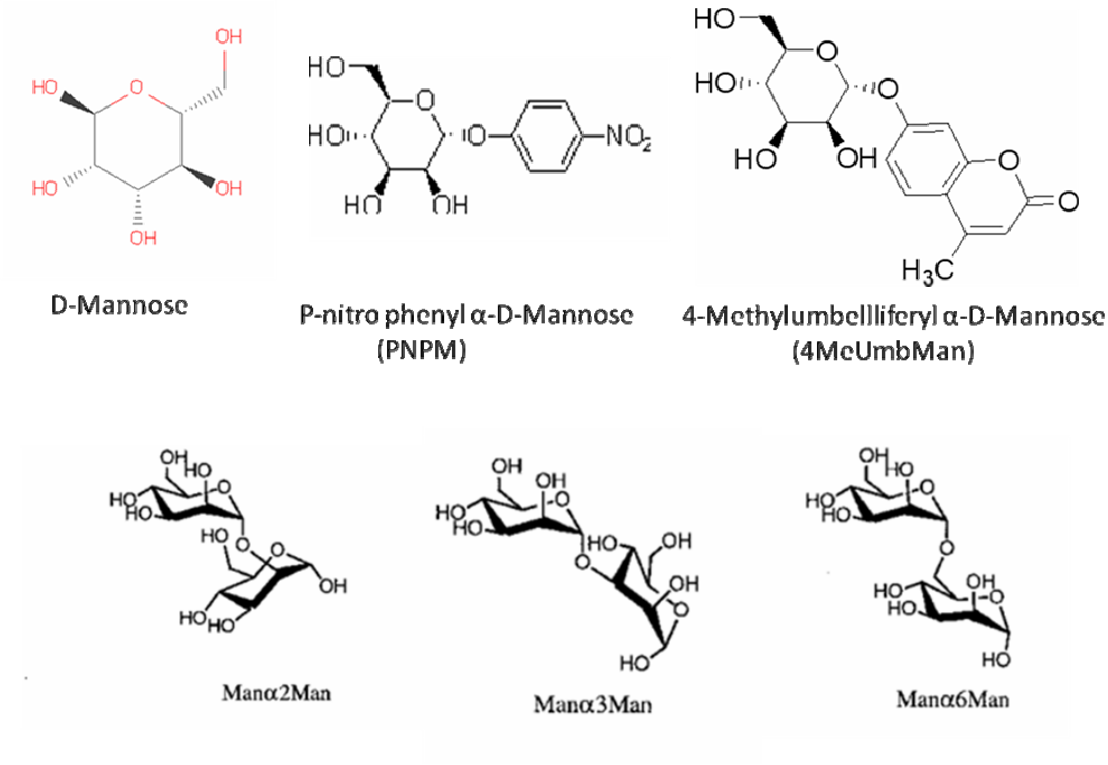

Figure 3.1: Structures of D-Mannose, aryl substrates (p-NPM and 4-MeUmbMan) and Mannobioses (Man α(1-2), Man α(1-3) & Man α(1-6)).

Table 3.1: Kinetic parameters of α-mannosidase for various substrates

Sl. No.	Substrate	K_m (μM)	V_{max}(μmol/min/mg)
1	PNPαMan	82.65 ± 4.13	0.2
2	4MeUmbαMan	7.31 ± 0.37	65
3	Manα(1-3)Man	839 ± 41.95	2.44
4	Manα(1-2)Man	1116 ± 55.80	1.74
5	Manα(1-6)Man	1455 ± 72.75	1.24

Reaction with mannobioses

The activity of α-mannosidase in presence of respective mannose disaccharides was determined at different temperatures at various substrates concentrations. The V_{max} and K_m values were calculated from Michaelis–Menten plots for each substrate at each temperature. The specificity constant K_{cat}/K_m of Man (α1-3) Man, Man (α1-2) Man and Man (α1-6) Man at 50 ^{0}C were 7488, 5376 and 3690M^{-1} min^{-1}, respectively, indicating affinity of the enzyme for the substrates and rate of the reaction is in the order α1-3 >α1-2>α1-6 linked mannobioses (Table 3.2).

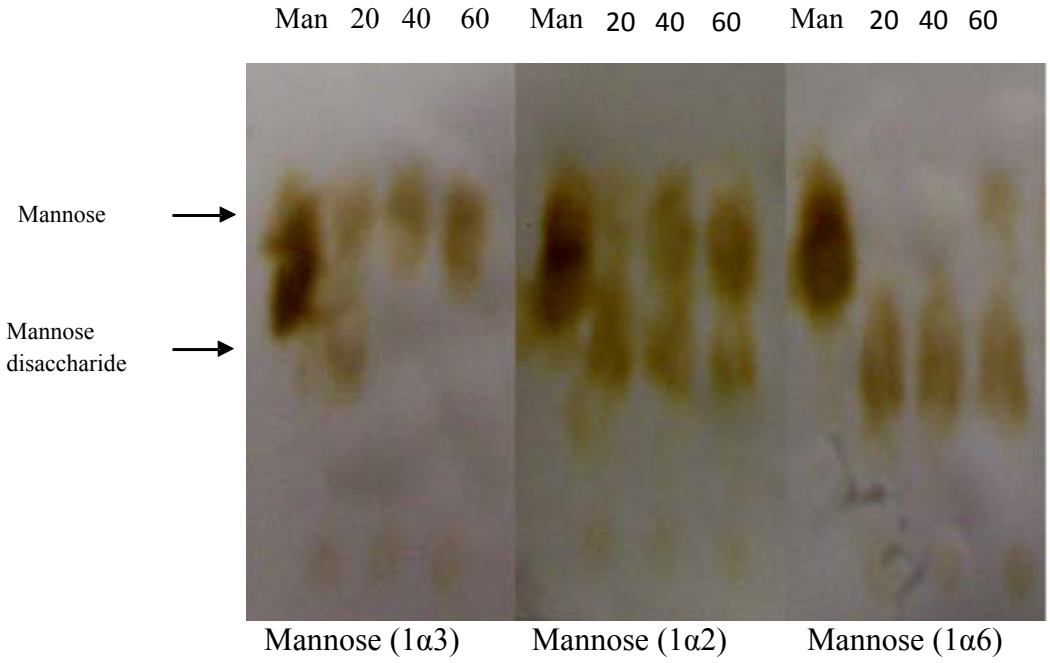

Figure 3.2: TLC plates showing the hydrolytic activity of the α-mannosidase towards differently linked disaccharides (0.2%, w/v) [Man(1-3)Man, Man(1-2)Man and Man(1-6)Man], monitored over 1.0 h incubation time at 50 ^{0}C, pH 6.5, using two ascents of butanol–ethanol–acetic acid–water 9:6:3:1. The plate was developed by dipping in 0.1M Ce(SO4)2 diluted in 15% (v/v) H_2SO_4 and the sugar spots visualized at 100 ^{0}C for 15 min. Mannose (0.5%, w/v) control (Lane 1), digestion rate at 20 min (Lane 2) 40 min (Lane 3) and at 60 min (Lane 4) time interval, respectively.

From the slope of the plot of ln V_{max} versus 1000/T (Fig. 3.2A) (R = 0.98 and 0.99), energy of activation, E_a for all the substrates was calculated. Among the mannose disaccharides, the E_a of hydrolysis of Manα(1-3)Man (15.14 kJ/mol) is three times lower than that of Manα(1-2)Man (47.43 kJ/mol) and 4.6 times lower than that of Manα(1-6)Man (71.21 kJ/mol), respectively (Table 3.2). The hydrolysis of Manα(1-3)Man occurring at faster rate could be due to the easy access of the glycosidic linkage to the carboxylic groups at the active site. There must be more constraints for Manα(1-2) Man and still more for Manα(1-6) Man during binding as well as catalysis due to which the hydrolysis is slow. Affinity of the substrates towards the enzyme and the rates of reaction seem to be reflecting the E_a.

Table 3.2: Energy of activation and free energy of binding of α-mannosidase from *Aspergillus fischeri* with physiological and synthetic substrates.

Substrate ↓	**K_{cat}/K_m (M^{-1} min^{-1})**	**Ea (KJ/Mol)**	**K_m (μM)**	**ΔG KJ/Mol**
Man-α-(1-3)-man	7488	15.14	839±41.95	-19.02
Man-α-(1-2)-man	5376	47.43	1116±55.80	-18.26
Man-α-(1-6)-man	3690	71.21	1455±72.75	-17.54
pNPα-Man	356000	38.70	82.65±4.13	-25.22
MeUmbα-Man	461000	8.92	7.31±0.37	-31.74

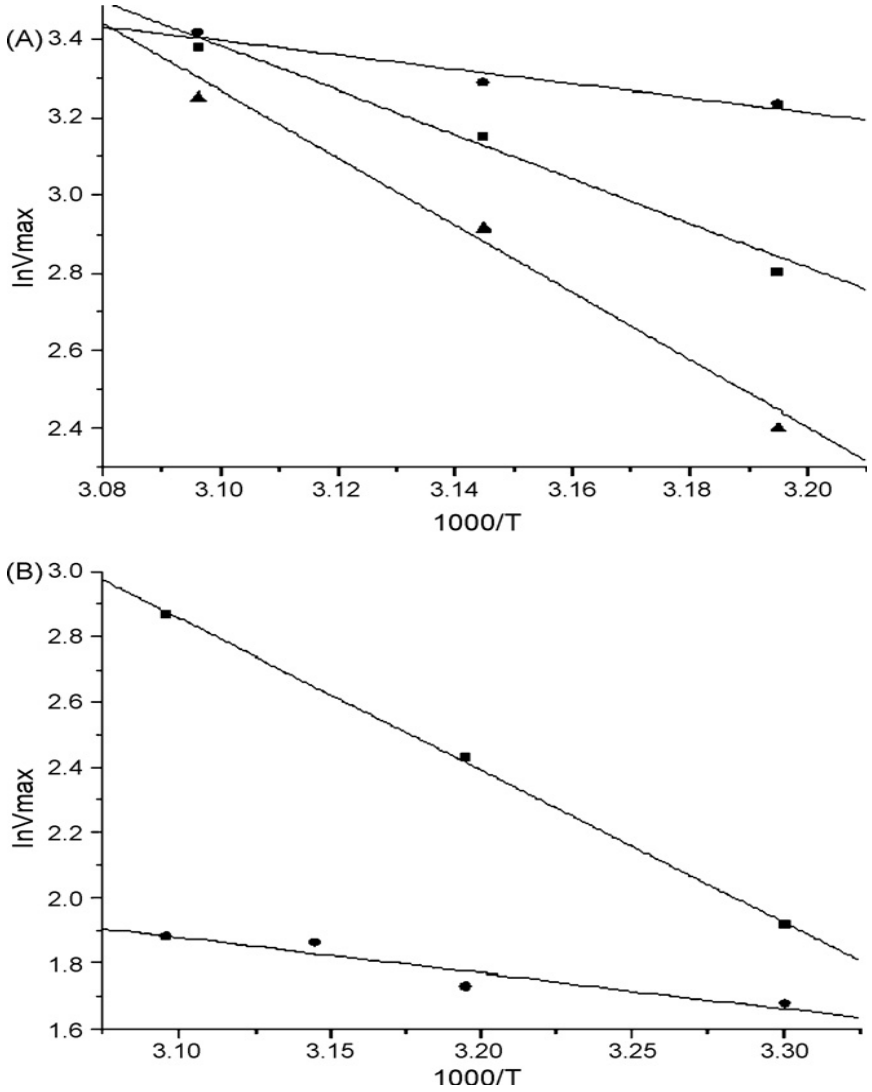

Figure 3.3: Energy of activation of α-mannosidase with mannose disaccharides and aglycon containing substrates. 0.144μM enzyme was taken for the assay of pNPαMan and 4-MeUmbαMan while 2.88μM enzyme was taken for mannobiose assay. The reaction mixtures containing different concentrations of substrates were incubated at different temperatures. Values of V_{max} were taken from Michaelis–Menten plots. (A) Disaccharides: Manα(1→2) (■), Manα(1→3) (●), Manα(1→6) (▲), and (B) 4-methylumberlliferyl-α-mannopyranoside (●) and pNP-α-mannopyranoside (■).

Reaction with synthetic substrates

4-MeUmbαMan has higher specificity constant towards the enzyme (K_{cat}/K_m 4.61×105M^{-1} min^{-1}) as compared to pNPαMan (K_{cat}/Km 3.56×105M^{-1} min^{-1}) (Table 3.2). E_a is four times less for 4-MeUmbαMan (8.92 kJ/mol) as compared to pNPαMan (38.70 kJ/mol) (Fig. 3.3B). The free energy of binding of pNPαMan and 4-MeUmbαMan is much lower than that of mannose disaccharides indicating easier binding of these substrates. The higher specificity (or lower K_m) of the enzyme to 4-MeUmbαMan as compared to pNPαMan can be explained with the structures. The tilted structure in the 4-MeUmbαMan makes easy accessibility of the glycosidic bond to the active site of the enzyme and there by hydrolyzing at faster rate. The flattened structure of pNPαMan could not be easily accessible to the active site and hence there is lower affinity for pNPαMan as compared to 4-MeUmbαMan. It is generally known that half-boat shaped substrates are easily hydrolyzed by the mannosidases.

Inhibition kinetics of α-mannosidase

Table 3.3: IC_{50}, Ki and Type of inhibition of Swainsonine and 1-deoxymannojirimycin for α-mannosidase from *A. fischeri*.

Inhibitor	IC_{50} (µM) at 50 ^{0}C	Ki (µM)	Type of Inhibition
Swainsonine	110	101	Competitive
1-Deoxymannojirimycin	284	286	Competitive

Inhibition studies of the enzyme in presence of inhibitors of α-mannosidase were carried out. The type of inhibition was found to be competitive (Fig. 3.4) for Swainsonine and 1-deoxymannojirimycin as they are the substrate analogues. IC_{50} values for Swainsonine and 1-deoxymannojirimycinwere 110 and 284µM, respectively. Swainsonine, specific

inhibitor of Class II α-mannosidases exhibited three times lower *K*i (101μM) than that for 1-deoxymannojirimycin (286μM), specific inhibitor of Class I enzymes (Table 3.3).

The binding of both the inhibitors was found to be low up to 40 ^{0}C and increased at 50 ^{0}C. The K_i was found to be decreasing (or K_a increasing) (Table 3.4) with increasing temperature indicating kind of the reaction to be endothermic and increased association of the inhibitor to the enzyme. This could be due to the optimum reactive state of the active site of enzyme at 50 ^{0}C. Δ*H* for Swainsonine and 1-deoxymannojirimycin are 101.43 and 59.36 kJ/mol at 40–50 ^{0}C, respectively. The K_i for Swainsonine reported here is 1000 times higher than those reported for the Class II mannosidases from plant and animal sources (Jack beans α-mannosidase; 0.4–0.1μM, rat liver lysosomal α-mannosidase; 0.07–0.2μM and rat liver Golgi α-mannosidase; 0.08–0.2μM), which could be due to the difference in the active site geometry of the respective enzyme.

Table 3.4: Binding of the inhibitors to α-mannosidase from *Aspergillus fischeri*.

Inhibitor↓	**K_a M^{-1}**			**Temperature range ºC**	**ΔG KJmol^{-1}**	**ΔH KJmol^{-1}**
	30^{0}C	**40^{0}C**	**50^{0}C**			
Swainsonine	2100 ±105	2950 ±147.5	9900 ±495	30-40	-20.79	26.83
				40-50	-24.7	101.43
1-Deoxymannojirimycin	2360 ±118	2420 ±121	3500 ±175	30-50	-21.91	59.36

Three-dimensional structure of the enzyme will show the clear picture of the active site. Dorling et al. [16] have reported the inhibition of two α-mannosidases by Swainsonine, the acid form and a neutral form. Since pK_a of Swainsonine is 7.4, it is fully ionized at pH4.0 and hence strongly inhibits the acid form of enzyme while the neutral form of the enzyme is inhibited up to 60% at the same concentration at pH 6.5.

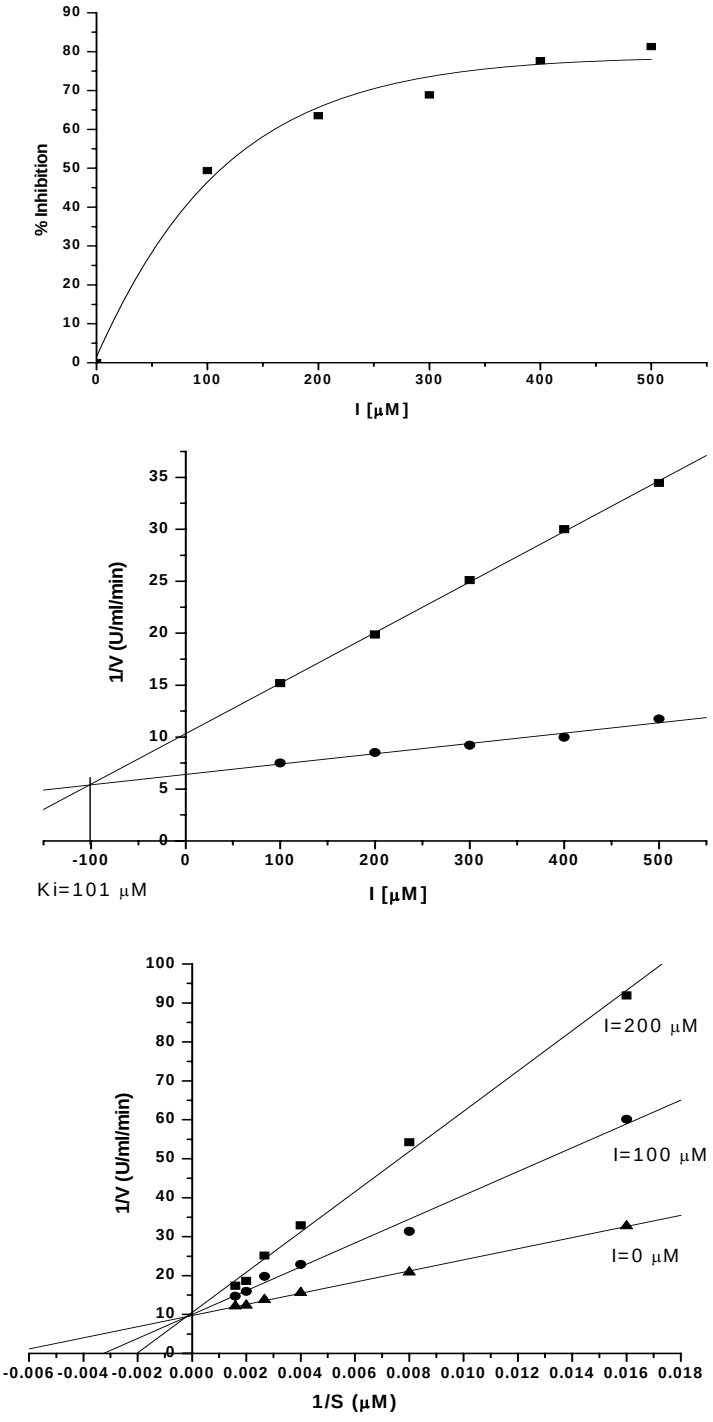

Figure 3.4: IC_{50}, Ki and L-B Plot of Swainsonine inhibition.

Inhibition with polyhydroxy substituted piperidine derivatives

The poor cellular bioavailability of swainsonine, its side effects, as well as the undesired co-inhibition of lysosomal enzymes has resulted in the search for new, more selective, α-mannosidase inhibitors. Recently, there are several reports on polyhydroxy-pyrrolidine derivatives as selective and competitive inhibitors of α-mannosidase from jack bean, [17-20] and it has also been demonstrated for promising anti-proliferative activities on human glioblastoma and melanoma cells for the cell-permeant ester of this compound.

As reported by Pandey et al [14] the polyhydroxy substituted piperidine derivative compounds synthesized and tested for mannosidase inhibition showed different degrees of inhibition (Table 3.5). Out of 11 compounds tested, five compounds (**20, 22, 32, 33** and **39**) at very low concentration showed inhibition of enzyme activity. The IC_{50}, Ki and Type of inhibition were determined. Out of these five said compounds, three turned out to be competitive inhibitors (**20**, **32** and **39**) the other two, **22** and **33** showed non-competitive and mixed type of inhibition, respectively. We selected three inhibitors (**20, 32** and **39**) once which inhibited the enzyme strongly and competitively, to study further the energetics of inhibition. Structures of the compounds are shown in Materials and Methods. Compound no. **32** (IC_{50}=31μM) and **39** (IC_{50}=51μM) strongly and **20** (IC_{50}=237μM) moderately inhibited the α-mannosidase activity. The L-B plots are shown in the Figure 3.5 A, B and C.

The energetics of the inhibition for these three compounds (**20, 32** and **39**) was studied. Table 3.6 shows the decreasing values of inhibition constants with increasing temperature indicating increasing association of the inhibitor with the enzyme accordingly. The binding is endothermic and entropically driven. The increase in entropy due to the release of water molecules from enzyme active site region and the inhibitor due to binding must be much higher than the decrease in entropy due to the restriction on movement of inhibitor and enzyme. Benzyl group in compounds **39** and **32** seems to enhance the binding to the enzyme as compared to compound **20**. Higher positive entropy on binding of the compound **32** than **39** to the enzyme shows the added effect of amine group.

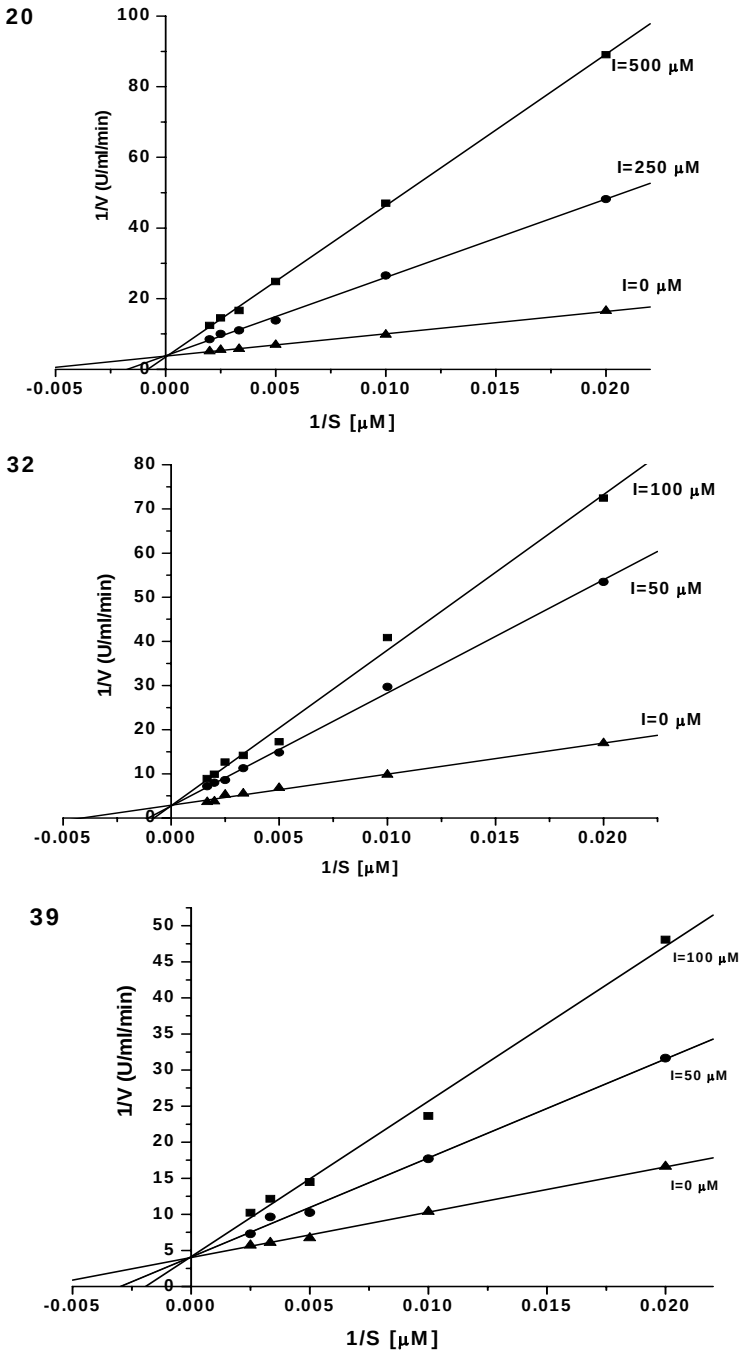

Figure 3.5: L-B Plots for the compounds **20**, **32** and **39** showing competitive type of inhibition for α-mannosidase.

Table 3.6: Thermodynamic parameters of binding of the synthetic inhibitors to α-mannosidase from *Aspergillus fischeri*

Inhibitor↓	IC_{50} (M) 10^{x-6} at 50°C	K_i X 10^{-6} M				ΔG* KJ/mol	ΔH KJ/mol	ΔS* J/mol/K
		30^0C	40^0C	45^0C	50^0C			
20	247	374	310	271	235	-22.44	18.56	127.04
39	51	130	85	73	48	-26.70	38.29	200.45
32	31	254	143	89	45	-26.88	67.83	291.74

* Values reported are at 50 ^{0}C

We have already shown above that the inhibition of the α-mannosidase by Swainsonine, class II enzyme inhibitor and 1-deoxymannojirimycin, class I enzyme inhibitor exhibits K_i as 101 μM and 256 μM, respectively. The binding of both the inhibitors to the enzyme was found to be endothermic. Structure of compound **20** resembles with deoxymannojirimycin and has comparable IC_{50} as 247μM with that of 1-deoxymannojirimycin as 286 μM.

Besides providing tools for the exploration of the physiological role of the endomannosidase-initiated processing pathway these derivatives yield valuable insights into the substrate recognition site of the enzyme.

References:

[1] Herscovics, A. (1999) *Biochimica et Biophysica Acta* **1473**, 96-107.

[2] Dennis, J.W., Granovsky, M. and Warren, C.E. (1999) *Biochimica et Biophysica Acta* **1473**, 21-34.

[3] Jean, M.H.E., Kuntz, D.A. and Rose, D.R. (2001) *The EMBO Journal* **20**, 3008–3017.

[4] Goss, P.E., Reid, C.L., Bailey, D. and Dennis, J.W. (1997) *Clin Cancer Res* **3**, 1077–1086.

[5] Sinnot, M.L. (1990) *Chem Rev* **90**, 1171-1202.

[6] Svensson, B. and Sogaard, M. (1993) *J Biotechnol* **29**, 1-37.

[7] Borea, P.A., Dalpiaz, A., Varani, K., Gilli, P. and Gilli, G. (2000) *Biochem Pharmacol* **60**, 1549-1556.

[8] Varani, K. et al. (2008) *Osteoarthritis and Cartilage* **16**, 1421-1429.

[9] Epps, D.E., Cheney, J., Schostarez, H., Sawyer, T.K., Prairie, M., Krueger, W.C. and Mandell, F. (1990) *Journal of Medicinal Chemistry* **33**, 2080-2086.

[10] Lowry, O.H., Rosebrough, N.J., Farr, A.L. and Randall, R.J. (1951) *J Biol Chem* **193**, 265-75.

[11] Somogyi, M.J. (1952) *J Biol Chem* **195**, 19-23.

[12] Athanasopoulos, V.I., Niranjan, K., Rastall, R.A. (2005) *Carbohydr Res* **340**, 609–617.

[13] Dixon, M. (1953) *Biochem J* **55**, 170-171.

[14] Pandey, G., Bharadwaj, K.C., Khan, M.I., Shashidhara, K.S. and Puranikc, V.G. (2008) *Org Biomol Chem* **6**, 2587–2595.

[15] Gaikwad, S.M., Keskar, S.S. and Khan, M.I. (1995) *Biochim Biophys Acta* **1250**, 144-8.

[16] Dorling, P.R., Huxtable, C.R. and Colegate, S.M. (1980) *Biochem J* **191**, 649-51.

[17] Gerber-Lemaire, S., Popowycz, F., Rodriguez-Garcia, E., Carmona Asenjo, A.T., Robina, I. and Vogel, P. (2002) *ChemBioChem* **5**, 466-470.

[18] Popowycz, F., Gerber-Lemaire, S., Demange, R., Rodriguez-Garcia, E., Asenjo, A.T., Robina, I. and Vogel, P. (2001) *Bioorg Med Chem Lett* **11**, 2489-93.

[19] Popowycz, F., Gerber-Lemaire, S., Rodriguez-García, E., Schütz, C. and Vogel, P. (2003) *Helvetica Chimica Acta* **86**, 1914-1948.

[20] Popowycz, F., Gerber-Lemaire, S., Schütz, C. and Vogel, P. (2004) *Helvetica Chimica Acta* **87**, 800-810.

CHAPTER: 4

FOLDING - UNFOLDING STUDIES

Summary: The conformational transitions of an oligomeric and high molecular weight class II α-mannosidase from *Aspergillus fischeri* were examined using fluorescence and CD spectroscopy under various denaturing conditions. The enzyme activity was labile i) above 55 ^{0}C ii) in presence of 1.0 M GdnHCl iii) below pH 5.0 or above pH 8.0. The enzyme lost the biological activity first and then the overall folded conformation and secondary structure. The midpoint values of GdnHCl mediated changes measured by inactivation, fluorescence and negative ellipticity were 0.48 M, 1.5 M and 1.9 M, respectively. The protein almost completely unfolded in 4.0 M GdnHCl but not at 90 ^{0}C. The inactivation and unfolding were irreversible. The protein exhibited molten-globule like intermediate with rearranged secondary and tertiary structures and exposed hydrophobic amino acids on the surface. This species showed not only increased accessibility of Trp to the neutral and anionic quenchers but also got denatured with GdnHCl in a different manner than that of the native enzyme. The insoluble aggregates of a thermally denatured protein could be detected only in the presence of 0.25 – 0.75 M GdnHCl.

Introduction:

Specific biological functions of proteins emerge directly from their unique three-dimensional structure, attained in a very short time after their synthesis. The three dimensional structure of a protein is held together by non-covalent interactions viz. hydrogen bonds, ionic interactions, hydrophobic interactions, van der Waals forces and covalently by disulfide linkages. Conditions which disturb these stabilizing forces affect the native conformation of the protein by changing a majority of its physical properties apart from its biological activity. The extent and balance between different stabilizing forces, studied under various denaturing conditions, is interpreted in terms of conformational stability. Determination of the stability of a protein generally based on the analysis of denaturant or thermally induced unfolding transition measured either spectroscopically or calorimetrically [1-3].

It has become increasingly evident that a polypeptide chain can adopt conformations different from the functional, native conformation of the protein. It is well established that protein folding goes through few kinetic intermediates, which can accumulate in the folding process. To understand the principles governing protein folding it is important to study these partly folded conformations [4-6]. The best way to do this is to study protein unfolding by strong denaturants such as urea or GdnHCl since these denaturants can really transform proteins in a more or less completely unfolded state [7]. The development of wide range of sensitive techniques has led to the identification and characterization of stable intermediates in several proteins [8]. By recording changes in intrinsic tryptophan fluorescence and the secondary and tertiary structural features of protein in response to tailored changes in surroundings, one can establish presence of interesting structural intermediates relevant to structure-function relationship of the protein.

The aggregation of the protein is a phenomenon associated with many neurodegenerative diseases such as amyloidoses, prion disease and cataracts, that are caused by non-specific protein interactions [9]. In this regard, different agents such as temperature, pH, chaotropic agents and denaturants, either individually or in combination of the denaturants were used to study the conformational stability of the proteins. Denaturation is followed by monitoring the changes in any measurable physical property of the protein such as intrinsic fluorescence, CD spectra and corresponding change in the protein activity are checked.

The purification, characterization, and chemical modification of α-mannosidase from *A. fischeri* have already been reported (Chapter 2). The energetics of catalysis and inhibition of the enzyme has recently been studied (Chapter 3). The environment of tryptophans in the native and denatured states also has been studied by steady state and time- resolved fluorescence spectroscopy (chapter 5). As a next step towards the understanding of a correctly folded structure and conformational stability of the α-mannosidase from *A. fischeri*, folding and unfolding experiments on α-mannosidase were carried out with

different denaturants like pH, Urea and Guanidium hydrochloride and transitions in the structure were monitored by biophysical techniques correlating with activity.

Material and methods:

1-anilino-8-naphthalenesulfonate (ANS), Guanidine hydrochloride (GdnHCl), Urea were obtained from Sigma, USA. All other reagents used were of analytical grades. Solutions prepared for spectroscopic measurements were in MilliQ water.

Production and Purification of α-mannosidase

Production, purification and enzyme assay were carried out as described in chapter 2.

Protein concentration estimation

Protein concentration was determined according to the method of Lowry[10] using bovine serum albumin as standard.

Zymogram of α-mannosidase

The enzyme (25 µg) was loaded on to the SDS gel (7.5 %) and allowed to run for 2hrs. The gel was removed and suspended in 50 µM 4-methylumbelliferyl α-mannopyranoside for 20 min in water both at 50 ^{0}C. The gel was washed with water to remove excess of 4-methylumbelliferylα-mannopyranoside and visualized under UV light.

Fluorescence Measurement

Intrinsic fluorescence of the enzyme was measured using a Perkin-Elmer Luminescence spectrometer LS50B connected to a Julabo F20 water bath. The protein solution of 1.44 µM was excited at 280 nm and the emission was recorded in the range of wavelength 300-400 nm at 30 ^{0}C. At 280 nm, although major fluorescence is due to tryptophan residues, tyrosine fluorescence also contributes to it and the overall conformation can be monitored under different conditions. The slit widths for the excitation and emission were set at 7.0 nm, and the spectra were recorded at 100 nm/min. To eliminate the background emission the signal produced by either buffer solution or buffer containing the appropriate quantity of denaturants was subtracted.

Thermal Inactivation of α-mannosidase

Effect of temperature on α-mannosidase was studied using a thermostatic cuvette holder connected to an external constant temperature circulation water bath. The protein sample (1.44 μM) was incubated for 10 min at specified temperature before taking the scan. For renaturation experiments the samples were cooled to 30 ^{0}C and left for 2 h before recording the spectra. Fluorescence spectra were recorded as described above. Time course of temperature effect on α-mannosidase was carried out by incubating the enzyme in the temperature range of 40-60 ^{0}C, for 2 h. The aliquots were removed after 20 min interval and the activity was checked under standard assay conditions. Activity at zero minute at 30^{0}C was taken as 100%.

Effect of pH

Samples of α-mannosidase (0.72 μM) were incubated in an appropriate buffer over the pH range of 1-12 for 3 h at 30 ^{0}C. The following buffers (50 mM) were used for these studies: Glycine-HCl for pH 1-3, acetate for pH 4-5, phosphate for pH 6-7, Tris-HCl for pH 8-9 and Glycine-NaOH for pH 10-12. pH of the reaction remained stable till the end when it was checked. For refolding experiments, the pH of each sample was adjusted back to pH 7 and incubated at 30 ^{0}C for 1 h before recording the spectral measurement. Fluorescence spectra were recorded as described above.

Quenching studies

Fluorescence quenching experiments were carried out by the addition of a small aliquot of acrylamide, KI or CsCl stock solution (5 M) to the protein solution (0.90 μM) previously incubated at pH 2 or 6.5 at 25 ^{0}C for 2 h and the fluorescence intensities were determined. Protein was excited at 295 nm and emission spectra were recorded in the range of 300-400 nm. Slit widths of 7 nm each were set for excitation and emission monochromators.

Iodide stock solution contained 0.2 M sodium thiosulfate to prevent formation of tri-iodide (I^{-3}). For quenching studies of a denatured protein, the protein was incubated with

6 M GdnHCl overnight at room temperature. Fluorescence intensities were corrected for volume changes before further analysis of quenching data.

The steady-state fluorescence quenching data obtained with different quenchers were analyzed by Stern–Volmer (Eq. 1) and modified Stern–Volmer (Eq. 2) equations in order to obtain quantitative quenching parameters[11].

$$Fo/Fc = 1 + Ksv\,[Q] \quad (1)$$

$$Fo/\Delta F = f_a^{-1} + 1/[K_a f_a\,(Q)] \quad (2)$$

Where Fo and Fc are the relative fluorescence intensities in the absence and presence of the quencher, respectively, (Q) is the quencher concentration, Ksv is Stern–Volmer quenching constant, $\Delta F = Fo - Fc$ is the change in fluorescence intensity at any point in the quenching titration, K_a is the quenching constant for accessible fraction and f_a is the fraction of the total fluorophore accessible to the quencher. Equation (2) shows that the slope of a plot of $Fo/\Delta F$ versus $(Q)^{-1}$ (modified Stern–Volmer plot) gives the value of $(K_a f_a)^{-}1$ and its Y-intercept gives the value of f^{-1}_a .

Guanidium Hydrochloride (GdnHCl) Mediated Unfolding

Protein samples (1.44 μM) were incubated in 0-6 M denaturant solution at pH 6.5 for 3 h to attain the equilibrium. Fluorescence spectra were recorded as described above. After taking the scans suitable aliquots were removed from the samples to check for activity. Refolding experiments were conducted on samples diluted 10 times to dilute the GdnHCl and incubated at 30 ^{0}C and left for 2 h before recording the spectra. Fluorescence spectra were recorded as described above.

Urea-Mediated Unfolding

Protein samples (1.44 μM) were incubated in 0-6M denaturant solution at pH 6.5 for 3h to attain the equilibrium. Fluorescence spectra were recorded as described above.

Denatured protein samples were allowed to renature by diluting them ten times and incubating at 30 ^{0}C for 2 h. Fluorescence spectra were recorded as described above.

ANS-binding Assay

The intermediate states of denatured and native α-mannosidase under different denaturing conditions were analyzed by the hydrophobic dye (ANS) binding. The final ANS concentration used was 50 μM, excitation wavelength, 375 nm and total fluorescence emission was monitored between 400-550 nm. Reference spectrum of ANS in each buffer of respective pH and GdnHCl was subtracted from the spectrum of the sample.

Light Scattering

Protein aggregation upon thermal, pH and GdnHCl denaturation was detected using light scattering method. The same experimental setup used for fluorescence studies was employed for this purpose. Both excitation and emission wavelengths were set at 400 nm. Excitation and emission slit widths were set at 5 nm and 2.5 nm respectively. Scattering was recorded for 120 seconds.

Circular Dichroism Measurements

The CD spectra were recorded on a J-175 Spectropolarimeter with a PTC343 Peltier unit (Jasco, Tokyo, Japan) at 25 ^{0}C in a quartz cuvette. Each CD spectrum was accumulated from eight scans at 50 nm/min with a 1 nm slit width and a time constant of 1 s for a nominal resolution of 0.5 nm. Far UV CD spectra (2.6 μM) were collected in the range of wavelengths of 200-250 nm using a cell path length 0.1 cm for monitoring secondary structure. All spectra were corrected for buffer contributions and observed values were converted to molar ellipticity. The tertiary structure of the enzyme (8.6 μM) was monitored with near UV CD spectra in the wavelength 250-300 nm using path length 1 cm. Results were expressed as mean residue ellipticity (MRE) in deg cm^2 dmol^{-1} defined as

$$MRE = M\,\theta_\lambda / 10\,d\,c\,r$$

Where M is the molecular weight of the protein, θ_λ is CD in millidegree, d is the path length in cm, c is the protein concentration in mg/ml and r is the average number of amino acid residues in the protein. Helical content was calculated from the MRE values at 222 nm using the following equation

% helix = (MRE 222nm – 2340)/30300 *100.

Results and discussion:

Thermal Denaturation of α-mannosidase

Monitoring the activity of α-mannosidase from *Aspergillus fischer*i, incubated at different temperatures for different time intervals revealed the maximum stability of the enzyme to be at 50 ^{0}C for 40 min (Fig. 4.1A).The intrinsic fluorescence of the protein was monitored at different temperatures to correlate the thermal instability with conformation. The fluorescence spectrum of native enzyme showed a plateau in the range of 338 - 350 nm (Fig. 4.1B) indicating Trp residues present in differential environment (Chapter 5). The fluorescence intensity of the enzyme gradually decreased with increasing temperature which could be due to the deactivation of the single excited state by non-radiative process. At 70 ^{0}C, the spectrum showed a peak at 350 nm and at 90 ^{0}C, at 353 nm due to the exposure of buried Trp of partially unfolded protein to the solvent.

The Far UV CD spectra of the enzyme were recorded at different temperatures to monitor the changes in secondary structure (Fig. 4.1C). Gradual decrease in the ellipticity was observed with increase in temperature. The inset of the figure 4.1C shows slow decrease in the α-helix content of the protein on thermal denaturation. The α-helical content of the protein was reduced by 8 % at 50 ^{0}C while positive ellipticity at 190 – 195 nm was almost same in the temperature range of 35 – 50 ^{0}C. The activity is not affected in this range. At 60 ^{0}C, 18 % and at 70 ^{0}C and above, 25 % loss in the α-helical content of the protein was observed with significant decrease in the positive ellipticity. Although the

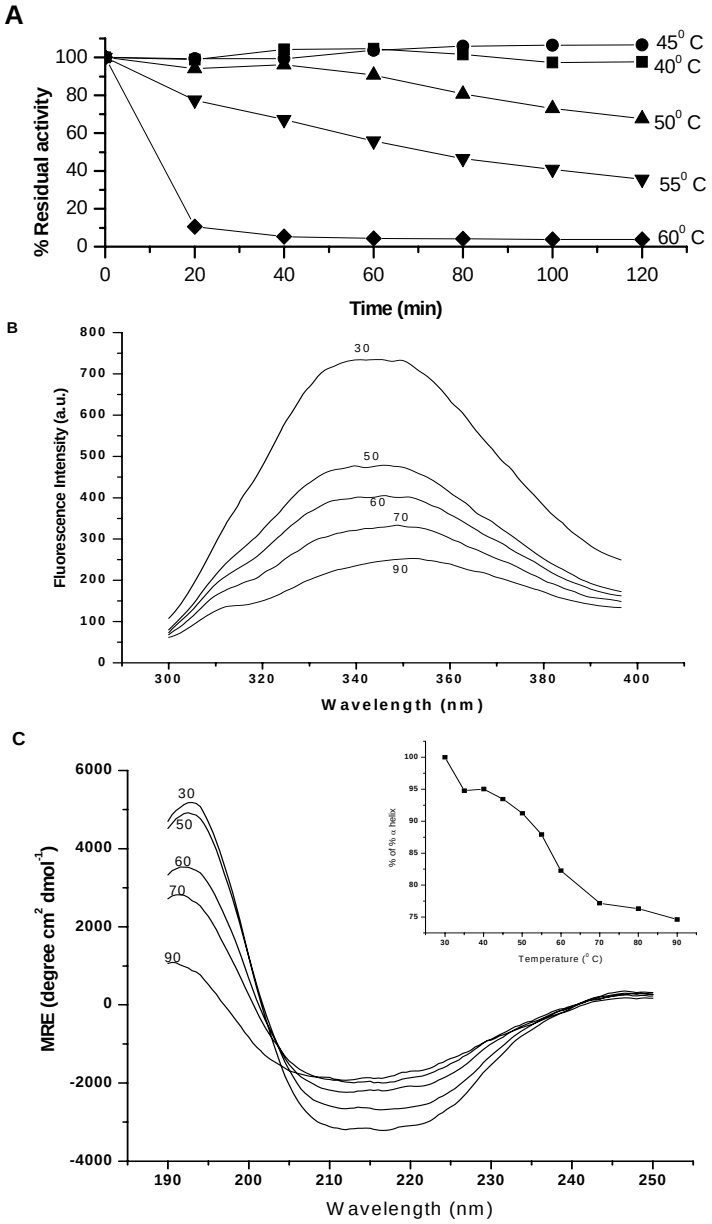

Figure 4.1: Thermoinactivation and denaturation of α-mannosidase: (A) Time course study of the enzyme at different temperature. (B) Flurorescence Scans of protein (1.44 μM) incubated at different temperature for 10 min. (C) Far UV CD spectra of α-mannosidase at different temperature. 2.60 μM of protein was used, each sample was incubated for 10 min at the respective temperature and then scans were recorded. **Inset**: The per cent α helical content of protein calculated by the formula given in material and methods.

λ_{max} of the fluorescence spectrum is at 355 nm indicating unfolding of the protein, major unfolding of the protein does not take place even at 90^0C, as evident from the far UV CD spectra.

No change in the light scattering intensity of the protein was observed till 90 ^{0}C, as there was no aggregation due to thermal denaturation. Renaturation or cooling of the heated protein samples to 30 ^{0}C did not lead to reactivation of enzyme indicating irreversibility of the thermal inactivation of α-mannosidase. Thermal inactivation of the enzyme taking place before any structural change has been reported in BSH [12].

Effect of pH on α-mannosidase

The enzyme shows maximum activity at pH 6.0-6.5 and is most stable in range of pH 5.0 – 7.0. Inactivation of the enzyme is fast below pH 5.0 and slow above pH 8.0 and is irreversible.

The fluorescence scans at different pH show decrease in the fluorescence intensity at pH 1, 2 and 3 than at pH 6.5 (Fig. 4.2A) which could be due to the acid quenching and neutralization of COO^- groups on amino acid in the vicinity of tryptophan [13]. Under extreme pH conditions, red shift in the λ_{max} to 353 nm was observed indicating partial unfolding of the protein, which was further characterized by hydrophobic dye binding.

ANS binding for α-mannosidase was carried out at different pH. The protein could bind ANS only at extreme acidic pH, maximum at pH 2.0 showing blue shift in the λ_{max} from 520 to 480 nm and four times increase in the fluorescence intensity (Fig. 4.2B). Partial unfolding of the protein was observed at pH 2.0, as the λ_{max} of intrinsic fluorescence scan was red shifted to 353 nm. The binding of hydrophobic dye (ANS) to α-mannosidase indicated the exposure of hydrophobic patches in protein at extreme acidic pH.

Far UV CD-spectrum at pH 6.5 showed a trough with minima at 210 nm and 222 nm indicating presence of both α and β structures in the enzyme (Fig. 4.3A). The secondary structure elements calculated using the software CD Pro are 24% (Helix), 23.6% (Sheet), 21.2% Turn and 31.3% unordered structure (RMSD 0.028 and NRMSD 0.012). At pH

2.0, there is substantial rearrangement of the secondary structural elements as compared to pH 6.5.

Near UV CD spectrum of α-mannosidase (Fig. 4.3B) at pH 2.0 shows decrease in the overall ellipticity indicating change in the environment of the aromatic amino acid residues during which, the hydrophobic patches must be getting exposed on the surface of the protein. An inactive but compact intermediate with rearranged secondary structure, altered tertiary structure, exposed hydrophobic amino acids on the surface of the protein together show that the molten-globule like intermediate exists at pH 2.0. Structural changes of α-mannosidase at extreme pH were found to be irreversible as indicated by unaltered λ_{max} of the fluorescence spectra of the protein samples under renaturing conditions.

Acids and bases are known to denature proteins by disrupting their electrostatic interactions. Protonation of all ionizable side chains below pH 3.0 leads to charge-charge repulsion and consequently protein unfolding. This induces loosening of side chain packing and the exposure of hydrophobic groups to solvent. Several proteins have been shown to exist in molten globule form at extremely acidic pH, Glucose/Xylose Isomerase [14], α-crystalin [15], Xylanase [16], glutathione transferase [17] and glucose oxidase [18]. Molten globule may be one of the first conformations embraced by the polypeptide chain in folding from the unfolded state [19].

The molten-globule like structure was further characterized by applying denaturation conditions and performing solute quenching studies. At pH 2.0, the enzyme treated with GdnHCl (0-6M) showed gradual increase in the fluorescence intensity with increase in the GdnHCl concentration (Fig. 4.4). The denaturation profile was different than that of protein at pH 6.5 which is presented in the section 3.3. The tyrosine peak became prominent, the intensity of which increased with increase in the concentration of GdnHCl. This unusual pattern of fluorescence spectra could be due to the complex mechanism of energy transfer. There was no ANS binding with protein at pH 2.0 under these conditions.

A

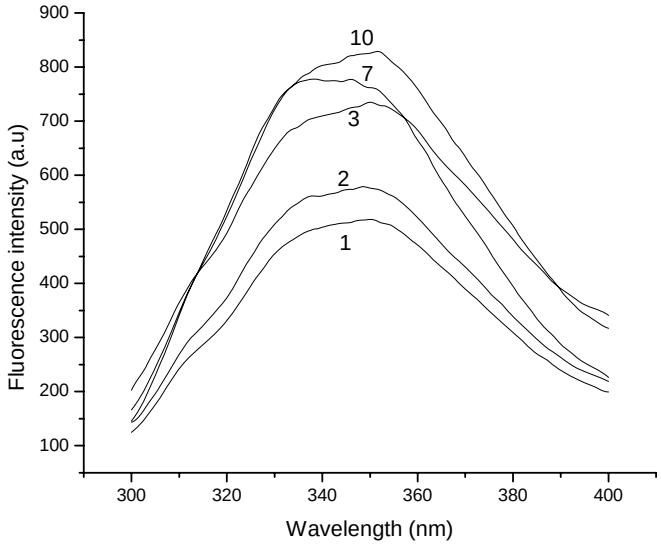

B

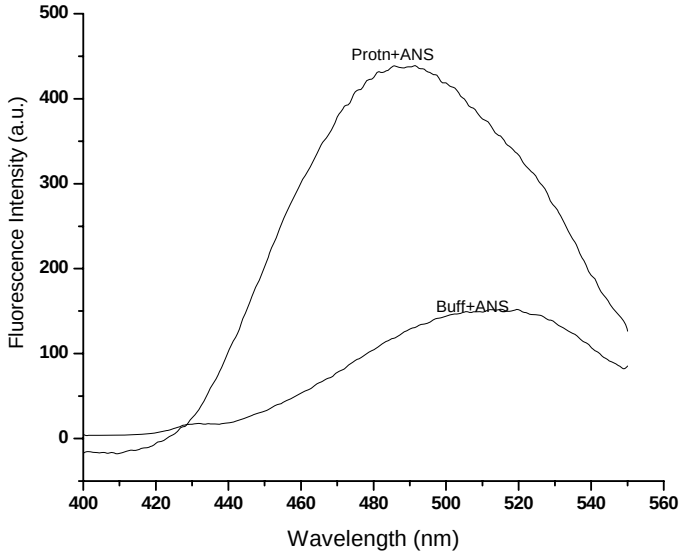

Figure 4.2: pH dependent denaturation: (A) Fluorescence spectra of α-mannosidase (1.44 μM) at different pH. The numbers on the spectra indicate the respective pH of the sample. (B) Fluorescence spectra showing ANS binding of α-mannosidase (1.44 μM) at pH 2.0.

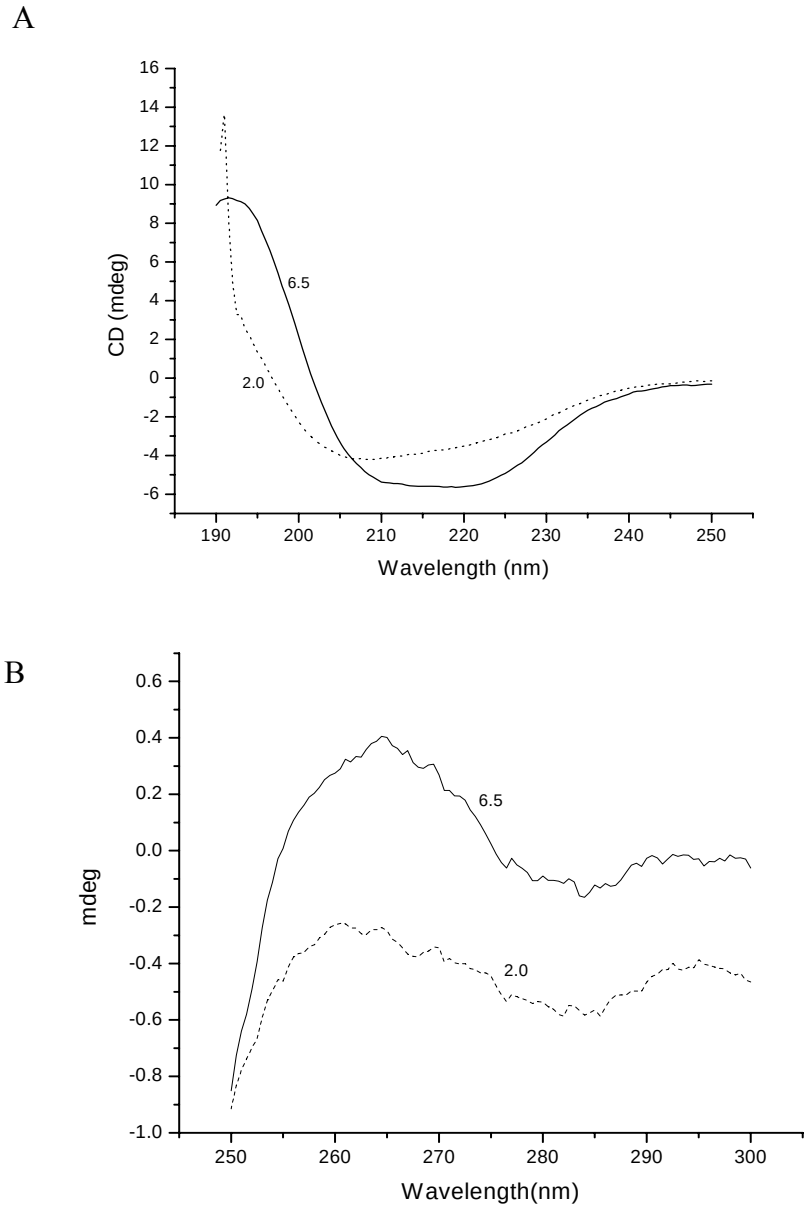

Figure 4.3: pH dependent denaturation: (A) Far UV CD spectrum of the α-mannosidase (2.6 μM) at pH 6.5 and 2.0. (B) Near UV CD spectrum of α-mannosidase (8.6 μM) at pH 6.5 and 2.0. The protein samples were incubated for 2 h at respective pH for both the experiments.

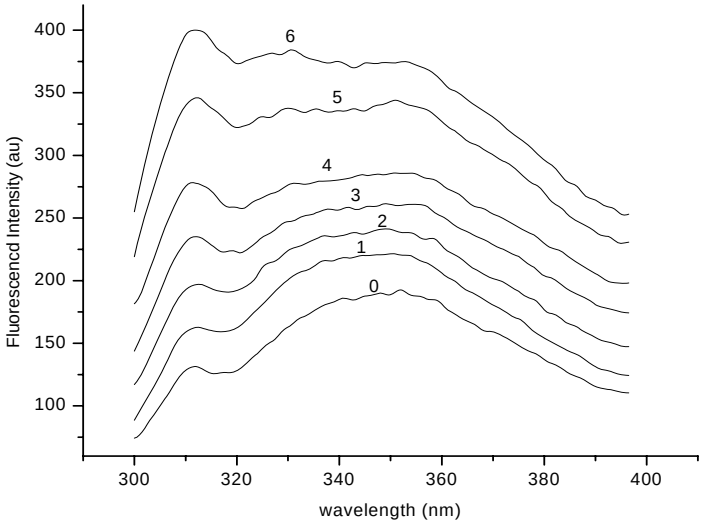

Figure 4.4: pH dependent denaturation: Fluorescence spectra of α-mannosidase treated with different concentrations of GdnHCl (0-6 M) at pH 2.0. The protein (0.72 μM) was incubated with GdnHCl (0-6M) for 2 h and fluorescence scans were recorded.

Quenching of α-mannosidase at pH2.0

Fluorescence quenching studies were carried out with quenchers like acrylamide, KI and CsCl at pH 2.0 (Table 4.1). Total fluorescence accessible to acrylamide was more (100%) at pH 2.0 while that under native condition accessibility was 73% (Chapter 5). For KI, fraction accessible at pH 2.0 was 67% which is double that of native protein. CsCl showed six times more accessibility as compared to native state which could be due to the redistribution of the charge density.

Ksv, the collisional quenching constant, for KI is more at pH 2.0 than native and denatured ones due to more positive charge and more exposure as compared to native protein. Ksv for KI is more than CsCl which can be again explained by the same property of protein at lower pH i.e., protein become more positively charged, so KI which is positive quencher quenches more as compared to CsCl. Stern-Volmer plots were biphasic in case of KI at pH 2.0 which shows the heterogeneity in tryptophan environment.

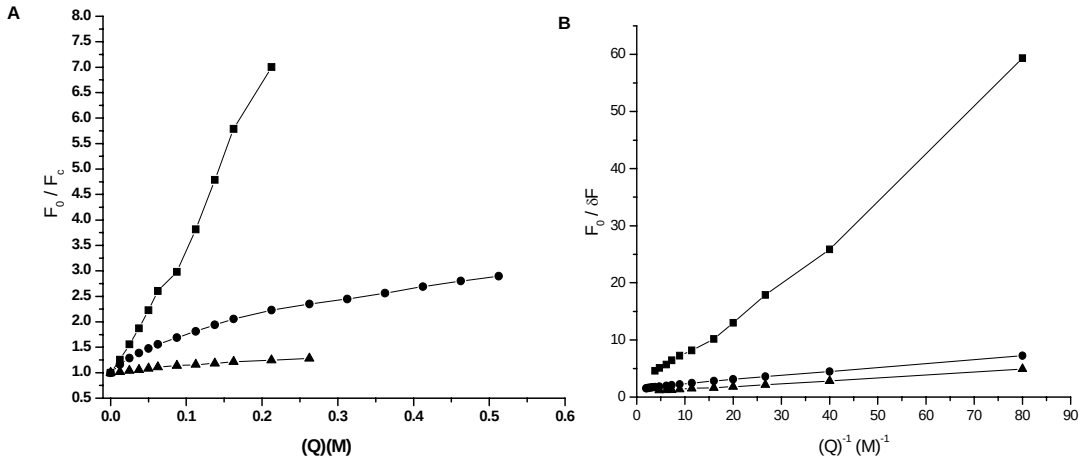

Figure 4.5: Fluorescence Quenching at pH 2.0: (A) Stern-Volmer plot and (B) Modified Stern-Volmer plot for quenching of α-mannosidase (■) Acrylamide (●) KI (▲) CsCl.

Table 4.1: Summary of parameters obtained from the intrinsic fluorescence quenching of α-mannosidase at pH 2.0.

Quencher and condition*	K_{sv1} (M^{-1})	K_{sv2} (M^{-1})	*f*a	K_q
Acrylamide				
Native	3.414	-	0.73	6.72
Native + GdnHCl 6M	10.634	-	1.00	8.57
pH 2.0	28.89	-	1.00	16.64
KI				
Native	1.821	0.835	0.33	9.65
Native + GdnHCl 6M	3.670	-	0.71	7.90
pH 2.0	6.966	2.462	0.665	21.37
CsCl				
Native	1.017	0.311	0.124	10.32
Native + GdnHCl 6M	1.050	-	0.380	5.84
pH 2.0	0.368	-	0.697	1.511

* Values for the Native and denatured protein have been taken from the Chapter 5, **Table 5.2**.

CsCl showed lesser Ksv values than native and denatured samples. This may be again due to lower pH of the protein environment.

Effect of GdnHCl and Urea on α-mannosidase

The enzyme lost 54% and 70% of the original activity in 0.5M and 1.0M GdnHCl, respectively (Fig. 4.6) which could be due to the modification of carboxylate group at the active site of α-mannosidase. Specific chemical modification studies of the enzyme have revealed presence of one carboxylate group at the active site region of the protein. The positively charged guanidinium group electro statically interacts with the carboxylate group causing inactivation. With urea the effect is milder as compared to GdnHCl. At 0.5M Urea, the enzyme loses just 4% of the activity within 30 min and at 1.0M urea, the enzyme lost around 35% of the activity (Fig. 4.6). This shows at low concentrations urea is not affecting the enzyme activity much.

Fluorescence spectra of the enzyme treated with 0-6M GdnHCl at pH 6.5 show decrease in the intensity up to 3M GdnHCl (Fig. 4.7A), λ_{max} of the fluorescence of the inactivated protein in 2M GdnHCl shifted to 352 nm indicating partial unfolding of the protein. The broad fluorescence spectrum of the protein was transformed into the sharper one with λ_{max} 352 nm, in presence of 1.5 M GdnHCl. The λ_{max} consequently shifted to 355 nm at higher concentration indicating the gradual unfolding of the protein. Increase in fluorescence intensity of the protein in presence of $\geq$ 4.0 M GdnHCl could be due to the change in the microenvironment of tryptophan of the unfolded protein. In case of urea denaturation, the fluorescence spectra followed the same pattern as that of GdnHCl treated samples but the fluorescence intensities above 4M urea are more than that of native protein.

The far UV CD spectra of GdnHCl treated samples (Fig. 4C and inset) show that there is insignificant decrease in the α-helical content of the protein in presence of 1.0 M GdnHCl. Significant loss in the α-helical content of the protein in presence of 1.5 M and drastic loss at ≥ 2.0 M GdnHCl was observed. Major loss of enzyme activity in presence

of 1.0 M GdnHCl takes place before any significant change in the secondary structure of the protein.

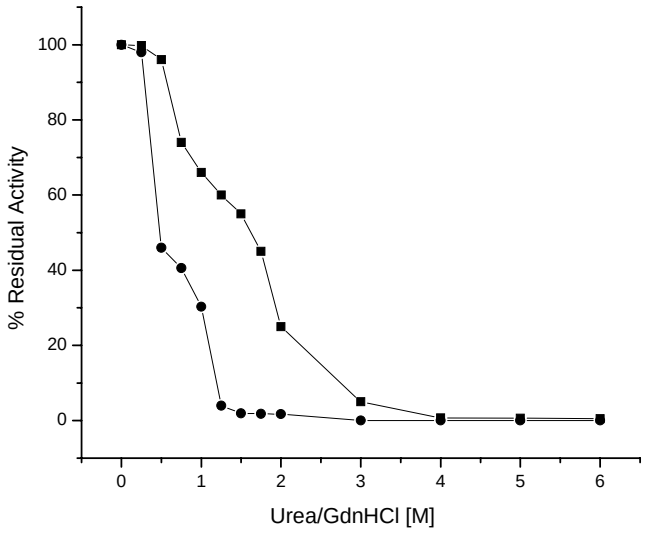

Figure 4.6: Per cent residual activity of α-mannosidase at different concentrations of (●) GdnHCl and (■) Urea.

Under denaturing conditions the energy transfer from Tyr or Trp residues does not occur any more and frequently results in increased tyrosine emission in the fluorescence spectra [20]. In the present studies, tyrosine peak becomes prominent and intensity increases with increase in GdnHCl concentration. There is initial decrease in fluorescence intensity and then increase in presence of higher concentrations of GdnHCl (> 4M). The excited states of tryptophan interact with water molecules to form excited state complexes and such a process competes with the radiative relaxation and leads to diminution of the fluorescence intensity [21-23].

The enzyme did not get reactivated after dilution of 0.5 or 1.0 M denaturant. After renaturation of the samples denatured with 3-6M GdnHCl, the ratio of fluorescence intensity (336/356) increased from 0.85 to 0.91 indicating irreversibility of denaturation.

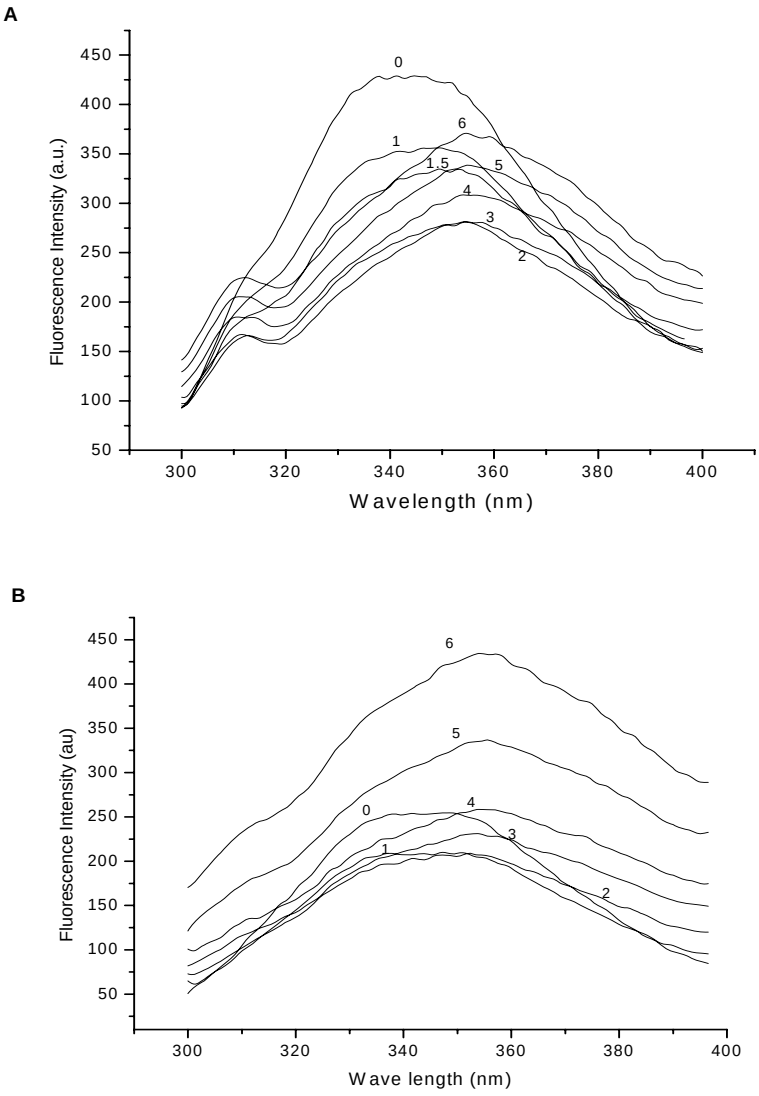

Figure 4.7: Fluorescence scans showing the spectra of α-mannosidase (1.44 μM) at different concentrations of (A) GdnHCl and (B) Urea. Numbers on the spectra indicate molarity of the denaturant.

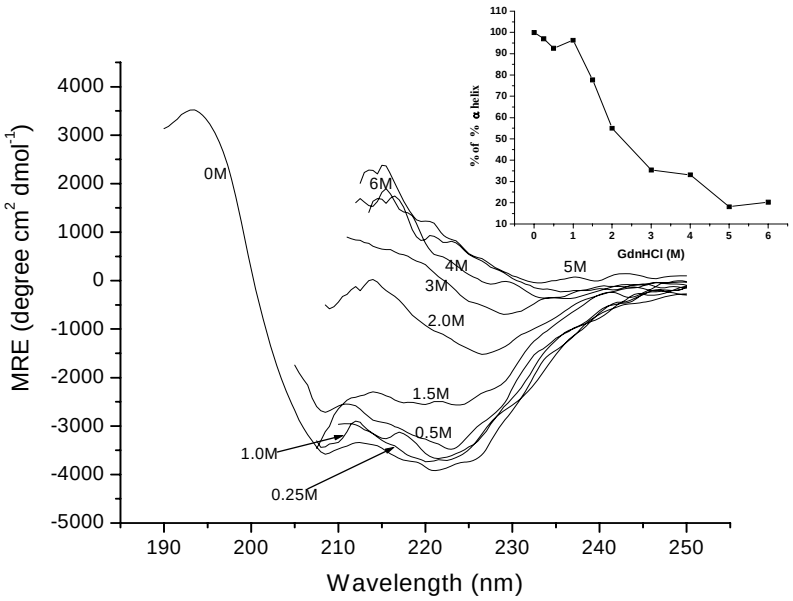

Figure 4.8: Far UV CD spectra of α-mannosidase at different concentrations of GdnHCl (0 – 6 M). All the protein samples were kept in denaturant for 2 h and scans were recorded. **Inset:** The per cent α helical content of protein calculated by the formula given in material and methods.

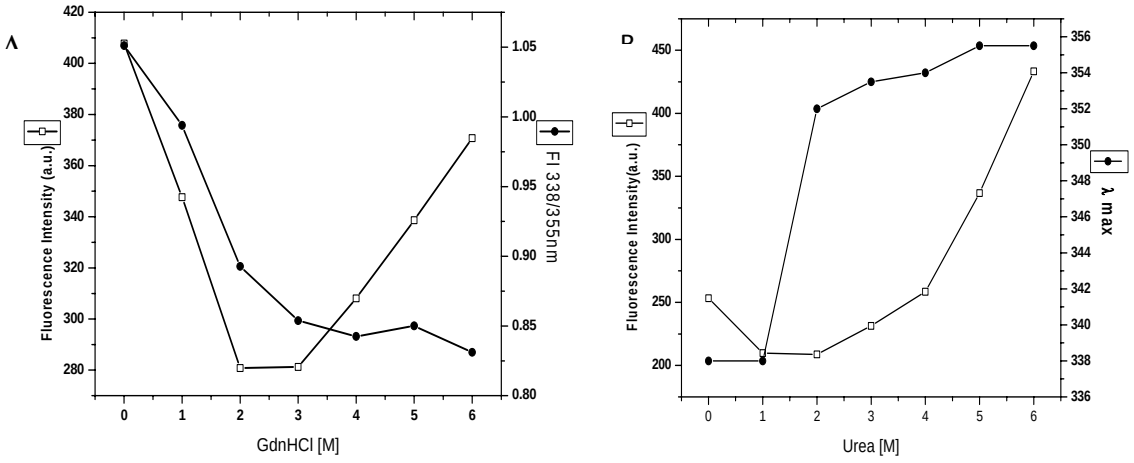

Figure 4.9: (A) Plot of fluorescence intensity (□) and ratio of FI at 338/355 (●) for GdnHCl denaturation. (B) Plot of fluorescence intensity (□) and λ_{max} (●) for Urea denaturation.

Allowing the protein to renature for more time did not help in reconstituting the tructure. The midpoint values of GdnHCl mediated changes measured by inactivation, fluorescence and negative ellipticity are 0.48 M, 1.5 M and 1.9 M, respectively.

The present native α-mannosidase has a molecular mass of 412 kDa and is composed of six subunits of 69 kDa [20]. The SDS-PAGE of the protein incubated at 50 ºC in presence and absence of SDS shows fluorescence by activity staining method (Fig. 4.10) This protein species on the gel showed molecular mass of 210 kDa. The hexameric protein existing in the native state could be the dimer of trimers which is the ultimate active oligomeric structure of the enzyme.

.

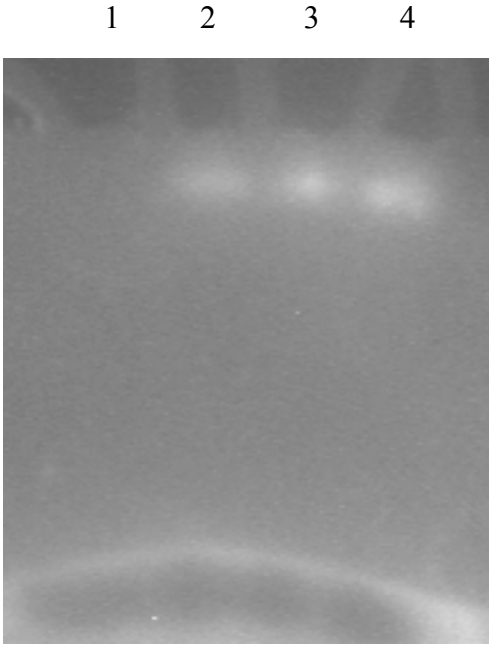

Figure 4.10: Zymogram showing the activity of α-mannosidase under different conditions: (1) Enzyme + SDS (0.1%) boiled (2) Enzyme + SDS (0.1%) kept at 50 ^{0}C for 10 min. (3) Enzyme + SDS (0.1%). (4) Enzyme.

The gel filtration of native and 1.5M GdnHCl treated enzyme on HPLC showed change in the retention time of the peak of the native enzyme indicating that the dissociation and unfolding of enzyme start simultaneously (data not shown)

Effect of GdnHCl at different temperature

Raylight scattering studies were carried out to monitor the formation of aggregates in the protein solution under different denaturing conditions. Exposure of the enzyme at 60 – 65 ^{0}C in presence of low concentrations of GdnHCl showed high light scattering intensity indicating the formation of insoluble aggregates (Fig. 4.11). In presence of 0.25 M and 0.5 M GdnHCl, the protein showed high light scattering intensity at 65 ^{0}C. No aggregation was observed at higher temperature in presence of ≥ 0.75 M concentration.

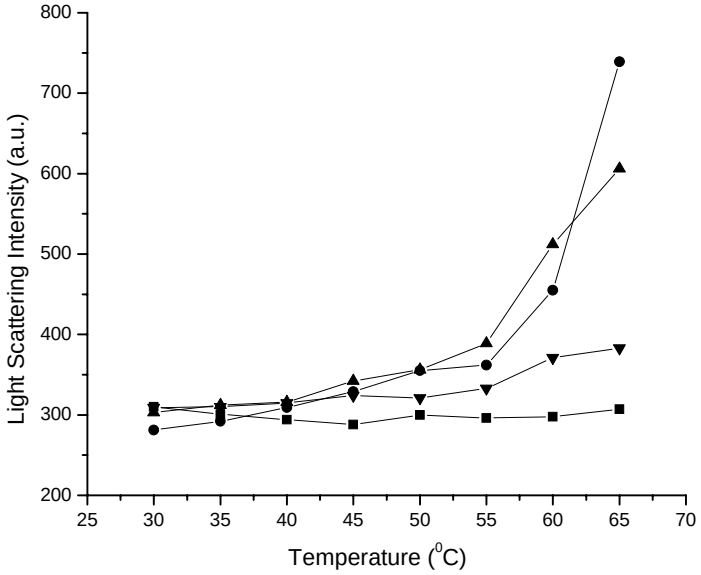

Figure 4.11: Light scattering by α-mannosidase (1.44 μM) in the presence of GdnHCl at different temperatures. Protein in the absence of (■) and in presence of 0.25 M (●), 0.5 M (▲) and 0.75 M (▼) GdnHCl was incubated at different temperatures for 10 min.

At 0.25 – 0.75 M GdnHCl, progressive inactivation and purturbance in the secondary structure of the enzyme was observed (Fig. 4.6A and 4.8). No aggregation of protein was observed due to thermal denaturation in the absence of GdnHCl. At 55 ^{0}C and above, the loss in the secondary structure has also been observed (Fig. 4.1C). There is a cumulative effect of disturbance in the secondary structure at 60 ^{0}C and in presence of GdnHCl.

Thus, due to distortion in the secondary structure, protein turns into insoluble aggregates on heating in presence of GdnHCl. The Trp environment of the α-mannosidase intermediate structure formed in the presence of 0.25 – 1 M GdnHCl showed decrease in fluorescence intensity. But the enzyme progressively lost catalytic activity and secondary structure. The protein under these conditions was susceptible to forming insoluble aggregates.

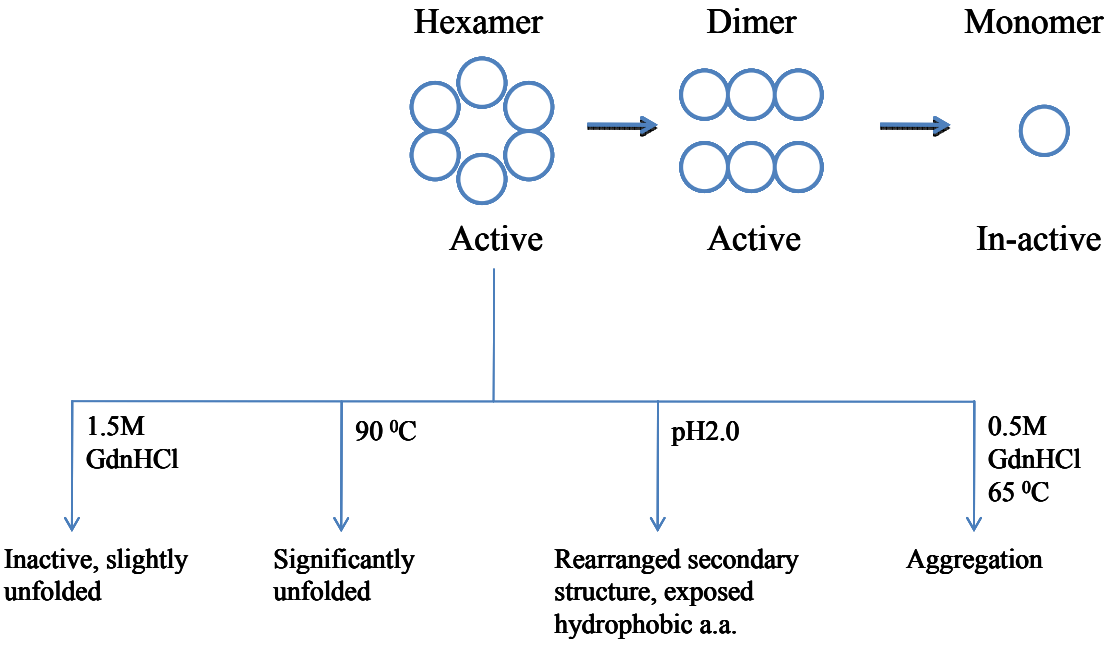

Figure 4.12: Schematic representation of different states of α-mannosidase under various denaturing conditions.

The aggregation process usually involves conformational change of the whole protein or of a specific domain and it is often attributed to the association of partially unfolded/folded molecules [21]. Aggregation process depends on temperature and it starts only after rearrangement of protein structure [22]. Irreversible unfolding of α-amylase was analyzed by unfolding kinetics, for all α-amylases the irreversible process

was found to be fast and the preceding unfolding transition was the rate limiting step [23].

During the course of the unfolding studies, i) the partially unfolded states at 90 °C and ii) in presence of 1.5 M GdnHCl, iii) molten globule-like structure at pH 2.0 and iv) heat aggregated state only in presence of low concentration of the denaturant were the interesting intermediates observed for the high molecular weight oligomeric enzyme. Loss of enzyme activity due to thermal and chemical denaturant, before any significant change in the conformation was also observed.

References:

[1] Nicholson, E.M. and Scholtz, J.M. (1996) *Biochemistry* **35**, 11369-11378.

[2] Agashe, V.R. and Udgaonkar, J.B. (1995) *Biochemistry* **34**, 3286-3299.

[3] Neet, K.E. and Timm, D.E. (1994) *Protien Sci* **3**, 2167-2174.

[4] Baldwin, R.L. (1991) *Chemtracts-Biochem Mol Biol* **2**, 379-389.

[5] Dill, K.A. and Shortle, D. (1991) *Annu Rev Biochem* **60**, 795-825.

[6] Dobson, C.M. (1992) *Curr Opin Stuct* **2**, 6-12.

[7] Tanford, C. (1968) *Adv Protein Chem* **23**, 121-282.

[8] Kuwajima, K. (1989) *Proteins* **6**, 87-103.

[9] Dobson, C.M. (2006) *Protein Pept Lett* **13**, 219-227.

[10] Lowry, O.H., Rosebrough, N.J., Farr, A.L. and Randall, R.J. (1951) *J Biol Chem* **193**, 265-75.

[11] Lehrer, S.S. (1971) *Biochemistry* **10**, 3254–3263.

[12] Kumar, R.S., Suresh, C.G., Brannigan, J.A., Dodson, G.G. and Gaikwad, S.M. (2007) *IUBMB Life* **59**, 118-125.

[13] Cowgill, R.W. (1975) *in Biochemical Fluorescence Concepts (Chen, R. F. and Edelhoch, H., Eds)*, pp 441-486, Marcel Dekker, New York.

[14] Pawar, S.A. and Deshpande, V.V. (2000) *Euro J Biochem* **267**, 6331-6338.

[15] Rajaraman, K., Raman, B. and Rao, M. (1996) *J Biol Chem* **271**, 27595-27600.

[16] Nath, D. and Rao, M. (2001) *Biochem Biophys Res Comm* **288**, 1218-1222.

[17] Luo, J.K., Hornby, J.A., Wallace, L.A., Chen, J., Armstrong, R.N. and Dirr, H.W. (2002) *Protein Sci* **11**, 2208-2219.

[18] Khatum Haq, S., Ahmad, F. and Khan, R.H. (2003) *Biochem Biophys Res Comm* **303**, 685-692.

[19] Vamvaca, K., Vogeli, B., Kast, P., Pervshin, K. and Hilvert, D. (2004) *Proc Natl Acad Sci USA* **101**, 12860-12864.

[20] Gaikwad, S.M., Keskar, S.S. and Khan, M.I. (1995) *Biochim Biophys Acta* **1250**, 144-8.

[21] Vetri, V. and Militello, V. (2005) *Biophys Chemistry* **113**, 83-91.

[22] Stirpe, A., Guzzi, R., Wijma, H., Ph. Verbeet, M., Canters, G., W., and Sportelli, L. (2005) *Biochem Biophys Acta* **1752**, 47-55.

[23] Duy, C. and Fitter, J. (2005) *J Biol Chem* **280**, 37360-37365.

CHAPTER: 5

STEADY STATE AND TIME RESOLVED FLUORESCENCE STUDY

Summary: Apart from the vital role in glycoprotein biosynthesis and degradation, α-mannosidase is currently an important therapeutic target for the development of anticancer agents. Fluorescence quenching and time-resolved fluorescence of α-mannosidase, a multitryptophan protein from *Aspergillus fischeri* were carried out to investigate the tryptophan environment. The tryptophans were found to be differentially exposed to the solvent and were not fully accessible to the neutral quencher indicating heterogeneity in the environment. Quenching of the fluorescence by acrylamide was collisional. Surface tryptophans were found to have predominantly positively charged amino acids around them and differentially accessible to the ionic quenchers. Denaturation led to more exposure of tryptophans to the solvent and consequently in the significant increase in quenching with all the quenchers. The native enzyme showed two different lifetimes, τ_1 (1.51 ns) and τ_2 (5.99 ns). The average lifetime of the native protein (τ) (3.187 ns) was not affected much after denaturation (τ) (3.219 ns), while average lifetime of the quenched protein samples was drastically reduced (1.995 ns for acrylamide and 1.537 ns for iodide). This is an attempt towards the conformational studies of α-mannosidase.

Introduction:

Fluorescence spectroscopy is widely used to study peptides and proteins. The aromatic amino acids, tryptophan, tyrosine, and phenylalanine, offer intrinsic fluorescent probes of protein conformation, dynamics, and intermolecular interactions. Of the three, tryptophan is the most popular probe. Tryptophan occurs as one or a few residues in most proteins and biologically active peptides. The fluorescence of the indole chromophore is highly sensitive to environment, making it an ideal choice for reporting protein conformation changes and interactions with other molecules. The emission spectrum of tryptophan in proteins varies from a structured band to a broad, diffuse band with wavelength maximum spanning a 40nm range[1].

Among the properties used are changes in the fluorescence intensity, wavelength maximum (λ_{max}), band shape, anisotropy, fluorescence lifetimes, and energy transfer.

They are applied to folding/unfolding, substrate binding, external quencher accessibility, etc. The power of this probe has been considerably amplified by the finding that Trp can often be substituted for other amino acids by site-directed mutagenesis, with minimal effect on structure and activity. Trp λ_{max} is quite sensitive to its local environment, ranging from ~308 nm (azurin) to ~355 nm (e.g., glucagon) and roughly correlates with the degree of solvent exposure of the chromophore [2].

Studies of indole fluorescence quenching by added solutes have provided valuable information regarding the structure and dynamics of proteins in solution [3-9]. The quenching reaction involves physical contact between the quencher and an excited indole ring, and can be kinetically described in terms of a collisional and a static component. Static quenching is readily detected in proteins that are denatured, or contain only a single fluorophor. Quenching patterns for most multi-tryptophan containing proteins are difficult to analyze precisely, but qualitative information can, nevertheless, be extracted [7]. The most significant finding with this technique is that even tryptophan (Trp) residues that are presumably deeply buried within globular proteins are able to be quenched by the uncharged quenchers oxygen and acrylamide with quenching rate constants in the order of $l0^9$ $M^{-1}S^{-1}$. These results have been interpreted as indicating that the quenchers are able to penetrate into the matrix of globular proteins, with the penetration being facilitated by small-amplitude fluctuations in the protein structure occurring on the nanosecond time scale [5,7]. Ionic quenchers, being charged and heavily hydrated, should be able to quench only surface tryptophanyl residues [3,10].

In phosphorescence and fluorescence quenching study, Calhoun et al. [11] have emphasized another possible interpretation of the quenching of buried Trp residues. They have argued for a mechanism involving the local unfolding of a protein to expose internal residues to the solvent, followed by quenching of the transiently exposed residues by quencher. With increasing quencher size, one would expect decrease in the rate of penetration into a globular protein dramatically due to the increase in the amplitude of the required fluctuations [12]. Size of the quencher has little influence on the quenching by a local unfolding mechanism [11].

Steady-state measurements provide an intensity weighted average of the underlying decay processes. Therefore, steady-state signals are often proportional, not to the most populated state, but simply to the state that emits the most light. Time-resolved studies, however, can provide detailed information concerning the population distribution of molecular species in the excited state. Time-resolved fluorescence spectroscopy monitors events that occur during the lifetime of the excited singlet state. This time scale ranges from a few picoseconds to hundreds of nanoseconds. Relevant biological events that occur in this time domain include the rotation of whole proteins, of segments of polypeptide chains, and of individual amino acid side chains. In addition, the excited chromophore can interact with solvent molecules or neighboring amino acid residues [13].

Some pure fluorophores show monoexponential decay kinetics when they are dissolved in noninteracting solvents. In the case of biomolecules, multiexponential decay kinetics, nonexponential decay kinetics are more common. It is useful to consider possible origins of complex fluorescence decay in proteins. Clearly a mixture of fluorophores could give rise to multiexponential decay, with the number of decay constants equal to the number of components in the mixture. It might thus be possible to assign two decay constants found in a protein containing two tryptophans to the individual tryptophan residues. Likewise if a protein has only one tryptophan residue but exists in two conformations, biexponential decay kinetics might reflect these two states of the protein and could be used to investigate their interconversion. Microheterogeneity can also be more subtle. Tryptophan zwitterion itself shows biexponential decay, and one interpretation of this finding suggests that tryptophan exists in microheterogeneous (rotameric) forms. Multi- or non-exponential decay behavior may also arise from a pure homogeneous fluorophore undergoing an excited-state reaction.

In the present chapter, we report, on the basis of steady state fluorescence, solute quenching technique and time-resolved fluorescence, the exposure and environment of the tryptophan residues in the enzyme.

Materials and Methods:

Production and Purification of α-mannosidase

Production, purification and enzyme assay were carried out as described in chapter 2.

Protein concentration estimation

Protein concentration was determined according to the method of Lowry[14] using bovine serum albumin as standard.

Modification of Trp residue with N-bromosuccinimide (NBS)

Enzyme solution (1 ml, 5.8 μM) was titrated with freshly prepared N-bromosuccinimide (NBS) (2 mM) with different installments (5 μl each) till the protein to NBS ratio reached 1:10. Modification of protein with NBS was accompanied by a decrease in the absorbance of modified protein at 280 nm. The NBS modification was also carried out under denaturing conditions (6 M guanidium hydrochloride (Gdn-HCl)) and number of Trp residues modified were determined spectrophotometrically, assuming the molar absorption coefficient of 5,500 $M^{-1}cm^{-1}$ for the modified Trp at 280 nm [15].

Solute quenching studies by steady state fluorescence

Fluorescence measurements were performed for native and denatured protein with different quenchers like acrylamide (5 M), succinimide (2.5 M) (neutral quenchers), iodide (5 M) and cesium ions (5 M) (charged quenchers), on Perkin-Elmer LS 50B spectrofluorimeter at 30°C. α-Mannosidase samples of <0.1 OD were excited at 295 nm and emission spectra were recorded in range of 300–400 nm. Slit widths of 7.0 nm each were set for excitation and emission monochromators. Small aliquots of quencher stocks were added to protein samples and fluorescence spectra were recorded after each addition. Iodide stock solution contained 0.2 M sodium thiosulfate to prevent formation of tri-iodide (I^{-3}). For quenching studies with denatured protein, the protein was incubated with 6 M Gdn-HCl overnight at room temperature. Fluorescence intensities were corrected for volume changes before further analysis of quenching data.

The steady-state fluorescence quenching data obtained with different quenchers were analyzed by Stern–Volmer (Eq. 1) and modified Stern–Volmer (Eq. 2) equations in order to obtain quantitative quenching parameters [3].

$$F_o/F_c = 1+ K_{sv} [Q] \quad (1)$$

$$F_o/\Delta F = f^{-1}_a + 1/[K_a f_a(Q)] \quad (2)$$

Where F_o and F_c are the relative fluorescence intensities in the absence and presence of the quencher, respectively, (Q) is the quencher concentration, K_{sv} is Stern–Volmer quenching constant, $\Delta F=F_o-F_c$ is the change in fluorescence intensity at any point in the quenching titration, Ka is the quenching constant and fa is the fraction of the total fluorophores accessible to the quencher. Equation (2) shows that the slope of a plot of $F_o/\Delta F$ versus $(Q)^{-1}$ (modified Stern–Volmer plot) gives the value of $(K_a f_a)^{-1}$ and its Y-intercept gives the value of f^{-1}_a.

Lifetime measurement of fluorescence decay

Lifetime measurements were carried out on Edinburgh Instruments' FLS-920 single photon counting spectrofluorimeter. An H_2 flash lamp of pulse width 1.0 ns was used as excitation source and a Synchronization photomultiplier was used to detect the fluorescence. The diluted Ludox solution was used for measuring Instrument response function (IRF). The samples (1 mg/ml) were excited at 295 nm and emission was recorded at 336 nm. Slit widths of 15 nm each were used on the excitation and emission monochromators. The resultant decay curves were analyzed by a Reconvolution fitting program supplied by Edinburgh Instruments.

The bimolecular quenching constant K_q was calculated as $K_q = K_{sv}/\tau$ where τ is the average life time of the protein in the absence of a quencher. The average life time was calculated using the formula,

$$(\tau) = \sum_i \alpha_i \tau^2_i / \sum_i \alpha_i \tau_i, \text{ where } i = 1,2\ldots\ldots \quad (3)$$

Results and Discussion:

As described in earlier report [16], one tryptophan residue is essential for the activity of α-mannosidase from *A. fischeri*. In the present work, kinetics of the NBS modified enzyme with 45% residual activity was studied (chapter 2). There was no change in the K_m values (100 μM for native and 97.5 μM for modified enzyme) coupled with a decrease in the V_{max} values (0.286 μmol/min/mg for native and 0.122 μmol/min/mg for the modified enzyme) indicating that the tryptophan residue can be essential for the catalytic conformation. Tryptophan is also shown to be essential for the activity of α-mannosidase from Phaseolus vulgaris [17].

The number of tryptophans detected by NBS modification in the native enzyme and under denaturing conditions was found to be two and seven, respectively. Thus, five tryptophans seem to be present in the hydrophobic interior of the protein and two are exposed to solvent. The studies of tryptophan environment were taken up further.

Steady-state fluorescence of α-mannosidase and quenching studies

The spectrum of the native enzyme (Fig. 5.1A, spectrum 1) shows maximum fluorescence intensity between 333 nm to 348 nm indicating several populations of Trp, few in the hydrophobic environment and others, differentially exposed to the polar environment. The denatured protein shows λmax red shifted to 355 nm upon denaturation indicating polar environment due to exposure of the tryptophans (Fig. 5.1B, spectrum 1).

Tryptophan residues appear to be uniquely sensitive to quenching by a variety of solutes as a result of a propensity of the excited indole nucleus to donate electrons while in the excited state. Fluorescence spectra of the native and denatured α-mannosidase recorded in the absence and in the presence of increasing concentrations of acrylamide displayed higher extent of quenching in the presence of 6 M Gdn-HCl, clearly revealing that unfolding results in a significant increase in the accessibility of the tryptophan residues to the quencher. Also, denaturation led to a significant increase in the extent of quenching

with the other quenchers used in this study, namely succinimide, iodide and cesium (Table 5.1). The percentage quenching was calculated on the basis of raw data.

Of the four quenchers used, acrylamide was the most effective, quenching 67.0% of the total intrinsic fluorescence of the protein (at 0.46 M) whereas bulkier succinimide (0.30 M) quenched only 35.0% of the total available fluorescence. The ionic quenchers, iodide (0.30 M) and cesium ion (0.30 M), which cannot penetrate into the protein matrix and can access only surface exposed tryptophans were found to quench only 31.0% and 15.0%, respectively, of the total fluorescence intensity of *A. fischeri* α-mannosidase.

Significantly lower quenching observed with the neutral quencher succinimide, must be due to the bulkier nature of the molecule. The lower quenching with charged quenchers (I^- and Cs^+) with native α-mannosidase indicated most of the fluorescent tryptophan residues in the protein to be buried in the hydrophobic core of the protein. Additionally, lowest quenching observed with Cs^+ appears to be due to the inability of this quencher to access the fluorophores. This may be due to the presence of positively charged residues in the vicinity of some of the exposed (or partially exposed) tryptophan residues, which repel the positively charged cesium ion, but allow the neutral acrylamide and succinimide and the negatively charged iodide ion to approach the indole moieties of the tryptophan residues in their neighborhood.

The iodide ions could get concentrated in a positively charged environment in the vicinity of tryptophans which increased the probability of iodide ions colliding with them and quenching the fluorescence. Besides, the inherently low quenching efficiency of Cs^+ may also be partly responsible for the lower quenching observed with it [18].

Denaturation resulted in a significant increase in the quenching by all the four quenchers, with the extent of quenching observed being 85.0%, 57.0%, 57.0% and 30.0% with acrylamide, succinimide, iodide and cesium ion, respectively (Table 5.1). Even after denaturation, some residual conformation was present in the enzyme which prevented the access of the neutral quenchers to the tryptophan therein.

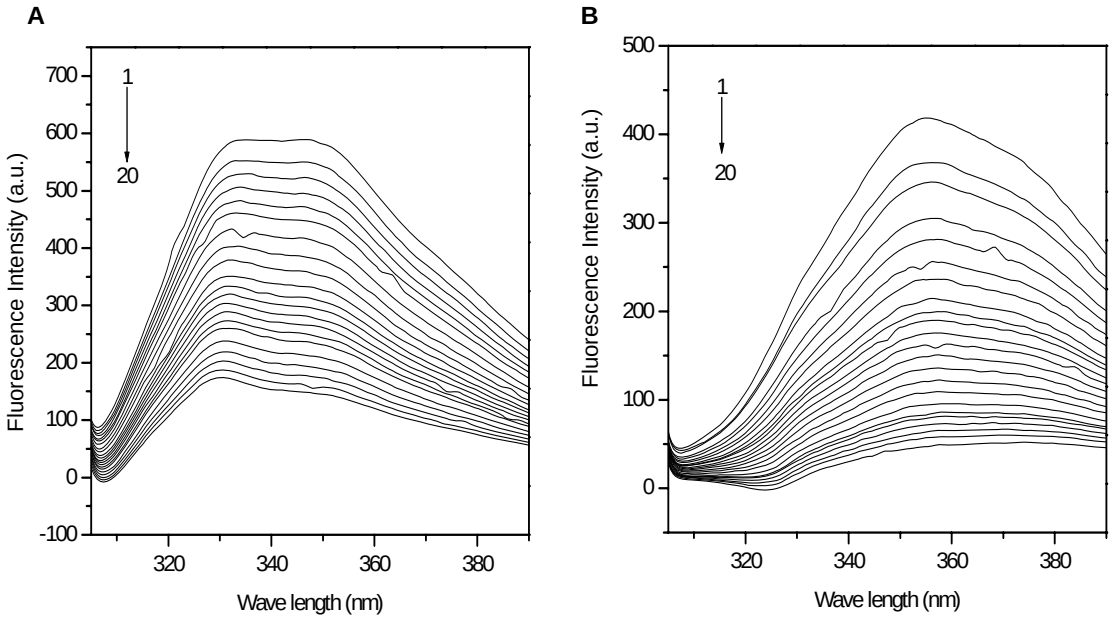

Figure 5.1: Fluorescence spectra of α-mannosidase in the absence and presence of acrylamide. (**A**) Under native conditions, (**B**) under denaturing conditions (6 M Gdn-HCl). Spectrum 1corresponds to protein alone and spectra 2–20 correspond to the protein in presence of increasing concentrations of acrylamide. The final concentration of the quencher in both **A** and **B** is 0.46 M.

Table 5.1: Extent of fluorescence quenching of *A. fischeri* α-mannosidase with different quenchers.

Quencher	**Quenching (%)**[a]	
	Native	**In 6 M GdnHCl**
Acrylamide(0.46 M)	67.0	85.0
Succinimide(0.30M)	35.0	57.0
Iodide ion(0.30M)	31.0	57.0
Cesium ion(0.30M)	15.0	30.0

[a] Quenching % was calculated from raw data.

Analysis of fluorescence quenching Data

The Stern–Volmer plots for the quenching of the protein with different quenchers are shown in Fig. 5.2. The quenching profiles obtained for native and denatured protein with acrylamide follow linear dependence on the quencher concentration (Fig. 5.2a) indicating collisional type of quenching. The profiles obtained with succinimide, iodide and cesium ion for native protein exhibited negative curvature (Fig. 5.2b–d) showing that certain tryptophans are selectively quenched before others in a protein. At low concentration of quencher, the slope of the Stern–Volmer plots reflects largely the quenching of the more accessible residues. At higher concentrations, the easily quenched fluorescence has been depleted, and those tryptophans having lower quenching constants become dominant. Similar quenching patterns have been observed for several multi-tryptophan proteins [3,19,20].

For denatured protein, all the four quenchers showed linear Stern–Volmer plots making it clear that upon denaturation, even buried tryptophans become exposed to solvent and are more accessible for quenching. These results indicate that tryptophans in *A. fischeri* α-mannosidase are present in different environments, some residues are partially or fully exposed to solvent while others are buried inside hydrophobic environment. These observations are in good agreement with the fluorescence spectrum of the native enzyme and also with the results of chemical modification experiments with NBS, where only two tryptophan residues in α-mannosidase could be modified under native condition and seven tryptophan residues could be modified upon denaturation of protein. This heterogeneity has also been shown by fluorescence life time measurements which is discussed later.

From the slopes of the two linear components of the Stern–Volmer plots, collisional quenching constants, K_{sv1} and K_{sv2} were obtained for succinimide, I^- and Cs^+ and are listed in Table 5.2. K_{sv1} is considerably greater than the K_{sv2} in case of succinimide, iodide and cesium giving substantial evidence for selective tryptophan quenching by these quenchers. Upon denaturation, the K_{sv1} increased nearly twice in acrylamide and

iodide ion, and slight increase in the value was observed for succinimide and cesium ion (Table 5.2). The Ksv value for Cs^+ is lower than that for I^-. The higher K_{sv} value of I^- as compared to Cs^+ indicates higher efficiency of quenching by I^- due to the presence of an electropositive environment around Trp residues in the enzyme.

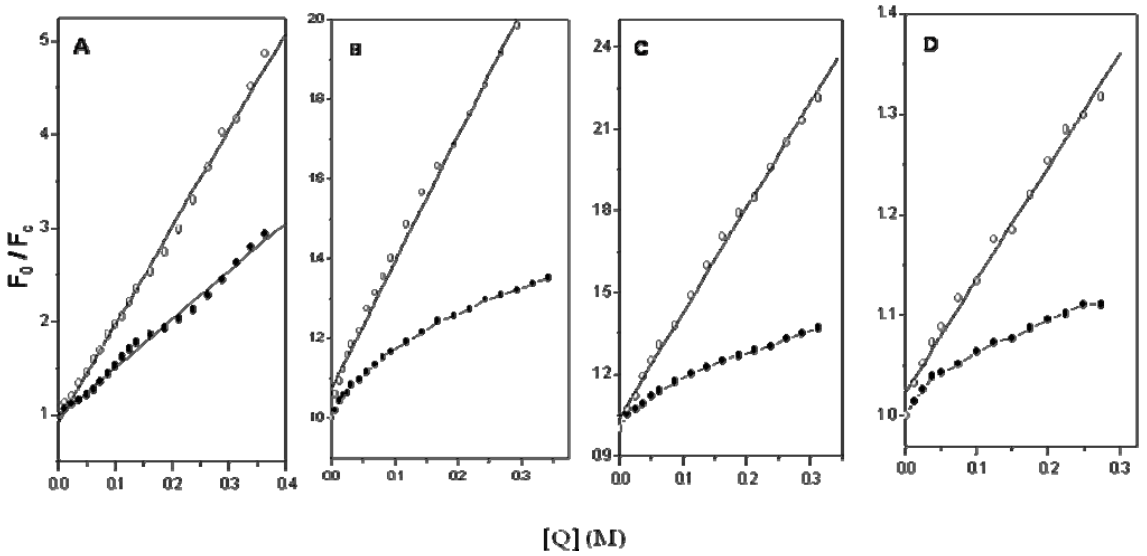

Figure 5.2: Stern–Volmer plots for the quenching of the intrinsic fluorescence of α-Mannosidase with different quenchers **A**, acrylamide; **B** succinimide; **C**, cesium ion; and **D**, iodide ion of the native enzyme (closed circles) and in the presence of 6 M Gdn-HCl (open circles). Titrations were carried out as described in the "Materials and methods" section.

Modified Stern–Volmer plots obtained with all four quenchers are shown in Fig. 5.3 from which f_a or fractional accessibility and K_a, quenching constant were obtained according to Eq. 2 and listed in Table 5.2. Based on the f_a values of the four quenchers used, 73.0% and 29.0% of the total fluorescence was found to be accessible to acrylamide and succinimide respectively, and 33.0% and 12.4% was accessible to I^- and Cs^+, respectively.

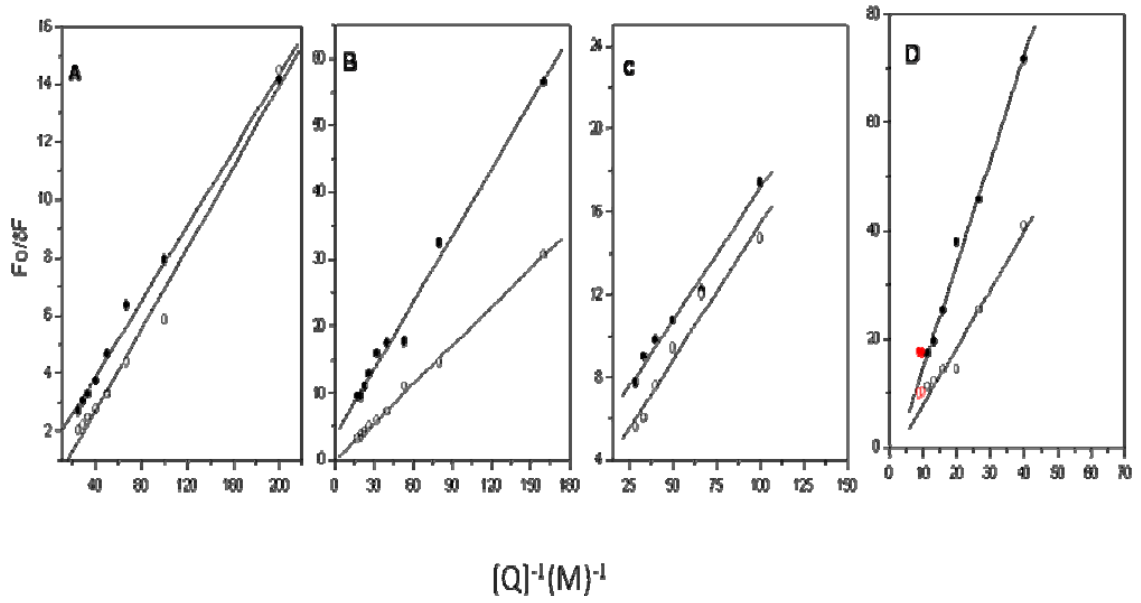

Figure 5.3: Modified Stern–Volmer plots for the quenching of the intrinsic fluorescence of α-mannosidase with different quenchers. A; acrylamide, **B;** succinimide, **C;** cesium ion, and **D;** iodide ion of the native enzyme (closed circles) and in the presence of 6 M Gdn-HCl (open circles). Titrations were carried out as described in the "Materials and methods" section.

Denaturation of protein with 6 M Gdn-HCl led to 100% accessibility with acrylamide. For succinimide, I^- and Cs^+, the fraction accessible increased to 57.0%, 71.0% and 38.0%, respectively. The complete accessibility of tryptophan residues to acrylamide and increased accessibility to other quenchers (succinimide, iodide and cesium) clearly indicated that the protein unfolds upon treatment with 6 M Gdn-HCl. The extent of the quenching achieved with Cs^+ is significantly lower than that observed with I^-, as explained above; it is quite likely that a larger fraction of the tryptophan residues have positively charged residues in their close proximity.

Table 5.2: **Summary of parameters obtained from the intrinsic fluorescence quenching of *A. fischeri* α-D-mannosidase with different quenchers.** K_{sv1} and K_{sv2} are Stern–Volmer quenching constants, K_{q1} and K_{q2} are bimolecular quenching constants, f_a is the fraction of accessible residues and K_a is the quenching constant obtained from modified Stern–Volmer analysis.

Quencher and Condition	**K_{sv1} (M^{-1})**	**$K_{q1}\times10^{-9}$ (M^{-1} S^{-1})**	**K_{sv2} (M^{-1})**	**$K_{q2}\times10^{-9}$ (M^{-1} S^{-1})**	**f_a**	**K_a**
Acrylamide						
Native	3.41	1.07			0.73	6.72
Native+Gdn. HCl 6M	10.63	3.30			1.00	8.57
Succinimide						
Native	3.12	0.98	0.55	0.17	0.29	11.55
Native+Gdn. HCl 6M	3.15	0.98			0.57	12.12
KI						
Native	1.82	0.57	0.84	0.26	0.33	9.65
Native+Gdn. HCl 6M	3.67	1.14			0.71	7.90
CsCl						
Native	1.02	0.32	0.31	0.1	0.124	10.32
Native+Gdn. HCl 6M	1.05	0.33			0.380	5.84

The bimolecular quenching constants K_{q1} and K_{q2} are also presented in Table 5.2. The K_q values for acrylamide and iodide quenching of the native enzyme do increase after denaturation while they are not affected in case of succinimide and Cs^+ quenching. Due to some residual conformation present even after denaturation, succinimide, the bigger

molecule will not have an easy access to deeply buried tryptophans and quenching by Cs^+ ions will still be restricted due to positive charge around tryptophans. Low K_q values reflect low collisional frequency.

Fluorescence lifetime measurement

The dynamics of the steady state fluorescence of α-mannosidase from *A. fischeri* was resolved to correlate the photo physical parameters of the protein to the structural properties. The intrinsic emission decay of the enzyme was studied in nanosecond domain (Fig. 5.4) and could be described by two decay components τ_1 and τ_2. The corresponding relative amplitudes α1 and α2 were obtained from reconvolution fit. The decay curves obtained from the lifetime measurement of intrinsic fluorescence of α-mannosidase could be fitted well into a bi-exponential curve (χ^2<1.01), since mono-exponential curves gave large errors (χ^2>1.2). From these fits, two decay times τ_1 (1.51 ns) with 37.19% contribution and τ_2 (5.992 ns) with 62.81% contribution for the Trp fluorescence of the native enzyme were obtained (Table 5.3), indicating the presence of more than one fluorophores differentially emitting the energy. In the present enzyme, the components having longer lifetime have major contribution to the total quantum yield.

For the denatured enzyme, again two decay times τ_1 (1.16 ns) and τ_2 (4.656 ns) with 39.28% and 60.72% contribution to the total fluorescence, respectively were observed. This can be due to the change in the conformation of the protein. The fact that this cannot be correlated with the steady state fluorescence spectrum of the denatured enzyme reflects the heterogeneity of the tryptophan environment of the multitryptophan enzyme.

The enzyme with one Trp modified (with NBS) and 40% residual activity was analyzed for the life time measurement of fluorescence decay. The shorter lifetime was reduced to 1.28 ns from 1.51 ns while longer lifetime was reduced to 5.88 ns from 5.99 ns. But, the contribution of shorter fluorescence lifetime component was decreased nearly by 4%, from 39.48% of native to 35.62% of the NBS modified, whereas for longer fluorescence lifetime component, same amount of contribution, about 4.0%, was increased from 60.72% of the native to 64.38% for NBS modified one. Thus, active site Trp does

contribute to the fluorescence to marginal extent. Steady state fluorescence titration of the native enzyme with NBS (1:8 enzyme: NBS ratio) had shown 4% decrease in the total fluorescence (data not shown) confirming the marginal contribution of the active site Trp to the total fluorescence of the protein.

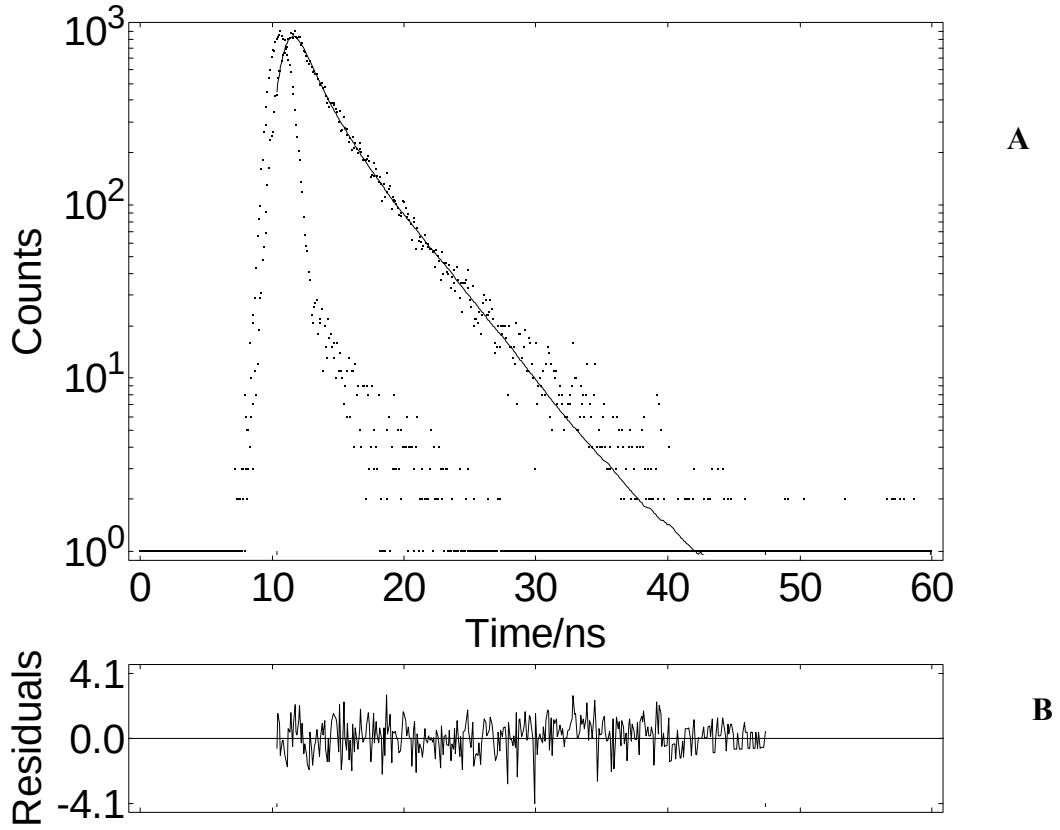

Figure 4: (A) Time-resolved fluorescence intensity decay of α-mannosidase under native conditions. Typical fluorescence decay data obtained at 25°C using an excitation wave length of 295 nm (slit width 15 nm) and observing the fluorescence emission at 333 nm (slit width 15 nm). The protein concentration was 1.0 mg/ml in 50 mM potassium phosphate buffer of pH 6.5. The calibration time for each channel was 1.0 ns. On the Y-axis, the photon counts are presented in a logarithmic scale. The fast decaying, noisy solid line represents the IRF (instrument response function) used as the excitation source. The slower decaying line represents the experimental fluorescence decay curve. **(B)** Plot of the auto correction function of the weighted residual used to judge the goodness of fitting.

Table 5.3: Lifetimes of fluorescence decay of *A. fischeri* α-D-mannosidase under different conditions

Sample description	α_1	τ_1	α_2	τ_2	(τ)	χ^2
Native	0.073	1.51	0.011	5.992	3.181	1.083
NBS modified	0.070	1.28	0.030	5.880	3.120	1.001
Denatured (6M GdnHCl)	0.080	1.16	0.028	4.656	3.219	1.006
Native + 0.5M Acrylamide	0.115	1.04	0.006	5.452	1.995	1.036
Native + 0.5M KI	0.178	0.446	0.018	3.082	1.537	1.007
Native + 0.5M CsCl	0.092	1.144	0.013	4.112	2.153	0.942

The average lifetime (τ) of the fluorescence decay of the native enzyme (3.187 ns) does not change much after denaturation (3.219) although both shorter and longer life times show decrease in the values. The average lifetime drastically decreases for all the samples of enzyme treated with the quenchers (1.995 ns for acrylamide, 1.537 ns for iodide quenched samples). The contribution of shorter lifetime component increases from 37.19% to 79.63% for acrylamide, to 58.64% for I^- and to 66.82% for Cs^+ quenched samples. The contribution of the longer life time decreases from 62.81% to 20.37% for acrylamide, to 41.36% for I^- and to 35.18% for Cs^+ treated samples. The fluorescence seen after maximum quenching could be due to the inaccessible tryptophans. This could be due to the differentially exposed tryptophans in the protein.

In summary, α-mannosidase, a multi-tryptophan protein from *A. fischeri* shows maximum fluorescence intensity between 333–348 nm indicating several populations of tryptophans, few of which are in the hydrophobic environment and others differentially exposed to the polar environment. These tryptophans are inaccessible to the neutral quencher under native conditions. The quenching by neutral quencher was found to be collisional. Tryptophans on the surface of a protein have predominantly positively charged environment and differentially accessible to I^-. The heterogeneity of the tryptophan environment is reflected into the lifetime of the fluorescence of the native as well as after treatment of the enzyme with denaturant or quenchers.

References:

[1] Eftink, M.R. 1991 *in Methods of Biochemical Analysis (Suelter, C. H., Ed.)* **35**, pp.127-205. John Wiley and Sons, New York.

[2] Vivian, J.T. and Callis, P.R. (2001) *Biophysical Journal* **80**, 2093–2109.

[3] Lehrer, S.S. (1971) *Biochemistry* **10**, 3254–3263.

[4] Lehrer, S.S. and Leavis, P.C. (1978) *Methods Enzymol* **49**, 222-236.

[5] Lakowicz, J.R. and Weber, G. (1973) *Biochemistry* **12**, 4171- 4 179.

[6] Lakowicz, J.R., Maliwal, B.P., Cherek, H. and Balter, A. (1983) *Biochemistry* **22**, 1741-1752.

[7] Eftink, M.R. and Ghiron, C.A. (1976) *Biochemistry* **15**, 672-680.

[8] Eftink, M.R. and Ghiron, C.A. (1977) *Biochemistry* **16**, 5546-5551.

[9] Eftink, M.R. and Ghiron, C.A. (1981) *Anal Biochem* **114**, 199-227.

[10] Burstein, E.A., Vedenkina, N.S. and Ivkova, M.N. (1973) *Photochem Photobiol* **18**, 263-272.

[11] Calhoun, D.B., Vanderkooi, J.M. and Englander, S.W. (1983) *Biochemistry* **22**, 1533-1539.

[12] Richards, F.M. (1979) *Carlsberg Res Commun* **44**, 47-63.

[13] Beechem, J.M. and Brand, L. (1985) *Ann Rev Biochem* **54**, 43-71.

[14] Lowry, O.H., Rosebrough, N.J., Farr, A.L. and Randall, R.J. (1951) *J Biol Chem* **193**, 265-75.

[15] Spande, T.F., and Witkop, B., . (1967) *Methods Enzymol* **11**, 498-506.

[16] Sushama, M.G., M. Islam, Khan and Sulbha, S. Keskar. (1997) *Biotechnology and Applied Biochemistry* **25**, 105-108.

[17] Paus, E. (1978) *Biochim Biophys Acta* **533**, 446-456.

[18] Komath, S.S. and Swamy, M.J. (1999) *J Photochem Photobiol* **50**, 108–118.

[19] Teale, F.W.J. and Badley, R.A. (1970) *Biochem J* **116**, 341–348.

[20] Sultan, N.A. and Swamy, M.J. (2005) *J Photochem Photobiol B: Biol* **80**, 93–100.

CHAPTER: 6

GENERAL DISCUSSION AND CONCLUSION

Mannosidases are involved in both glycoprotein biosynthesis (Golgi mannosidases) and degradation (lysosomal mannosidases) from yeast to human beings. [1,2]. The absence of this enzyme causes the genetic lysosomal storage disease α-mannosidosis in humans and cattle [3]. The enzymes are categorized as class I and class II mannosidases and based on the sequence alignments; they belong to family 47 and family 38 glycosidase, respectively in Henrissat's glycosidase classification [1,4]. A number of these enzymes have been cloned and sequenced; also some success has been achieved in their high level expression. There has been widespread interest in α-mannosidase in recent years, in particular, mammalian Golgi mannosidase-II involved in glycoprotein biosynthesis and is currently an important therapeutic target for the development of anticancer agents [5].

Microbial α-mannosidases have been studied widely [6] and categorized into two Classes. In Class I, the enzymes hydrolyze specifically linked α-D-mannosidic bonds (α1–2). These enzymes have strict stereo-chemical requirements. Class I enzymes cannot hydrolyze aryl substrates like para-nitro phenyl α-D-mannopyranoside (pNPM) and 4-mehtyl umbelliferylα-mannopyranoside. In Class II, the enzyme hydrolyzes nonreducing terminal α-mannosidic linkages regardless of the aglycon moiety. It includes those enzymes which act on para-nitro phenyl α-D-mannopyranoside (pNPM) and do not have strict linkage specificity i.e. they act on α(1–2), α(1–3), α(1–4) and α(1–6) linkages although with different rates [4]. During last 10 years several reports on fungal α-mannosidases have been published [7-12].

The genus *Aspergillus* is one of the most important filamentous fungal genera causing some diseases in plants. *Aspergillus* species are used in the fermentation industry. *Aspergilli* are the major producers of the α-mannosidases. These include *Aspergillus niger* [13], *Aspergillus oryzae* [14], *Aspergillus nidulans* [15], Aspergillus saitoi [16], *Aspergillus fumigatus* [17] and *Aspergillus flavus* [18]. The Class II α-mannosidases from different fungal and yeast species studied so far are from *Aspergillus niger*, *A. saitoi*, *Trichoderma reesei*, *Candida albicans* and *Saccharomyces cerevisiae*. Detail studies of active site, energetics of catalysis and conformational characteristics have hardly been

reported for the enzyme. In the present study, α-mannosidase has been produced from *Aspergillus fischeri* NCIM 508 which is collection from National Collection of Industrial Microorganisms (NCIM), National Chemical Laboratory, Pune, India.

Discussion:

The α-mannosidase from *Aspergillus fischeri* was produced as an extracellular enzyme in a medium with yeast extract powder (2%) as carbon source as well as an inducer of α-mannosidase. The activity was maximum when the culture was grown in a medium containing $MgSO_4$ (0.1%), $(NH_4)_2SO_4$ (0.1%), KH_2PO_4 (0.2%) and Yeast Extract Powder (2%) for seven days. The enzyme was purified to homogeneity by conventional procedure involving an ion exchange chromatography followed by preparative poly acrylamide gel electrophoresis. The effort to purify the protein on gel filtration chromatography after ion-exchange chromatography failed. The reported fungal α-mannosidase are purified through conventional chromatographic methods [7,16,19,20] and even in some places where affinity chromatography has been used (*Trypanosoma cruzi* [21], *Aspergillus oryzae* [22]), they had to pass through conventional chromatography methods before loading on to affinity chromatography.

It is a hexameric protein with a 412 kDa mass and has pI around 4.5. Majority of the fungal mannosidase showed the pI towards acidic side only (*Penicillium citrinum* 4.6, *Aspergillus saitoi* 4.5). Amino analysis revealed that α-mannosidase contains remarkably high percentage of Glycine (20.6%), Arginine (11.2%) and Alanine (11.1%) and essential amount of hydrophobic amino acids (18.43%) and basic amino acids (17.5%). ASX and GlX were found to 6.4% and 9.4%, respectively. The enzyme contains one cysteine residue per sub unit. There is no Methionine in the protein.

Far UV CD-spectrum at pH 6.5 showed a trough with minima at 210 nm and 222 nm indicating presence of both α and β structures in the enzyme. The secondary structure elements determined using the software CD Pro (continell) are 24% (Helix), 23.6% (Sheet), 21.2% Turn and 31.3% unordered structure (RMSD 0.028 and NRMSD 0.012). The helix and sheet content of the protein are in equal proportion.

The pH-activity profile obtained revealed the participation of two ionizable groups with pK_a values of 5.75 and 7.84. The pK_a of amino acid towards acidic side shows involvement of carboxylate and the one towards basic side shows the presence of either His or Cys. Chemical modification of the amino acids with the group specific reagents further proved this result. In addition to carboxylate, histidine, cysteine, tryptophan and one arginine is present at the active site of the enzyme from *Aspergillus fischeri*.

Kinetics of the modified enzyme showed that there is decrease in the V_{max} values of the enzyme modified with almost all the reagents. However, the K_m values of the enzyme modified with EDAC, pHMB and NBS were almost unchanged indicating that the carboxylate, cysteine and Trp residues must be involved either in the catalysis or holding the catalytic conformation. The enzyme modified with pNPG and DEPC showed increase in K_m values indicating decrease in the substrate affinity, along with decrease in the V_{max}. So, Arg and His could be involved in substrate binding and holding the reactive groups in proper position. The inactivation could be prevented by the substrate to substantial extent confirming the specific modification of the amino acids at the active site.

The catalytic mechanism of α-mannosidase normally requires the presence of two carboxylate groups, one acts as a general base by removing a proton from water and the other acts as general acid by donating the proton to the leaving group[23]. The reason for getting one residue from the double reciprocal plot in the present work could be due to the fast reactive nature of one carboxylate residue. EDAC was used alone for modification which rules out the possibility of cross linking with the other amino acids. Presence of carboxylate group at the active site of α-mannosidase has been shown by chemical modification of the enzyme from *Aspergillus saitoi* [24] and *Penicillium citrinum* [25] and by radiolabelling of the enzyme from Jack bean [26]. Aspartic acid is known to be conserved in the Class II α-mannosidase active site. Thus, Asp can be assigned as one of the carboxylate amino acid present at the active site of *A. fischeri* α-mannosidase.

There are no disulfide bonds in the enzyme as revealed by modification of the protein with DTNB under reducing conditions. Incubation of enzyme with β-mercaptoethanol or dithiothreotal [DTT] did not show any effect on the activity of α-mannosidase. The Cu^{++} is known to bind cysteine residues in the protein [27]. The drastic inactivation of the present enzyme by Cu^{++} could be due to the binding of these metal ions to the cysteine near the active site. As described in our earlier report [28], one Trp residue was found to be essential for the α-mannosidase activity and the other residues react slowly. Trp is also shown to be essential for the activity of α-mannosidase from *Phaseolus vulgaris* [29]. His and Trp residues are in the proximity with each other at the active site of α-mannosidase from *A. fischeri*.

The class II α-mannosidases are neither metal ion dependent nor they get inactivated by EDTA. The number of metal ions were checked for the effect on the enzyme. None of the metal ions showed positive effect on the enzyme activity. The effect of Cu^{++}, Co^{++} and Hg^{++}, Se^{++} and Pb^{++} ions strongly inactivated the enzyme. Ca^{++} which is known to be required in case of Class I α-mannosidase does not show any effect on the enzyme. Inhibition of neutral α-mannosidase from Japanese quail oviduct by copper has been reported [30].

The K_i values determined from the Dixon plot were 22nm, 28 μM, and 1.2 mM for Cu^{++}, Se^{++} and Co^{++} ions, respectively. The reason for Co^{++} being competitive inhibitor could be the co-ordination with carboxylate ions at the active site. Cu^{++} and Se^{++} could be interfering the catalysis since the K_m of the enzyme in presence of these metal ions remained same. Also, there was no recovery of the enzyme activity after dialyzing out the metal ions. Co^{++} is known to activate the α-mannosidase from Japanese oviduct and rat liver [30,31].

The α-mannosidase can hydrolyze different mannose disaccharides like Man (α1-3) Man, Man (α1-2) Man and Man (α1-6) Man. The specificity constant K_{cat}/K_m of Man (α1-3) Man, Man (α1-2) Man and Man (α1-6) Man at 50 ^{0}C were 7488, 5376 and 3690M^{-1} min^{-1}, respectively, indicating affinity of the enzyme for the substrates and rate of the

reaction is in the order α1-3 >α1-2>α1-6 linked mannobioses. Among the mannose disaccharides, the E_a of hydrolysis of Manα(1-3)Man (15.14 kJ/mol) is three times lower than that of Manα(1-2)Man (47.43 kJ/mol) and 4.6 times lower than that of Manα(1-6)Man (71.21 kJ/mol), respectively. The hydrolysis of Manα(1-3)Man occurring at faster rate could be due to the easy access of the glycosidic linkage to the carboxylic groups at the active site. There must be more constraints for Manα(1-2) Man and still more for Manα(1-6) Man during binding as well as catalysis due to which the hydrolysis is slow. Affinity of the substrates towards the enzyme and the rates of reaction seem to be reflecting the E_a.

4-MeUmbαMan has higher specificity constant towards the enzyme (K_{cat}/K_m 4.61×10^5 M^{-1} min^{-1}) as compared to pNPαMan (K_{cat}/Km 3.56×10^5 M^{-1} min^{-1}). E_a is four times less for 4-MeUmbαMan (8.92 kJ/mol) as compared to pNPαMan (38.70 kJ/mol) (Fig. 3.2B). The free energy of binding of pNPαMan and 4-MeUmbαMan is much lower than that of mannose disaccharides indicating easier binding of these substrates. The higher specificity (or lower K_m) of the enzyme to 4-MeUmbαMan as compared to pNPαMan can be explained with the structures. The tilted structure of 4-MeUmbαMan makes easy accessibility of the glycosidic bond to the active site of the enzyme, thereby hydrolyzing at faster rate. The flattened structure of pNPαMan showed lower affinity as compared to 4-MeUmbαMan towards the enzyme. It is generally known that half-boat shaped substrates are easily hydrolyzed by the mannosidases.

Inhibition of the enzyme was found to be competitive for Swainsonine and 1-deoxymannojirimycin as they are the substrate analogues. IC_{50} values for Swainsonine and 1-deoxymannojirimycin were 110 and 284 μM, respectively. Swainsonine, specific inhibitor of Class II α-mannosidases exhibited three times lower Ki (101μM) than that for 1-deoxymannojirimycin (286μM), specific inhibitor of Class I enzymes.

The binding of both the inhibitors was found to be low up to 40 ^{0}C and increased at 50 ^{0}C. The K_i was found to be decreasing (or K_a increasing) with increasing temperature indicating the kind of reaction to be endothermic and increased association of the

inhibitor to the enzyme. This could be due to the optimum reactive state of the active site of enzyme at 50 ^{0}C. ΔH for Swainsonine and 1-deoxymannojirimycin are 101.43 and 59.36 kJ/mol at 40–50 ^{0}C, respectively. The K_i for Swainsonine reported here is 1000 times higher than those reported for the Class II mannosidases from plant and animal sources (Jack beans α-mannosidase; 0.4–0.1 μM, rat liver lysosomal α-mannosidase; 0.07–0.2 μM and rat liver Golgi α-mannosidase; 0.08–0.2 μM), which could be due to the difference in the active site geometry of the respective enzyme.

Three-dimensional structure of the enzyme will show the clear picture of the active site. Dorling et al. [32] have reported the inhibition of two α-mannosidases by Swainsonine, the acid form and a neutral form. Since pK_a of Swainsonine is 7.4, it is fully ionized at pH4.0 and hence strongly inhibits the acid form of enzyme while the neutral form of the enzyme is inhibited up to 60% at the same concentration at pH 6.5.

The enzyme used in the present work is a Class II α-mannosidase from *Aspergillus fischeri* as revealed by the substrate specificity, inhibition by swainsonine and independency on the metal ion/s for activity.

The polyhydroxy substituted piperidine derivative compounds tested for mannosidase inhibition showed different degrees of inhibition. The energetics of the inhibition for these compounds (**20, 32** and **39**) showed the decreasing values of inhibition constants with increasing temperature indicating increasing association of the inhibitor with the enzyme accordingly. The binding is endothermic and entropically driven. The increase in entropy due to the release of water molecules from enzyme active site region and the inhibitor due to binding must be much higher than the decrease in entropy due to the restriction on movement of inhibitor and enzyme. Benzyl group in compounds **39** and **32** seems to enhance the binding to the enzyme as compared to compound **20**. Higher positive entropy on binding of the compound **32** than **39** to the enzyme shows the added effect of amine group. The inhibition of the α-mannosidase by Swainsonine, class II enzyme inhibitor and 1-deoxymannojirimycin, class I enzyme inhibitor show K_i 101 μM and 256 μM, respectively and endothermic binding to the enzyme. Structure of

compound **20** resembles with deoxymannojirimycin and has comparable IC_{50} as 247μM with that of 1-deoxymannojirimycin as 286 μM.

Besides providing tools for the exploration of the physiological role of the endomannosidase-initiated processing pathway these derivatives yield valuable insights into the substrate recognition site of the enzyme.

Effect of different chemical and physical denaturants such as urea, guanidine thiocynate, temperature and pH on structural stability of α-mannosidase from *A. Fischeri* was monitored by fluorescence spectroscopy and circular dichroism. The enzyme activity was labile i) above 55 ^{0}C ii) in presence of 1.0 M GdnHCl iii) below pH 5.0 or above pH 8.0. The enzyme lost the biological activity first and then the overall folded conformation and secondary structure. The intrinsic fluorescence of the protein was monitored at different temperatures. The fluorescence spectrum of native enzyme showed a plateau in the range of 338 - 350 nm indicating Trp residues present in differential environment. The fluorescence intensity of the enzyme gradually decreased with increasing temperature which could be due to the deactivation of the single excited state by non-radiative process. At 70 ^{0}C, the spectrum showed a peak at 350 nm and at 90 ^{0}C, at 353 nm due to the exposure of buried Trp of partially unfolded protein to the solvent. In far UV-CD spectra, gradual decrease in the ellipticity was observed with increase in temperature but there is no total unfolding of the protein even at 90^{0}C.

No change in the light scattering intensity of the protein was observed till 90 ^{0}C, as there was no aggregation due to thermal denaturation. Renaturation or cooling of the heated protein samples to 30 ^{0}C did not lead to reactivation of enzyme indicating irreversibility of the thermal inactivation of α-mannosidase. Thermal inactivation of the enzyme taking place before any structural change has been reported in BSH [33].

The fluorescence scans at different pH show decrease in the fluorescence intensity at pH 1, 2 and 3 than at pH 6.5 which could be due to the acid quenching and neutralization of COO^- groups on amino acid in the vicinity of tryptophan [34]. The protein could bind ANS only at extreme acidic pH, maximum at pH 2.0, indicating the exposure of

hydrophobic patches in protein at extreme acidic pH. At pH 2.0, there is substantial rearrangement of the secondary structural elements as compared to pH 6.5. The decrease in the tryptophan fluorescence of α-amylases from *Bacillus licheniformis* and *Bacillus amyloliquefaciens* accompanied by red shift at acidic pH was observed [35]. These results indicate changes in the conformation of the enzyme at acidic pH resulting in exposure of the buried tryptophan residues to polar solvents.

The midpoint values of GdnHCl mediated changes measured by inactivation, fluorescence and negative ellipticity were 0.48 M, 1.5 M and 1.9 M, respectively. The protein almost completely unfolded in 4.0 M GdnHCl but not at 90 ^{0}C. The inactivation and unfolding were irreversible. The protein exhibited molten-globule like intermediate with rearranged secondary and tertiary structures and exposed hydrophobic amino acids on the surface at pH 2.0. This species showed not only increased accessibility of Trp to the neutral and anionic quenchers but also got denatured with GdnHCl in a different manner than that of the native enzyme. Several proteins have been shown to exist in molten globule form at extremely acidic pH, Glucose/Xylose Isomerase [36], α-crystalin [37], Xylanase [38], glutathione transferase [39], α-amylases [35] and glucose oxidase [40]. Molten globule may be one of the first conformations embraced by the polypeptide chain in folding from the unfolded state [41]. Urea is milder denaturant as compared to GdnHCl. The insoluble aggregates of a thermally denatured protein could be detected only in the presence of 0.25 – 0.75 M GdnHCl. α-amylase from *Bacillus subtilis* is prone to aggregate at low temperature (37 ^{0}C) and neutral pH (pH 7) when the protein concentration is relatively high (>1μM) [42].

During the course of the unfolding studies, i) the partially unfolded states at 90 °C and ii) in presence of 1.5 M GdnHCl, iii) molten globule-like structure at pH 2.0 and iv) heat aggregated state only in presence of low concentration of the denaturant were the interesting intermediates observed for the high molecular weight oligomeric enzyme. Loss of enzyme activity due to thermal and chemical denaturant, before any significant change in the conformation was also observed.

Fluorescence quenching and time-resolved fluorescence of α-mannosidase, a multitryptophan protein from *Aspergillus fischeri* were carried out to investigate the tryptophan environment. The tryptophans were found to be differentially exposed to the solvent and were not fully accessible to the neutral quencher indicating heterogeneity in the environment. Quenching of the fluorescence by acrylamide was collisional. Surface tryptophans were found to have predominantly positively charged amino acids around them and differentially accessible to the ionic quenchers. Similar quenching patterns have been observed for several multi-tryptophan proteins [43-45]. Denaturation led to more exposure of tryptophans to the solvent and consequently in the significant increase in quenching with all the quenchers.

The native enzyme showed two different lifetimes, τ_1 (1.51 ns) and τ_2 (5.99 ns). The average lifetime of the native protein (τ) (3.187 ns) was not affected much after denaturation (τ) (3.219 ns), while average lifetime of the quenched protein samples was drastically reduced (1.995 ns for acrylamide and 1.537 ns for iodide). This is an attempt towards the conformational studies of α-mannosidase.

Conclusions:

1. The α-mannosidase was isolated from *Aspergillus fischeri* NCIM 508 using yeast extract powder (2%), which acts as both inducer of the enzyme and carbon source for the organism. The enzyme was purified using ion-exchange chromatography and preparative-PAGE.

2. It showed high specificity for Man α(1-3) Man which is energetically favored as compared to α(1-2) and α(1-6) linkages. 4-MeUmbαMan is also energetically favored than pNPαMan.

3. Active site characterization showed involvement of one residue each of carboxylate group, Arg, Hist, Cyst and Trp and also proximity of Trp to Hist at active site.

4. Inhibition of the enzyme activity by swainsonine (class II inhibitor) was higher as compared to 1-deoxymannojirimycin (class I inhibitor) but lower as compared to plant α-mannosidase. Poly-hydroxy substituted piperidine derivatives showed quite high level of inhibition of the enzyme activity.

5. Enzyme lost the activity at lower level of all the denaturants but was conformationally stable even up to 80 ^{0}C. At pH 2.0, enzyme showed molten globule like structure, with rearranged but compact secondary structure and loose tertiary structure with hydrophobic amino acids exposed on the surface.

6. Aggregation of the protein could be observed at high temperature only in GdnHCl at lower concentrations.

7. The tryptophans were found to be in the non-polar as well as polar environment show two lifetimes, in the time-resolved fluorescence.

Reference:

[1] Moremen, K.W., Trimble, R.B. and Herscovics, A. (1994) *Glycobiology* **4**, 113-125.

[2] Liao, Y.F., Lal, A. and Moremen, K.W. (1996) *J Biol Chem* **271**, 28348-58.

[3] Neufeld, E.F. (1991) *Annu Rev Biochem* **60**, 257-280.

[4] Henrissat, B., , and Bairoch, A. (1991) *Biochem J.* **316**, 695-696.

[5] Goss, P.E., Baker, M.A., Carver, J.P., Dennis, J.W. (1995) *Clinical Cancer Res* **1**, 935-944.

[6] Keskar, S.S., Gaikwad, S.M., Khan, M.I. . (1996) *Enz Micro Tech* **18**, 602-604.

[7] Eneyskaya, E.V., Kulminskaya, A.A., Savel'ev, A.N., Shabalin, K.A., Golubev, A.M. and Neustroev, K.N. (1998) *Biochem Biophys Res Commun* **245**, 43-49.

[8] Kelly, S.J., Herscovics, A. . (1998) *J Biol Chem* **263** 14757–14763.

[9] Reyna, A.B.V., Noyola, P.P., Mendez, C.C., Romero, E.O., Carreon, A.F. (1999) *Glycobiology* **9**, 533–537.

[10] Mares, M., Callewaert, N., Piens, K., Claeyssens, M., Martinet, W., Dewalele, S., Contreras, H., Dewerte, I., Penttila, M., Contreras, R. (2000) *J Biotechnol* **77**, 255–263.

[11] Tatara, Y., Lee, B.R., Yoshida, T., Takahashi, K. and Ichishima, E. (2003) *J Biol Chem* **278**, 25289-94.

[12] Athanasopoulos, V.I., Niranjan, K., Rastall, R.A. (2005) *Carbohydr Res* **340**, 609–617.

[13] Swaminathan, N., Matta, K.L., Donoso, L.A. and Bahl, O.P. (1972) *J Biol Chem* **247**, 1775-1779.

[14] Yamamoto, K., Hitomi, J., Kobatake, K. and Yamaguchi, H. (1982) *J Biochem* **91**, 1971-1979.

[15] Eades, C.J. and Hintz, W.E. (2000) *Gene* **255**, 25-34.

[16] Amano, J. and Kobata, A. (1986) *J Biochem* **99**, 1645-54.

[17] Li, Y., Fang, W., Zhang, L., Ouyang, H., Zhou, H., Luo, Y. and Jin, C. (2009) *Glycobiology* **19**, 624-32.

[18] Augustin, J. and Sikl, D. (1978) *Folia Microbiol (Praha)* **23**, 349-50.

[19] Vazquez-Reyna, A.B., Ponce-Noyola, P., Calvo-Mendez, C., Lopez-Romero, E. and Flores-Carreon, A. (1999) *Glycobiology* **9**, 533-7.

[20] Zouchova, Z., Kocourek, J. and Musilek, V. (1977) *Folia Microbiol (Praha)* **22**, 98-105.

[21] Vandersall-Nairn, A.S., Merkle, R.K., O'Brien, K., Oeltmann, T.N. and Moremen, K.W. (1998) *Glycobiology* **8**, 1183-94.

[22] Tanimoto, K., Nishimoto, T., Saitoh, F. and Yamaguchi, H. (1986) *J Biochem* **99**, 601-4.

[23] Petergem, V.F., Contreas, H., Contreas, R., Beeumen, V.J. (2001) *J Mol Biol* **312**, 157-165.

[24] Yoshida, T., Shimizu, S., Ichisima, E., . (1994) *Phytochemistry* **35**, 267-268.

[25] Yoshida, T., Maeda, K., Kobayashi, M. and Ichishima, E. (1994) *Biochem J* **303** 97-103.

[26] Howard, S., He, S. and Withers, S.G. (1998) *J Biol Chem* **273**, 2067-72.

[27] Harrison, D.C. (1927) *Biochem J* **21**, 335-346.

[28] Sushama, M.G., M. Islam, Khan and Sulbha, S. Keskar. (1997) *Biotechnology and Applied Biochemistry* **25**, 105-108.

[29] Paus, E. (1978) *Biochim Biophys Acta* **533**, 446-456.

[30] Oku, H., Hase, S. and Ikenaka, T. (1991) *J Biochem* **110**, 29-34.

[31] Grard, T., Saint-Pol, A., Haeuw, J.F., Alonso, C., Wieruszeski, J.M., Strecker, G. and Michalski, J.C. (1994) *Eur J Biochem* **223**, 99-106.

[32] Dorling, P.R., Huxtable, C.R. and Colegate, S.M. (1980) *Biochem J* **191**, 649-51.

[33] Kumar, R.S., Suresh, C.G., Brannigan, J.A., Dodson, G.G. and Gaikwad, S.M. (2007) *IUBMB Life* **59**, 118-125.

[34] Cowgill, R.W. (1975) *in Biochemical Fluorescence Concepts (Chen, R. F. and Edelhoch, H., Eds)*, pp 441-486, Marcel Dekker, New York.

[35] Shokri, M.M., Khajeh, K., Alikhajeh, J., Asoodeh, A., Ranjbar, B., Hosseinkhani, S. and Sadeghi, M. (2006) *Biophysical Chemistry* **122**, 58-65.

[36] Pawar, S.A. and Deshpande, V.V. (2000) *Euro J Biochem* **267**, 6331-6338.

[37] Rajaraman, K., Raman, B. and Rao, M. (1996) *J Biol Chem* **271**, 27595-27600.

[38] Nath, D. and Rao, M. (2001) *Biochem Biophys Res Comm* **288**, 1218-1222.

[39] Luo, J.K., Hornby, J.A., Wallace, L.A., Chen, J., Armstrong, R.N. and Dirr, H.W. (2002) *Protein Sci* **11**, 2208-2219.

[40] Khatum Haq, S., Ahmad, F. and Khan, R.H. (2003) *Biochem Biophys Res Comm* **303**, 685-692.

[41] Vamvaca, K., Vogeli, B., Kast, P., Pervshin, K. and Hilvert, D. (2004) *Proc Natl Acad Sci USA* **101**, 12860-12864.

[42] COLOMER-PALLAS, A., PETIT-GLATRON, M.F. and CHAMBERT, R. (2002) *J Biol Phy and Chem* **2**, 101-107.

[43] Lehrer, S.S. (1971) *Biochemistry* **10**, 3254–3263.

[44] Teale, F.W.J. and Badley, R.A. (1970) *Biochem J* **116**, 341–348.

[45] Sultan, N.A. and Swamy, M.J. (2005) *J Photochem Photobiol B: Biol* **80**, 93–100.

APPENDIX

CHARACTERIZATION OF α-MANNOSIDASE GENE

Characterization of α-mannosidase gene

Introduction:

The cloning and sequencing of the structural gene of an enzyme is useful for the overproduction of the protein for its potential biotechnological application and for mutagenesis, x-ray crystallography and structure function studies. The cloning of α-mannosidase is important since its production from native organism is low as compared to over expressed proteins. α-mannosidase gene from *Saccharomyces cerevisiae* [1], *Aspergillus nidulans* [2,3], *A. saitoi* [4] and *A. oryzae* [5] are isolated, cloned and over expressed. The present study describes the cloning of a high molecular weight α-mannosidase from *Aspergillus fischeri* (*Neosartorya fischeri*).

Materials:

Ampicillin, Kanamycin, Tris, IPTG, X-gal, SDS, BSA, EDTA and Ethidium bromide were purchased from Sigma-Aldrich, USA. Agarose, restriction enzymes, T4 DNA ligase, RNase A and lysozyme were obtained from GIBCO-BRL (USA), Promega (USA) and Amersham (UK). Taq DNA polymerase was obtained from Bangalore Genei (India). Plasmid vectors pGEM-T Easy Vector is purchased from Stratagene (USA). All other chemicals and solvents of analytical grade were purchased from HIMEDIA, Qualigens Fine Chemicals and E-Merck Laboratories, India. Pipette tips and micro centrifuge tubes were purchased from Axygen (USA).

Methods:

Isolation of genomic DNA

The fungal culture *Aspergillus fischeri* was grown in 500 ml of Basal medium (pH 5.0) at 28 °C for 7 dyas with continuous shaking at 180 rpm. DNA was isolated according to the method described by Hopwood *et al.*, [6] with slight modifications. Mycelium (1g) washed in 5 ml TE buffer (pH 8.0) was centrifuged at 10,000 rpm for 10min. at 4^{o}C. The

pellet was freezed in liquid nitrogen and powdered for better access by lysozyme. The powdered pellet was resuspended in 5 ml TE containing 2 mg/ml lysozyme. It was incubated at 30 °C, triturating every 15 min. until a drop of suspension on a microscopic slide was completely cleared with a drop of 10% SDS (1 hour). Further, 1.2 ml of 0.5 M EDTA was added to the mixture followed by 0.7 ml 10% SDS. The solution was swirled and incubated at 37 °C for 2 h. Proteins were extracted from the aqueous phase by adding 6 ml of a mixture of phenol: chloroform: IAA (isoamyl alcohol) (25:24:1). The mixture was shaken for 5 min. and then centrifuged at 10,000 rpm, 4 °C for 10 min. This step was repeated again for the aqueous phase in a new tube. Finally, 40 µg/g of RNAase from a stock of 10 mg/ml was added to pre-weighed aqueous phase and incubated at 37 °C for 1 h. The genomic DNA was precipitated by adding equal volume of isopropanol and was stored at room temperature for 1h. DNA was spooled with a glass rod and transferred to a fresh tube and dissolved in 5 ml of TE buffer, pH 8.0.

Total RNA Isolation

Solutions: TRIzol® Reagent (Invitrogen, USA**),** Chloroform and Isoamyl Alcohol (24:1), Isopropanol, 70% ethanol in DEPC treated deionized water, DEPC treated deionized water.

RNase free environment was created and maintained as described by Blumberg (1987). All glass and plasticware was DEPC (0.1% in water) treated overnight and autoclaved. The pestle and mortar were also DEPC treated and then baked at 300 ºC for 6 h. All materials were dried in a vacuum oven.

Total RNA from fungal mycelium was isolated using Trizol reagent. The mycelium was collected, washed with DEPC treated water, frozen in liquid nitrogen and crushed to a fine powder. To 100 mg of the fine powder 1ml Biozol reagent was added and mixed thoroughly using a vortimix. Chloroform: isoamyl alcohol (300 µl) was added and mixed thoroughly using vortimix. The tubes were centrifuged at 4 ºC at 13,000 x g for 15 min. The supernatant was transferred to 1.5 ml tubes and the chloroform: isoamyl alcohol step repeated. The aqueous phase was transferred to 1.5 ml tubes and half volume isopropanol

added. It was mixed thoroughly and kept for RNA precipitation for 1 h. Total RNA was made to pellet by centrifugation at 13,000 x g for 15 min at 4 ºC. The RNA pellet was washed with 70% ethanol twice and dried in a SpeedVac centrifugal concentrator. RNA pellet was dissolved in 40 µl of DEPC treated water and stored at -80ºC in aliquots. Purity of RNA was confirmed by measuring OD at 260/280 nm and also by visualization on 1.5% TAE Agarose gel.

cDNA first strand synthesis by Reverse Transcription

Complementary DNA (cDNA) is synthesized from a mature mRNA template in a reaction catalyzed by the enzyme reverse transcriptase. In the present study cDNA first strand was synthesized using ImProm-II™ Reverse Transcription System (Promega, USA). The reactions were set up as per the manufacturer's guidelines.

A brief reverse transcription reaction of up to 1µg of total RNA performed in 20 µl reactions comprised of components of the ImProm-II. Reverse Transcription System. Experimental RNA was combined with the oligo$(dT)_{15}$ primer. The primer/template mix was isothermally denatured at 70 °C for 5 min and snap chilled on ice. A reverse transcription reaction mix was assembled on ice to contain nuclease-free water, reaction buffer, reverse transcriptase, magnesium chloride, dNTPs and ribonuclease inhibitor RNasin®. As a final step, the template-primer combination was added to the reaction mix on ice. Following an initial annealing at 25 °C for 5 min, the reaction was incubated at 42 °C for up to 1 h. The cDNA synthesized was directly added to amplification reactions.

The first strand reaction was set up as follows:

Experimental RNA (1µg)	1µl
Primer [Oligo$(dT)_{15}$ or Random (10pmol)]	1µl
Nuclease-Free Water	3µl
Final volume	5µl

The tubes were incubated at 70 °C for 5 min and then chilled in ice-water for 5 min. Tubes were briefly spun in a micro centrifuge to collect the condensate and maintain the original volume. The tubes were kept closed and on ice until addition of the reverse transcription reaction mix.

The reverse transcription reaction mix was prepared by combining the following components of the ImProm-II Reverse Transcription System in a sterile 1.5 ml micro centrifuge tube on ice.

Nuclease-free water	6.5 µl
ImProm-II. 5X Reaction Buffer	4.0 µl
$MgCl_2$ (15 mM)	2.0 µl
dNTP Mix (7.5 mM)	1.0 µl
RNasin® Ribonuclease Inhibitor (40U μl^{-1})	0.5 µl
ImProm-II Reverse Transcriptase	1.0 µl
Final volume	15.0 µl

An aliquot of 1.0 µg total RNA and oligo $(dT)_{15}$ or Random hexamer primer (10 pmol) mix was added to the above reaction for a final reaction volume of 20 µl per tube. The tube was incubated at 25 °C for 5 min for primer annealing and then at 42 °C for 1 h for cDNA first strand synthesis. Reverse transcriptase was thermally inactivated by incubation at 70 °C for 15 min prior to proceeding with PCR amplification [7,8].

Polymerase Chain Reaction (PCR)

PCR is a powerful technique to amplify a desired nucleotide sequence using sequence specific primers. This amplification may be either of and from a single template or of a template from a mixture of templates [9,10]. This technique has been successfully used for various purposes like fishing out of gene(s) from genomic DNA or from cDNA

population [11], introducing restriction sites of interest in the amplified product for directional cloning etc.

In the present study applications of PCR were exploited for a few of the above specified applications. The PCR reaction mixture and cycling conditions used were as follows:

Reaction mixture

Sterile deionized water	6.2 µl
Template (50 ng μl^{-1})	1.0 µl
Forward primer (6 pmol)	1.0 µl
Reverse primer (6 pmol)	1.0 µl
dNTPs (0.2 mM)	4.0 µl
10 x Buffer (Mg+2 1.5 mM)	1.5 µl
Taq Polymerase (1U μl^{-1})	0.3 µl
Total volume	15.0 µl

PCR cycle conditions

1 cycle	95ºC	5 min
35 cycles	95ºC	1 min
	45-65ºC	30-45 s (annealing temperature was dependent on primer T_m)
	72ºC 1-1	min 30 s
1 cycle	72ºC	5 min
1 cycle	4ºC	hold

Extraction and purification of DNA from agarose gels

The restriction digested DNA or PCR amplified products were run on an agarose gel in 1X TAE buffer. The gel was stained with ethidium bromide (0.5 µg ml^{-1}) and viewed using a hand held long wavelength UV illuminator. The fragment of interest were excised from the gel and weighed. A 50-200 mg gel slice was transferred to a 1.5 ml micro centrifuge tube and 0.5 ml GEX buffer (AuprepTM GEL^X kit, Life Technologies, USA) added. The tube was incubated at 60 °C for 5 to 10 min with intermittent mixing until the gel slice was completely dissolved. The gel mixture was cooled down to room temperature. Approximately 0.7 ml dissolved gel mixture was loaded into the GEL^X column which was placed on the collection tube. The assembly was centrifuged at 12,000 x g for 2 min and the flow-through was discarded. The procedure was repeated for the balance of the dissolved gel mixture. The column was washed with 0.5 ml of WF buffer by centrifuging for 30-60 s. The flow-through was discarded and the column washed with 0.7 ml of WS buffer. The flow through was discarded and the column again centrifuged at 12,000 x g for 3 min to remove residual ethanol. The column was placed onto a new 1.5 ml centrifuge tube. About 30-50 µl of elution buffer or sterile distilled water was added onto the center of the column membrane. The column was allowed to stand for 1-2 min and then centrifuged at 12,000 x g to elute the DNA. The eluted DNA was stored at -20 °C.

Ligation reaction

The pGEM-T vector and PCR amplified product were mixed in a molar ratio of 1:2 and suspended in 5 µl of DNA ligase buffer. To the mixture, 1unit of ligase was added and incubated for 4 h at 16 °C.

***Escherichia coli* transformation and selection**

LB medium (50 ml) was inoculated with 1% of the overnight grown *E. coli* culture and allowed to grow till 0.5 O.D. at 600 nm. The cells were harvested by centrifugation at 5,000 x g for 10 min at 4 °C, suspended in 100 mM ice-cold $CaCl_2$ and kept on ice for 30

min. Cells were centrifuged, the pellet suspended in 1 ml of 100 mM ice-cold $CaCl_2$ and stored as aliquots of 200 µl at 4 °C. The competent *E. coli* cells, thus formed, were transformed according to Sambrook *et al*., [12]. To 200 µl of competent *E. coli* 5 µl of the ligation mixture was added, mixed by gentle swirling and stored on ice for 30min. The cells were given heat shock in a water bath at 42 °C exactly for 45 seconds and immediately transferred to an ice bath to chill for 1-2 min. To these cells, 800 µl LB was added and was incubated at 37 °C for 45 min. The culture was centrifuged at 3000 rpm for 5 min, the supernatant was discarded and the pellet was resuspended in 200 µl LB broth. About 100 µl of the transformed competent cells was spread onto LB plates containing appropriate antibiotic, IPTG and X-gal as per need [12].

Solutions	*Stock*	*Final conc*
1) IPTG stock solution	200 mg ml^{-1} in sterile distilled water	40 µg ml^{-1}
2) X-gal stock solution	20 mg ml^{-1} in dimethylformamide	40 µg ml^{-1}

Screening of positive transformants

In order to differentiate between the colonies containing recombinant plasmids from the non-recombinant colonies, blue white selection of the colonies was performed. To the LB plates containing ampicillin (40 µg/ml), 40 ml of a stock solution of X-gal (20 µg/ml in dimethylformamide) and 4 ml solution of isopropylthio-β-D-galactoside (IPTG) (200 µg/ml). The mixture of X-gal and IPTG were spread uniformly onto the surface of agar plates and incubated at 37 °C. The transformants were plated onto the plates and incubated at 37 °C for 12-16 h. After the appearance of the colonies, the plates were placed at 4 °C for several hours to allow the blue color to develop fully.

Isolation of plasmid DNA from *E. coli* cells

Solutions

TEG Buffer (Soln. I): 25 mM Tris-HCl (pH 8.0), 10 mM EDTA (pH 8.0), 50 mM Glucose.

Soln. II: 0.2 N NaOH, 1% SDS (freshly prepared)

Soln. III: 3.0 M Potassium acetate (pH 4.8)

Chloroform, absolute ethanol, 3.0 M Sodium acetate, 70% ethanol, deionized water

The alkaline lysis method of Sambrook *et al.*, [12] was improvised upon so that 12-24 samples could be processed conveniently for plasmid DNA extraction within 3 h, with yields of 5-30 µg per 1.5 ml culture depending on the host strain and the plasmid vector. An important feature of this protocol was the use of PEG for purification, which resulted in precipitation of high quality super-coiled plasmid DNA free of contamination. The bacterial cultures were grown overnight (O/N) with shaking (200 rpm) at 37 °C in LB broth, with appropriate antibiotic(s). About 1.5 to 3 ml culture was centrifuged for 1 min at 4,000 x g to pellet the bacterial cells. The pellet was resuspended in 100 µl of TEG buffer by vigorous pipetting, 200 µl of Soln. II was added, mixed by inversion till the solution becomes clear and incubated on ice for 5 min. The cell lysate was neutralized by addition of 150 µl of Soln. III, mixed well and incubated on ice for 5 min. The cell debris was removed by centrifuging for 5 min at 12,000 x g at room temperature. The supernatant was transferred to a clean tube, RNase A to a final concentration of 20 µg ml^{-1} (Sambrook *et al.*,) [12] was added and incubated at 37 °C for 20 min. To the above solution 400 µl of chloroform was added, mixed for 30 s and centrifuged for 5 min at 12,000 x g at 4 ^{o}C. The upper aqueous layer was transferred to a clean tube, 1/10th volume sodium acetate and one volume absolute ethanol was added with mixing and kept at -20 °C for 1-2 h. The sample was centrifuged at 12,000 x g for 10 min at room temperature. The pellet was washed thrice with 70% ethanol and dried under vacuum. The dried pellet was dissolved in 40 µl of deionized water and 40 µl of PEG-NaCl

solution (20% PEG 8000 in 2.5 M NaCl) was added. The mixture was incubated on ice for 20 min and the plasmid DNA pelleted out by centrifugation at 12,000 x g for 15 min at 4 °C. The supernatant was aspirated carefully, the pellet washed with 70% ethanol and air dried. The dried pellet was resuspended in 20 µl deionized water and stored at -70°C.

Restriction digestion of DNA

Plasmid DNA restriction digestion was set up as per recommendations manufacturer.

Primer design for the α-mannosidase gene and its amplification

The whole genomic sequence of *Neosartorya fischeri* (*Aspergillus fischeri*) fungus is available in the NCBI website. The information on α-mannosidase gene reveals that it is Class I α-mannosidase. As reported in earlier chapter of this thesis, it is proved that the α-mannosidase of molecular weight 69200 Da (on SDS PAGE) from *Aspergillus fischeri* is a Class II enzyme. To confirm whether this is the same enzyme as reported in genome sequence, the tryptic digest of enzyme and peptide mass fingerprinting was done with MALDI-TOF. The peptide masses so obtained were compared with the peptide masses of theoretical tryptic digest of the protein sequence of reported α-mannosidase. 11 peptide masses were exactly matched with each other. Again, the molecular mass of the enzyme (69200 Da) studied is same as the reported. Based on this information, the reported α-mannosidase in website was confirmed same as the enzyme under study and the gene (cDNA) was used for the primer design.

Table A.1: The mass of peptides after tryptic digestion of α-mannosidase and analyzing on MALDI-TOF (The values of experimental digests are matching with values of theoretical digest of protein are shown in red color).

Experimental Digest	Theoretical Digest	Experimental Digest	Theoretical Digest	Experimental Digest	Theoretical Digest	Expemental Digest	Theoretical Digest
1103.42771	1321.6681	1763.67266	1579.7421	2704.93189	1871.9619		2567.1377
1210.51427	1326.6688	**1773.65287**	**1583.7608**	2722.01842	1886.9243		2583.1326
1279.50456	1336.6426	1776.74007	1584.8169	2848.86073	**1887.9568**		2611.3667
1393.51584	1352.6376	**1778.67369**	1599.7557	**2931.04759**	1906.8633		2719.3223
1400.55504	1356.7634	1884.65879	1602.7587		**1913.0855**		2760.4964
1440.53391	1364.7321	1885.68709	**1606.7431**		1926.8915		2776.4913
1472.52274	**1370.6811**	1893.67351	1622.738		1937.0617		2828.3137
1483.5513	**1393.7587**	1899.59304	1629.9422		**1978.0505**		2847.4173
1498.63381	**1400.6441**	**1913.65957**	1657.8373		2016.9549		2867.5149
1515.55831	1403.7199	1915.68184	1669.8293		2022.0026		2881.4254
1550.53854	1411.5729	1934.6447	1684.8878		2023.0165		**2929.4519**
1582.53231	1427.5678	1962.7861	1693.8755		2093.8916		2945.3734
1595.63408	1453.7785	1971.69327	1696.9116		2109.8865		2961.3683
1606.62805	1467.7954	**1977.77729**	1720.9493		2146.0914		2977.3495
1660.62693	1476.8533	2037.74486	1729.9595		2199.1907		3052.408
1667.64747	1486.6995	2070.86977	1737.7795		**2244.1077**		3178.4907
1678.60445	1502.6944	2125.86904	**1749.9759**		2260.1027		3194.4856
1679.61192	1507.6911	2167.91634	1753.7745		2291.1878		3237.4438
1680.60899	1520.8332	2189.7849	**1757.8163**		2293.1194		3253.4387
1692.61567	1545.7027	2212.78802	**1773.8112**		2323.2504		3263.616
1706.60559	1547.8176	**2243.84204**	**1786.0433**		2339.3194		3265.4387
1708.69323	1552.8264	**2529.95121**	1791.7966		2431.1717		3269.4336
1710.62641	1553.8071	**2558.96235**	1812.049		2484.2459		3281.4336
1749.64177	1568.8213	2663.02964	1832.9078		2562.3297		3297.4286
1757.62398	1577.7859	2694.08769	1861.0066		2563.1744		3302.5409

The genomic DNA was used as a template for the amplification of the α-mannosidase gene of interest. The following primers were designed based on the cDNA sequence available from the NCBI Gene Bank database. The NCBI Gene ID is 4594076. ACCESSION: XM 001267006 VERSION XM-001267006.1 GI: 119500499.

Table A.2: Oligonucleotide primer sequences.

Primer	**Sequence (5'→3')**
AfManF	ATG ATT CTA GGT CGC AGG CGC
AfManR	TGT ACG AGC AGA GGG ACG CTT'
AfManF-1	ATG ATT CTA GGT CGC AGG CG
AfManR-1	TGT ACG AGC AGA GGG ACG CT
AfManR-2	TGT ACG AGC AGA GGG ACG C
AfManNdeF	CAT ATG ATT CTA GGT CGC AGG CGC
AfMandIIIR	AAG CTT TGT ACG AGC AGA GGG ACG CTT

Primers with restriction site to be incorporated in the amplified product were flanked with restriction sites on the 5' end of the respective primers. The forward primer with Nde site forward (5' CAT ATG ATT CTA GGT CGC AGG CGC 3') and reverse primer with Hind III site reverse (5'AAG CTT TGT ACG AGC AGA GGG ACG CTT 3') were used for the study.

Bioinformatic analysis

Nucleotide and amino acid sequence analysis was done using software **pDRAW 32** and online bioinformatics analysis facility available at **www.justbio.com**, **www.expasy.org** and **www.ncbi.nlm.nih.gov**.

Results and Discussion:

Dissection of the α-mannosidase gene from *A. fischeri*

Genomic DNA was extracted and Primers were designed based on the gene sequence available in NCBI Gene data Bank as described in materials and methods. PCR reactions were set up with *A. fischeri* genomic DNA using all possible combinations of the forward and the reverse primers. A DNA fragment of ~2.0 Kb was amplified (Fig. A.1) with forward primer **AfManF [5'ATG ATT CTA GGT CGC AGG CGC 3']** and reverse primer **AfManR-2 [5' TGT ACG AGC AGA GGG ACG C 3'].**

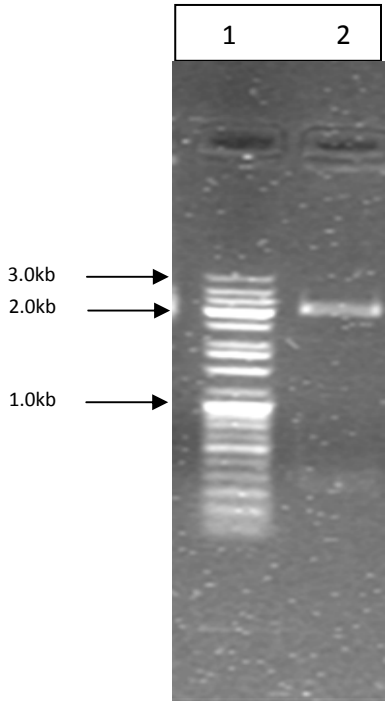

Figure A.1: PCR with *A. fischeri* genomic DNA template and primers **AfManF** and **AfManR-2**. DNA size marker (lane 1), PCR amplified product (lane 2).

Cloning of α-mannosidase gene

The amplicon obtained by primers AfManF forward and AfManR-2 reverse was cloned in to pGEM-T Easy Vector (Promega, USA) by TA cloning and transformed in to *E. coli*. The fact that *Taq* polymerase adds up poly A tail to the amplicon has been exploited in TA cloning. The pGEM-T has poly T at the cloning sites which make it easy to bind to the poly A of the PCR amplified fragment with poly A tail. The positive clones were selected based on the blue-white selection using IPTG and X-Gal. The positive clones were then cross checked for the presence of the gene by isolating the plasmid and sequencing it.

```
   1 CATATGATTC TAGTCGCAGG CGCTATCGCT ATGCCTTACC AACCTTTATT
  51 CTAATTCTCA TTACCTTCTT CCTTTTCTCG AGTCTACCGC CTGGCGCGGA
 101 ACCTCCCCTT GTCGACGACC ACTCATACTA CGCAGAATAC CATCCCCAAC
 151 CCCCGCAGAA CGATAACCGT ATCCATTGGA CCAAACATAC CGAAAGACAT
 201 CCTGTCCCCA GTTTTATTCC TCTCCCTACT CCCGCGCCAT CCGCAATTCC
 251 TCGTGTCCAG TACGACTTCG CGAAGGAATC ATGGCTTGGC CGGAGAAAAA
 301 GAGTGAACAG ACAGAAGGCC GTCAAGGAGG CCTTCACGCA TGCTTGGAAA
 351 GGGTACAAGC AGCATGCCTG GATGCGCGAT GAACTTTCGC CCCTCAGTGC
 401 TCGTTACAGA ACCACATTTG CTGGCTGGGC TGCCACTCTG GTGGACGCAC
 451 TTGACACTCT TGTCATTATG GGTATGGAAG ACGAGTTCAA GGATGCGTTG
 501 CATGCCATTG AGAGCATTGA TTTTACTACC ACCGATGCCA CCCAGATCAA
 551 TGTATTCGAG ACTACTATCC GATATGTAGG AGGGTTACTT GGCGCCTACG
 601 ACCTGACCGA CGGAAAACAC CCGATCCTTC TGAAGAAGGC TGTGGAACTG
 651 GCCGACGTGA TCTACGATGC TTTTGATACT AGCAAATAGG ATGCCCCAGT
 701 CTCGCTGGCA ATGGAGCAGT AAGCCGGCCA TTTGTTTCTG GAACCACTTA
 751 AAGCTGCTGT TAACTAGGCC ATAGATCTGC GCGAGGCCTG AGCATTCAAC
 801 CAAGCAGACA AACTATCCTC GCAGAATTGG GTTCATTGAA TCTAGAATTC
 851 ACCAGGCTGT CCCAGCTGAC TCATGATCCC AAGTACTTTG ATGCGGTCCA
 901 ACGAATTACA GACGTTCTCG ACGACGCTCA GAATAAGACC AAAATCCCTG
 951 GGCTGTGGCC TATGATGGTC AACGCTCAGG ATTTAGAGTT CACAGACCCT
1001 CGCTTTACTG TGGGTGGAAT GGCCGACTCA ACATATGAGT ATTTGCCGAA
1051 AGAGCATATG CTACTGGGAG CTCAGACGGA TCAATACCGC AAGATGTATG
1101 CCGCCGCCAT GGAGGCGATC AAGAAGCGCT TATTGTTTCG ACCCATGACC
1151 AAAAACGGCG AGGATCTCCT CTTCGCCGGG AACACCCACA CGAGTCTCGC
1201 AACTAACGCG CCCCCGGAGC CTCAATGGGA ACATCTGAAA TGCTTTTTTG
1251 GGGGCACTGT GGGCATCGGG GCCAAGGTTT TCAACCGCCC GGAGGAGCTC
1301 TCAATTGCAC GAAAGCTAAC AGATGGCTGT ATCTGGGCAT ACGATGTCAT
1351 GCCCACCGGA ATCATGCCGG AAATCATGCA TCTCAGCGCT TGCCAGAGTA
1401 TGGATAGTTG TGAATGGGAC GAGCAGAAGT GGTACCAAGA TGTCCGGCGG
1451 CGACTGGCCA AGGGATCAAA GGAGAGAGAC ACTGTTCAAG AAGCCAAGAC
1501 AATTATCCAG GAGAGTGGGC TTCAACCTGG CCTAACTGAG ATATCGGATC
1551 CGAGATATTT GCTGCGGTAT GTGATTTGCT GACAATTGAT TTTCGTCTTG
1601 CATCGGGTGT AGTAGTGCTG ATATTGGTTC TAGACCCGAG GCTATCGAGT
1651 CAGCTTTCAT CATGTACCGC ATCACTGGGG ACAAGAAATT GCAGGACGAT
1701 GCATGGAGAA TGTTTCAGAG CATTGAGAAA GCAACTCGAA CCAATCATGC
1751 CCATGCCGCG ATAGACGACG TCCGGGACGT GAAGACAACC CAGTTAGATT
1801 ACATGGAGAG TTTCTGGCTG GCAGAGACCT TGAAGTACTT CTATCTCGTC
```

```
1851 TTCTCCGAAC CAGGGCTTGT CAGCTTGGAT GATTACGTAC TGTATGTGCT
1901 GTTGTCTTGT GAGGCTCTCG CCAAAGCTAA CGATTAAGCA GGAACACGGA
1951 AGCACATCCA TTCAAGCGTC CCTCTGCTCG TACAAAGCTT
```

Figure A.2: Nucleotide sequence of GDNA amplicon of α-mannosidase (1990 bp).

The nucleotide sequences of α-mannosidase genomic clones were searched for sequence similarity in NCBI Gene Bank database and they showed sequence similarity with reported *Neosartorya fischeri* (*Aspergillus fischeri*) (100%) and *Aspergillus fumigatus* (94%) Class I α-mannosidase fungal genes.

Sequencing data analysis of gDNA of α-mannosidase showed that the clone was of 1990 bp long. The sequences upon alignment showed 100% sequence similarity with *Neosartorya fischeri* (*A. fischeri*) class I α-mannosidase. The calculated GC content (www.justbio.com) of the gene was 51.0 %. Manually, the intron / exon junctions in the clone were identified after doing BLAST search in gene bank. The α-mannosidase gDNA nucleotide sequences show presence of putative four exons and three introns. In the α-mannosidase gene clone the four exons spanned the nucleotide positions 4 - 719, 773 - 1566, 1633 - 1892 and 1942 - 1984. The putative introns spanned nucleotide positions 720 - 772, 1567 – 1632 and 1893 – 1941 (Fig. A.2).

```
Afishceri cDNA    ----ATGATTCTAGGTCGCAGGCGCTATCGCTATGCCTTACCAACCTTTATTCTAATTCTC
Afishceri gDNA    CATATGATTCTAG-TCGCAGGCGCTATCGCTATGCCTTACCAACCTTTATTCTAATTCTC
                     ********** ********************************************

Afishceri cDNA    ATTACCTTCTTCCTTTTCTCGAGTCTACCGCCTGGCGCGGAACCTCCCTTTGTCGACGAC
Afishceri gDNA    ATTACCTTCTTCCTTTTCTCGAGTCTACCGCCTGGCGCGGAACCTCCCCTTGTCGACGAC
                  ********************************************** ***********

Afishceri cDNA    CACTCATACTACGCAGAATACCATCCCCAACCCCCGCAGAACGATAACCGTATCCATTGG
Afishceri gDNA    CACTCATACTACGCAGAATACCATCCCCAACCCCCGCAGAACGATAACCGTATCCATTGG
                  ************************************************************

Afishceri cDNA    ACCAAACATACCGAAAGACATCCTGTCTCCAGTTTTATTCCTCTCCCTACTCCCGCGCCA
Afishceri gDNA    ACCAAACATACCGAAAGACATCCTGTCCCCAGTTTTATTCCTCTCCCTACTCCCGCGCCA
                  ************************* ******************************
```

```
Afishceri cDNA   TCCGCAATTCCTCGTGTCCAGTACGACTTCGCGAAGGAATCATGGCTTGGCCGAAGAAAA
Afishceri gDNA   TCCGCAATTCCTCGTGTCCAGTACGACTTCGCGAAGGAATCATGGCTTGGCCGGAGAAAA
                 ************************************************** ******

Afishceri cDNA   AGAGTGAACAGACAGAAGGCCGTCAAGGAGGCCTTCACGCATGCTTGGAAAGGGTACAAG
Afishceri gDNA   AGAGTGAACAGACAGAAGGCCGTCAAGGAGGCCTTCACGCATGCTTGGAAAGGGTACAAG
                 ************************************************************

Afishceri cDNA   CAGCATGCCTGGATGCGCGATGAACTTTCGCCCCTCAGTGCTCGTTACAGAACCACATTT
Afishceri gDNA   CAGCATGCCTGGATGCGCGATGAACTTTCGCCCCTCAGTGCTCGTTACAGAACCACATTT
                 ************************************************************

Afishceri cDNA   GCTGGCTGGGCTGCCACTCTGGTGGACGCACTTGACACTCTTGTCATTATGGGTATGGAA
Afishceri gDNA   GCTGGCTGGGCTGCCACTCTGGTGGACGCACTTGACACTCTTGTCATTATGGGTATGGAA
                 ************************************************************

Afishceri cDNA   GACGAGTTCAAGGATGCGTTGCATGCCATTGAGAGCATTGATTTTACTACCACCGATGCC
Afishceri gDNA   GACGAGTTCAAGGATGCGTTGCATGCCATTGAGAGCATTGATTTTACTACCACCGATGCC
                 ************************************************************

Afishceri cDNA   ACCCAGATCAATGTATTCGAGACTACTATCCGATATGTAGGAGGGTTACTTGGCGCCTAC
Afishceri gDNA   ACCCAGATCAATGTATTCGAGACTACTATCCGATATGTAGGAGGGTTACTTGGCGCCTAC
                 ************************************************************

Afishceri cDNA   GACCTGACCGACGGAAAACACCCGATCCTTCTGAAGAAGGCTGTGGAACTGGCCGACATG
Afishceri gDNA   GACCTGACCGACGGAAAACACCCGATCCTTCTGAAGAAGGCTGTGGAACTGGCCGACGTG
                 ************************************************************ **

Afishceri cDNA   ATCTACGATGCTTTTGATACTAGCAA-TAGGATGCCCCAGTCTCGCTGGCAATGGAGCAG
Afishceri gDNA   ATCTACGATGCTTTTGATACTAGCAAATAGGATGCCCCAGTCTCGCTGGCAATGGAGCAG
                 ************************* ********************************

Afishceri cDNA   ----------------------------------------------------------------------------------------ATCTG
Afishceri gDNA   TAAGCCGGCCATTTGTTTCTGGAACCACTTAAAGCTGCTGTTAACTAGGCCATAGATCTG
                                                                                                *****

Afishceri cDNA   CGCGAGGCCTGAGCATTCAACCAAGCAGACAAACTATCCTCGCAGAATTGGGTTCATTGA
Afishceri gDNA   CGCGAGGCCTGAGCATTCAACCAAGCAGACAAACTATCCTCGCAGAATTGGGTTCATTGA
                 ************************************************************

Afishceri cDNA   ATCTAGAATTCACCAGGCTGTCCCAGCTGACTCATGATCCCAAGTACTTTGATGCGGTCC
Afishceri gDNA   ATCTAGAATTCACCAGGCTGTCCCAGCTGACTCATGATCCCAAGTACTTTGATGCGGTCC
                 ************************************************************

Afishceri cDNA   AACGAATTACAGACGTTCTCGACGACGCTCAGAATAAGACCAAAATCCCTGGGCTGTGGC
Afishceri gDNA   AACGAATTACAGACGTTCTCGACGACGCTCAGAATAAGACCAAAATCCCTGGGCTGTGGC
                 ************************************************************

Afishceri cDNA   CTATGATGGTCAACGCTCAGGATTTAGAGTTCACAGACCCTCGCTTTACTGTGGGTGGAA
```

```
Afishceri gDNA    CTATGATGGTCAACGCTCAGGATTTAGAGTTCACAGACCCTCGCTTTACTGTGGGTGGAA
                  ************************************************************

Afishceri cDNA    TGGCCGACTCAACATATGAGTATTTGCCGAAAGAGCATATGCTACTGGGAGCTCAGACGG
Afishceri gDNA    TGGCCGACTCAACATATGAGTATTTGCCGAAAGAGCATATGCTACTGGGAGCTCAGACGG
                  ************************************************************

Afishceri cDNA    ATCAATACCGCAAGATGTATGCCGCCGCCATGGAGGCGATCAAGAAGCGCTTATTGTTTC
Afishceri gDNA    ATCAATACCGCAAGATGTATGCCGCCGCCATGGAGGCGATCAAGAAGCGCTTATTGTTTC
                  ************************************************************

Afishceri cDNA    GACCCATGACCAAAAACGGCGAGGATCTCCTCTTCGCCGGGAACACCCACACGAGTCTCG
Afishceri gDNA    GACCCATGACCAAAAACGGCGAGGATCTCCTCTTCGCCGGGAACACCCACACGAGTCTCG
                  ************************************************************

Afishceri cDNA    CAACTAACGCGCCCCCGGAGCCTCAATGGGAACATCTGAAATGCTTTTTTGGGGGCACTG
Afishceri gDNA    CAACTAACGCGCCCCCGGAGCCTCAATGGGAACATCTGAAATGCTTTTTTGGGGGCACTG
                  ************************************************************

Afishceri cDNA    TGGGCATCGGGGCCAAGGTTTTCAACCGCCCGGAGGAGCTCTCAATTGCACGAAAGCTAA
Afishceri gDNA    TGGGCATCGGGGCCAAGGTTTTCAACCGCCCGGAGGAGCTCTCAATTGCACGAAAGCTAA
                  ************************************************************

Afishceri cDNA    CAGATGGCTGTATCTGGGCATACGATGTCATGCCCACCGGAATCATGCCGGAAATCATGC
Afishceri gDNA    CAGATGGCTGTATCTGGGCATACGATGTCATGCCCACCGGAATCATGCCGGAAATCATGC
                  ************************************************************

Afishceri cDNA    ATCTCAGCGCTTGCCAGAGTATGGATAGTTGTGAATGGGACGAGCAGAAGTGGTACCAAG
Afishceri gDNA    ATCTCAGCGCTTGCCAGAGTATGGATAGTTGTGAATGGGACGAGCAGAAGTGGTACCAAG
                  ************************************************************

Afishceri cDNA    ATGTCCGGCGGCGACTGGCCAAGGGATCAAAGGAGAAAGACACTGTTCAAGAAGCCAAGA
Afishceri gDNA    ATGTCCGGCGGCGACTGGCCAAGGGATCAAAGGAGAGAGACACTGTTCAAGAAGCCAAGA
                  ********************************** **********************

Afishceri cDNA    CAATTATCCAGGAGAGTGGGCTTCAACCTGGCCTAACTGAGATATCGGATCCGAGATATT
Afishceri gDNA    CAATTATCCAGGAGAGTGGGCTTCAACCTGGCCTAACTGAGATATCGGATCCGAGATATT
                  ************************************************************

Afishceri cDNA    TGCTGCG-------------------------------------------------------------------------------
Afishceri gDNA    TGCTGCGGTATGTGATTTGCTGACAATTGATTTTCGTCTTGCATCGGGTGTAGTAGTGCT
                  *******
Afishceri cDNA    ------------------------ACCCGAGGCTATCGAGTCAGTTTTCATCATGTACCGCATCACTGGG
Afishceri gDNA    GATATTGGTTCTAGACCCGAGGCTATCGAGTCAGCTTTCATCATGTACCGCATCACTGGG
                                         ******************** ************************

Afishceri cDNA    GACAAGAAATTGCAGGACGATGCATGGAGAATGTTTCAGAGCATTGAGAAAGCAACTCGA
Afishceri gDNA    GACAAGAAATTGCAGGACGATGCATGGAGAATGTTTCAGAGCATTGAGAAAGCAACTCGA
                  ************************************************************
```

```
Afishceri cDNA    ACCAATCATGCCCATGCCGCGATAGACGACGTCCGGGACGTGAAGACAACCCAGTTAGAT
Afishceri gDNA    ACCAATCATGCCCATGCCGCGATAGACGACGTCCGGGACGTGAAGACAACCCAGTTAGAT
                  ************************************************************

Afishceri cDNA    TACATGGAGAGTTTCTGGCTGGCAGAGACCTTGAAGTACTTCTATCTCGTCTTCTCCGAA
Afishceri gDNA    TACATGGAGAGTTTCTGGCTGGCAGAGACCTTGAAGTACTTCTATCTCGTCTTCTCCGAA
                  ************************************************************

Afishceri cDNA    CCAGGGCTTGTCAGCTTGGATGATTACGTACTG----------------------------------------------
Afishceri gDNA    CCAGGGCTTGTCAGCTTGGATGATTACGTACTGTATGTGCTGTTGTCTTGTGAGGCTCTC
                  ********************************

Afishceri cDNA    ------------------------------------------AACACGGAAGCACATCCATTCAAGCGTCCCTCTGCTC
Afishceri gDNA    GCCAAAGCTAACGATTAAGCAGGAACACGGAAGCACATCCATTCAAGCGTCCCTCTGCTC
                                                  ************************************

Afishceri cDNA    GTACATAG---
Afishceri gDNA    GTACAAAGCTT
                  ***** **
```

Figure A.3: Nucleotide sequence of *A. fischeri* α-mannosidase genomic clone sequence and cDNA sequence and their nucleotide sequence alignment using Clustal W 1.8.

Restriction analysis of α-mannosidase gDNA was done using bioinformatic software **pDRAW32** (Fig. A.4). Analysis was limited to enzyme site cutting not more than two times in the sequence.

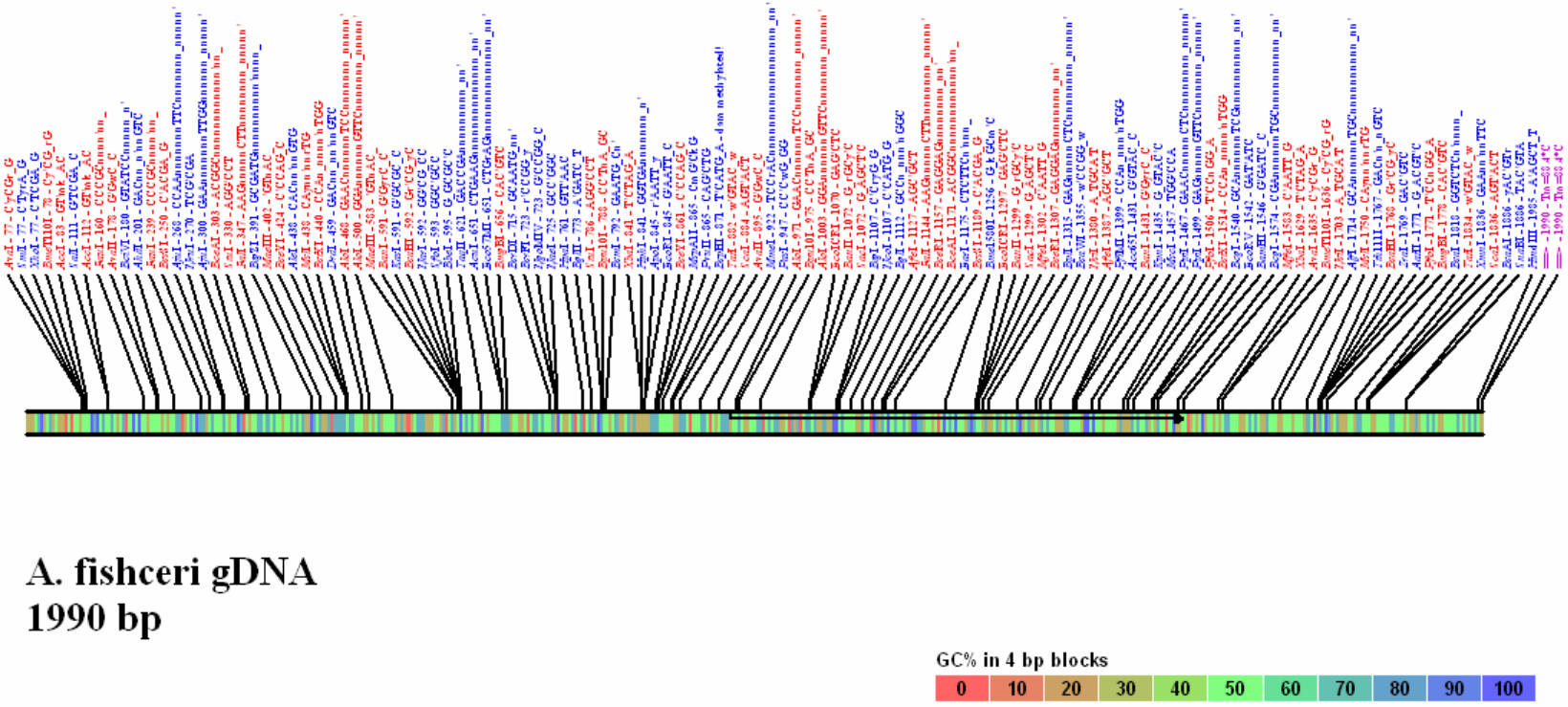

Figure A.4: Restriction analysis of α-mannosidase gDNA using pDRAW 32**.**

α-mannosidase gene isolation from *A. fischeri* by cDNA method

Total RNA was extracted from the *A. fischeri* and cDNA was synthesized as described in materials and methods. PCR reactions were set up with *A. fischeri* cDNA using all possible combinations of the forward and the reverse primers. A DNA fragment of ~1.8 Kb was amplified (Fig. A.3) with forward primer **AfManF [5'ATG ATT CTA GGT CGC AGG CGC 3']** and reverse primer **AfManR-2 [5' TGT ACG AGC AGA GGG ACG C 3'].**

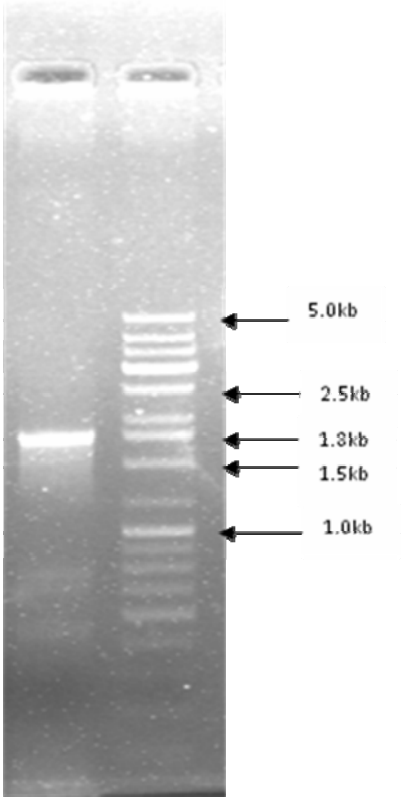

Figure A.3: PCR with *A. fischeri* cDNA template and primers **AfManF** and **AfManR-2**. DNA size marker (lane 1), PCR amplified product (lane 2).

Coclusion:

The α-mannosidase gene from *Aspergillus fischeri* was isolated by both genomic DNA and RNA method. Cloning of gene, isolation of recombinant plasmid and sequencing of genomic DNA gene showed that it is 1990 base pair long and analysis showed presence of three introns and four exons in the gene.

BLAST analysis revealed 100% similarity to the *Aspergillus fischeri* and 94% with *Aspergillus fumigatus* class I α-mannosidase reported in NCBI Gene Data Bank. But this sequence is not matching with any Class II α-mannosidase at gene level. The study from past four chapters (chapter 2-5) revealed that the enzyme is class II α-mannosidase.

As we have seen in Chapter 1 (page 16-17), there are three subfamilies of genes, Class IIA, IIB and IIC. Among these, Class IIC found in higher and lower eukaryotes and has very low sequence similarity to the other two subfamilies. The present α-mannosidase from *Aspergillus fischeri* could belong to the Class IIC subfamily.

	Class IIA α-mannosidase	**Class IIB α-mannosidase**	**Class IIC α-mannosidase**
1.	Occurs only in higher eukaryotes	Found only higher eukaryotes.	Found in higher and lower eukaryotes.
2.	Involved in N-glycan synthesis in golgi. Removes α, 1-3, 1-2, 1-6 linked mannose residues from N-glycans during their synthesis.	Involved in N-glycan breakdown, removal and recycling in the cytoplasm, lysosome and vacuole.	Involved in N-glycan breakdown, removal and recycling in the cytoplasm, lysosome and vacuole. Heterogeneous enzymes with a diversity of functions and cellular location. Low sequence similarity with the other two groups of enzymes.

Reference:

[1] Camirand, A., Heysen, A., Grondin, B. and Herscovics, A. (1991) *J Biol Chem* **266**, 15120-15127.

[2] Eades, C.J., Gilbert, A.M., Goodman, C.D. and Hintz, W.E. (1998) *Glycobiology* **8**, 17-33.

[3] Eades, C.J. and Hintz, W.E. (2000) *Gene* **255**, 25-34.

[4] Inoue, T., Yoshida, T. and Ichishima, E. (1995) *Biochim Biophys Acta* **1253**, 141-5.

[5] Akao, T. et al. (2006) *Biosci Biotechnol Biochem* **70**, 471-479.

[6] Hopwood, D.A. et al. (1985) *In: Genetic manipulation of Streptomyces- A laboratory manual.*, The John Innes foundation. Norwich. England.

[7] Sellner, L.N., Coelen, R.J. and MacKenzie, J.S. (1992) *Nucleic Acids Res* **20**, 1487-1490.

[8] Chumakov, K.M. (1994) *PCR Methods Appl* **4**, 62-64.

[9] Saiki, R., Scharf, S., Faloona, F., Mullis, K. B., Horn, G.T., Erlich, H. A., Arnheim, N. (1985) *Science* **230**, 1350-1354.

[10] Mullis, K.B., Faloona, F. A. (1987) *Methods Enzymol* **255**, 335-350.

[11] Todd, J.A., Bell, J. I., McDevitt, H. O. (1987) *Nature* **329**, 599-604.

[12] Sambrook, J., Fritsch, E. F., Maniatis, T. (1989) *Molecular cloning; A Laboratory Manual, 2nd ed., New York:* Cold Spring Harbor Laboratory Press, Cold Spring Harbor.